2012

Novel Shear-Thinning of Aged PDMS/Fumed Silica Admixtures and Properties of Related Silicone Elastomers

Wayne Brooke-Devlin
Virginia Commonwealth University

Novel Shear-Thinning of Aged PDMS/Fumed Silica Admixtures and Properties of Related Silicone Elastomers

A dissertation submitted in partial fulfillment of
the requirements for the degree of

Doctor of Philosophy
(Chemical and Life Science Engineering)

at Virginia Commonwealth University

By

Wayne William Brooke-Devlin
B.S. Chemical Engineering, University of South Florida, 1991

Dissertation Director: Kenneth J. Wynne, Ph.D.
Commonwealth Professor,
Department of Chemical and Life Science Engineering

Virginia Commonwealth University
Richmond, Virginia
December, 2012

Table of Contents

List of Tables

List of Graphs

List of Figures

Abstract

NOVEL SHEAR-THINNING OF AGED PDMS/FUMED SILICA ADMIXTURES AND PROPERTIES OF RELATED SILICONE ELASTOMERS

By Wayne William Brooke-Devlin, BS ChE

A dissertation submitted in partial fulfillment of the requirements for the degree of Doctor of Philosophy (Chemical and Life Science Engineering) at Virginia Commonwealth University.

Virginia Commonwealth University, 2012

Dissertation Director: Kenneth J. Wynne, Ph.D. Commonwealth Professor, Department of Chemical and Life Science Engineering

Fumed silica filler has long been used to structurally reinforce silicone elastomers. Unfortunately, the combination of as little as a few weight percent of untreated fumed silica nanoparticles [uFSN] with a siloxane polymer, such as PDMS, forms a difficult to process waxy solid admixture that even long periods of high shear mixing will not thin. In the course of the current work it was noted that after a period of storage certain solid admixtures would become viscous liquids when subjected to additional high shear mixing. It was further found that the required aging period could be decreased if the admixture storage temperature were increased. The only known interaction of PDMS and uFSN at moderate conditions is the adsorption of polymer on filler, and this interaction is also known to occur more quickly at higher temperature. This study examines the relationship between polymer adsorption and admixture liquefaction. Further, the mechanical properties of cured elastomers containing liquefied admixtures are examined to assess the degree of reinforcement that these materials afford.

Introduction

The first commercial silicone based product, Dow Corning Compound 4, was introduced in 1942. It was a greasy paste that exploited the high temperature stability, hydrophobicity, and weak dielectric properties of siloxanes to seal and electrically insulate the wiring harnesses of aircraft ignition systems. Its use was critical in inhibiting the water condensation, and consequent corona discharge, that caused engine failure during the extended operation of aircraft at high altitudes.[1] This compound remains in production to the present day. An examination of the MSDS for Compound 4 shows that it is composed of a mixture of polydimethylsiloxane [PDMS] and finely ground amorphous silica.[2] Later in the 1940's, methods were developed to crosslink PDMS, but the resulting elastomers were found to be weak. However, when mixtures of PDMS and silica (such as Compound 4) were crosslinked they were found to form much stronger silicone rubbers. Such mixtures are still the preferred starting material for many silicone elastomers. PDMS/silica mixtures are currently utilized in the production of lubricants, adhesives and high temperature gaskets, as sealants in electronic component assembly and general construction, and as both a mold making and casting material in the production of products as diverse as microfluidic devices, medical equipment, automotive parts, cooking utensils, and toys. These mixtures are a major part of the roughly $13 billion per year silicone industry. Therefore, it is humbling to realize that, after nearly 70 years, the exact nature of this seemingly simple binary mixture, and the ways in which that nature affects the properties of silica filled PDMS elastomers, remains far from understood.

Outline and Theses

This work begins with a "General Background" section that examines the history, synthesis, and properties of polydimethylsiloxane, silicone elastomers, and fumed silica. This section then examines the physical processes involved in compounding these materials, and describes the techniques employed to ease these processes. Wherever possible examples, data, or theoretically calculated values have been supplied specifically in terms of the particular polysiloxane and fumed silica utilized in the experimental work

of this study so that pertinent information derived from the literature might be available during later analysis.

As originally conceived, this work was intended to rationalize variations in the experimental results reported by three different researchers who examined similar fumed silica filled silicone elastomers. It was assumed that variations in processing conditions occasioned the variable results. Therefore, a "Study Specific Background" section has been included that begins by detailing and comparing the work of these three earlier investigators. While attempting to reproduce this earlier work, a novel process for producing viscous liquid admixtures of PDMS and untreated Fumed Silica Nanoparticles [uFSN] was discovered. In the literature only two relatively recent (1999 and 2007) articles were found that reported any similar softening in silicone/silica mixtures. The "Study Specific Background" section of this document therefore concludes with a detailed description of the content of these two papers.

An "Experimental" section follows the background sections. This section details the various materials and equipment utilized in the current work, and describes the procedures followed in sample preparation, and testing. These descriptions are given in sufficient detail that an interested researcher should be able to reproduce any experiment reported in this document.

The "Results and Discussion" section starts by relating the variety of techniques employed in attempts to recreate silicone elastomer films for comparison (by atomic force microscopy [AFM]) with images of films created by three earlier researchers. Based on the literature the probable reasons for the observed failure of these approaches are also discussed. The manner in which these failed attempts lead to the development of a process to liquefy PDMS/uFSN admixtures is also detailed. These viscous liquid admixtures made possible the production of elastomer films similar to the AFM image-able films produced by the earlier researchers. This section therefore also presents AFM images of the liquid admixture derived films (Appendix A) and makes comparisons with the results obtained by the earlier researchers. Possible reasons for the lack of any

crosslinker concentration based “disappearance” of surface silica under AFM, as reported by earlier investigators, are also discussed.

A secondary initial motivation for this work was a desire to determine the processing conditions that produce the “best” silicone rubber films. Students had encountered difficulty producing such films in an experiment performed for an undergraduate class. The unstated thesis here was that there exist optimal processing parameters for the production of visibly even, translucent, bubble-free, untreated fumed silica filled, alkoxy condensation cured silicone elastomer films. In pursuit of such conditions a considerable portion of the “Results and Discussion” section are given over to an examination of the products that result from varying elastomer production process conditions. In an extension of this thesis, since the improvement of mechanical properties is the reason for adding uFSN filler to silicone elastomer, it was felt that any process for producing uFSN filled silicone rubber films that did not also result in enhanced elastomer strength could not be deemed a “best” process. It was, however, believed that elastomers derived from the liquid PDMS/uFSN admixtures alkoxy cured with excess crosslinker display mechanical properties at least equal to those of elastomer filled with comparable quantities of treated (trimethylsilylated) fumed silica and equivalent quantities of crosslinker. In support of this thesis this section also presents and compares the results of mechanical testing of such materials.

The two literature sources that reported softening of siloxane/silica mixtures both proposed (for different reasons) that the adsorption of polymer on filler caused the observed weakening of aged silica/siloxane mixtures. This hypothesis was adopted here as a thesis for further experimental work with the new viscous liquid admixtures. The “Results and Discussion” section therefore concludes with an examination of the variation in filler adsorbed polymer (bound rubber) with temperature and over time, and the relation between bound rubber and liquefaction in these admixtures. Several other experiments to characterize admixture structure and behavior over time are also described and discussed.

Two final sections, one of "Conclusions" summarizing earlier discussions and one of "Future Work" proposing (in light of reported results) possibly fruitful directions for further research, close out this dissertation.

General Background

Poly(dimethylsiloxane)

History and Synthesis

Polydimethylsiloxane was first synthesized and identified by Eugene Rochow at General Electric in October of 1938. Earlier that year, during a visit to the Corning Glassworks, a colleague of Rochow's had learned of a method used by Corning's James Franklin Hyde to synthesize polyethylphenylsiloxane [PEPS]. Rochow employed a similar method in his PDMS synthesis.[3] Subsequently, each company would apply for patent protection (GE for the compound PDMS and the exact synthetic method, and Corning for the general synthetic method and all obvious resulting products, including PDMS) and a lively, extended patent dispute would result.[4, 5] In fact, both Rochow and Hyde had employed a Grignard synthesis published 30 years earlier by the pioneering English silicon chemist Frederick Stanley Kipping. In 1908 Dr. Kipping had reacted ethyl magnesium bromide with silicon tetrachloride in ether to form diethyldichlorosilane. When he added this compound to a large excess of water he was left with what he described as an "uninviting, oily" product.[6, 7] Kipping recognized that he had produced polydiethylsiloxane [PDES], but did not attach any great significance to the achievement. All three researchers carried out the reactions shown in eqs 1 – 4.

$$R_1MgBr + SiCl_4 \rightarrow R_1SiCl_3 + MgClBr \quad (1)$$

$$R_2MgBr + R_1SiCl_3 \rightarrow R_1R_2SiCl_2 + MgClBr \quad (2)$$

$$n(R_1R_2SiCl_2) + 2n(H_2O) \rightarrow n(R_1R_2Si(OH)_2) + 2n(HCl) \quad (3)$$

$$n\left(R_1R_2Si\begin{matrix}(OH)_2\\ \\ \end{matrix}\right) \rightarrow HO\text{-}(SiO)_nH + n\text{-}1(H_2O) \quad (4)$$

(In eq 4, R_1 and R_2 are the substituents on the silicon atom.)

In Kipping's synthesis R_1 and R_2 were both ethyl groups (C_2H_5-). Hyde's synthesis was like Kipping's, except that for R_2 he substituted a phenyl (C_6H_5-) group. Rochow's synthesis was likewise similar to Kipping's, except that R_1 and R_2 in his starting materials were both methyl groups (-CH_3).

Often intellectual property disputes can be very disruptive to scientific progress, but this was not the case in the Corning/GE litigation. In 1942 Corning felt confident enough of winning to begin limited Grignard based production of polyethylphenyl and polydimethyl siloxanes for use as oils and greases.[8] At that time (at the urging of Hyde) Corning entered into a joint venture with the Dow Chemical Company hastily forming the Dow Corning Corporation in a handshake deal that was not legally formalized until the following year. Dow, providentially, had begun producing both magnesium and halides from seawater in the late 1930's, and was in an excellent position to provide Corning with both essential raw materials and industrial scale chemical production expertise. By war's end Dow Corning silicone oils, greases, and resins were in widespread use as cooling/insulating materials in electrical transformers, and as temperature resistant, electrical wiring insulation.

General Electric was somewhat less sanguine about the chances for acceptance of their PDMS patent. At GE Rochow recognized that the expensive materials and low yields of the multistep Grignard reaction employed at Corning would severely hinder large scale production of silicones. Only the exigencies of war had made Dow Corning's small scale production economically feasible. Based on research conducted by Alfred Stock on silicon halides, Rochow began to seek a better synthetic route to PDMS. In mid 1940 he passed methyl chloride gas containing a small amount of hydrogen chloride over a heated, powdered bed of silicon that by chance contained a small amount of copper. He collected a cooled product and added it to an excess of water to form the now familiar PDMS. Further experimentation soon made it clear that the hydrogen chloride had served to etch the surface of the copper in the reactant bed and that the exposed metallic copper had catalyzed a reaction between methyl chloride and silicon.[9] The Rochow reactions are summarized in eqs 5 and 6.

$$2(CH_3Cl) + Si \xrightarrow{\text{Cu catalyst, } 300^{\circ}C} (CH_3)_2SiCl_2 \qquad (5)$$

$$n((CH_3)_2SiCl_2) + 2n(H_2O) \longrightarrow HO\text{-}\left(\begin{array}{c} CH_3 \\ | \\ SiO \\ | \\ CH_3 \end{array}\right)_n H + 2n(HCl) + n\text{-}1(H_2O) \qquad (6)$$

Unlike the Grignard based batch process, the starting materials for Rochow's process (methyl chloride, silicon and copper) were all cheaply and readily available in industrial quantities, and the fluidized bed reaction easily lent itself to continuous large scale production.

There were, of course, some difficulties to be overcome before the Rochow process could be implemented at a production scale. To begin with, though requiring activation temperatures of 300˚C, the first step of the reaction (eq 5) is highly exothermic. Preheating the methyl chloride followed by rapid cooling of the reaction product was found necessary to initiate the process while avoiding a runaway reaction. The next challenge to production was the discovery that the hydrolysis/condensation step (eq 6) required very pure (>99.98 mole %) dimethyldichlorosilane [DDS]. Only this difunctional product polymerizes to form long straight chain PDMS. The presence of mono or trifunctional reactants in the polymerization mixture causes chain termination or branching, respectively. Unfortunately, the first reaction step (eq 5) produced not just the dimethyldichloro- product, but also methyltrichloro-, trimethylchloro-, and tetrachloro-silicon products along with several chlorinated methyl silanes. Nevertheless, DDS comprised better than 80% of the first step (eq 5) yield, and by multiple distillations it proved possible to isolate it in high enough purity from the other products.[3, 10]

The last problem to be overcome was control of the hydrolytic polycondensation of dimethyldichlorosilane (i.e., Grignard reaction eqs 3 and 4, and Rochow reaction eq 6). In water chlorosilane rapidly hydrolyzes to hydroxysilane and acid (eq 7).

$$\equiv SiCl + H_2O \rightleftharpoons \equiv SiOH + HCl \quad (7)$$

From these products siloxane forms either via the heterofunctional condensation of hydroxysilane and chlorosilane (eq 8),

$$\equiv SiCl + \equiv SiOH \rightleftharpoons \equiv SiOSi\equiv + HCl \quad (8)$$

or it forms via the acid catalyzed homofunctional condensation of hydroxysilane (eq 9). In the homofunctional pathway (eq 9) HCl formed during hydrolysis (eq 7) catalyzes the reaction by protonating SiOH.

$$\equiv SiOH_2^+ + \equiv SiOH \rightleftharpoons \equiv SiOSi\equiv + H_2O + H^+ \quad (9)$$

Kipping, Hyde, and Rochow all added their dichloro- products to a large excess of water. Under these conditions, hydroxysilane and acid form quickly (eq 7) leaving little chlorosilane to react by the heterofunctional pathway (eq 8), so that homofunctional condensation (eq 9) predominates. Unfortunately, in addition to forming straight chains, this self-condensation pathway also forms low molecular weight non-functional cyclics (predominantly the cyclic tetramer). Overall, the hydrolytic polycondensation of dimethyldichlorosilane in excess water is found to give a mixture of cyclic (m) and linear (n) PDMS (eq 10).

$$(CH_3)_2SiCl_2 \xrightarrow[-HCl]{H_2O} (CH_3)_2Si(OH)_2 \xrightarrow[-H_2O]{} HO\text{-}((CH_3)_2SiO)_nH + ((CH_3)_2SiO)_m \quad (10)$$

$$n = 2, 3, 4\ldots \quad m = 3, \underline{4}, 5\ldots$$

It was later found that a solution containing almost exclusively linear siloxanediols resulted when the time that the intermediate hydroxy compound was left in contact with high concentrations of hydrochloric acid and water was minimized.[11] However, since the acid was responsible for catalyzing the polycondensation, short contact time also resulted in a solution of very low molecular weight (n = 2, 3, 4) linear hydroxy terminated PDMS.

In order to obtain higher molecular weight [MW] polysiloxanes, a second non-aqueous acid catalyzed polycondensation of the low MW linear siloxanediol (performed at low pressure to eliminate the aqueous product) was found necessary (eq 11).

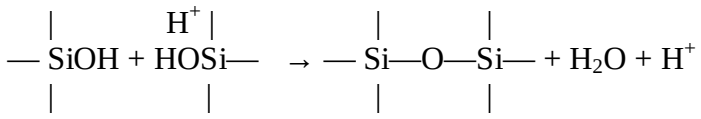

(11)

In bulk at 25˚C and with a high concentration of a strong protic acid this reaction is thermodynamically favorable for high MW siloxane formation: ΔH = -16.3 to -20.6 kJ/mol, and ΔS = -6.3 to -18 J/mol · K. In addition, the equilibrium constant for this reaction, K_{298} = 340 – 450, is high.[12]

The favorable thermodynamic driving force is thought to be due to multiple reaction pathways. In addition to the expected acid-catalyzed condensation of protonated silanol with unprotonated silanol (eq 11), a second chain growth mechanism is also believed to be at work. It is thought that short siloxanediol chains can self-catalyze by forming hydrogen bonds between opposite chain ends.[13] This intramolecular catalysis involves one hydroxy end group acting as a proton acceptor while the other acts as a proton donor. The oxygen of the donor hydroxy then nucleophilically attacks the silicon of a protonated silanol more vigorously than would the oxygen of a non-self-catalyzed hydroxy (eq 12). This mechanism not only results in condensation polymerization, but also regenerates a protonated silanol to perpetuate the reaction. [14, 15]

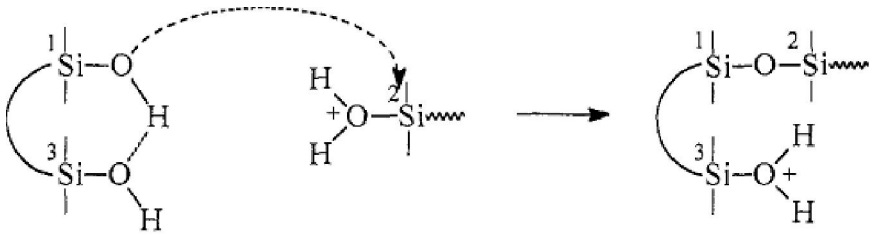

(12)

The reactivity of α, ω-oligosiloxanediols has been found to decrease with increasing chain length, and this is thought to be due to a decreased probability of intramolecular catalysis by widely separated chain ends. The decreased reactivity causes

long chains to condense with each other infrequently, while they nevertheless continue to grow in a step-like manner by condensing with smaller more reactive short chain siloxanediols. An important consequence of this variation in reactivity and multipath formation is that Rochow process PDMS exhibits the narrow molecular weight [MW] distributions commonly found in step-growth polymers.[16] Polymer Polydispersity Index [PDI] is defined as the ratio of the weight average and number average molecular weights of a polymer. A PDI close to one indicates a small variance in a polymer MW. Typical hydrocarbon step-growth polymers have a PDI of around two, and similar values are observed for Rochow process PDMS. For example, the Gelest, Inc. M_n = 26,000 g/mol hydroxy terminated PDMS [α, ω-hydroxyPDMS$_{26k}$] used in this study has a reported polydispersity index of 1.98.[17] The Rochow process therefore allows for the inexpensive manufacture of PDMS with molecular weights ranging from a few hundred to several hundred thousand g/mol, while also ensuring that any process synthesized PDMS of a particular MW varies only slightly from that weight.

By the mid 1940's the Rochow process became the preferred method for large scale production of PDMS. However, developing the process delayed GE's entry into the field of silicones. While Dow Corning opened their first dedicated silicone plant in 1945, it would be another two years before GE would open their first silicone manufacturing facility. Shortly after the end of the war, in a move that surprised both Dow Corning and GE, the courts awarded the PDMS patent to GE. It was judged that Kipping's published work on the Grignard based synthesis of polydiethylsiloxane constituted prior art that invalidated Dow Corning's claim to all products of the reaction. Therefore, GE could claim ownership of Grignard synthesized PDMS. This point was moot however, since in the interim GE had developed the much better Rochow process for PDMS production. During this period, while GE had been focused on PDMS production, Dow Corning had instead been developing techniques by which PDMS could be crosslinked to form useful polymeric materials. In light of the court's decision, and their respective wartime derived expertise, the two companies adopted an unusual arrangement that allowed them to share a number of silicone synthesis and crosslinking patents. Thus, in the immediate postwar

period both Dow Corning and GE were well positioned to develop an emerging silicone product market.[18]

In 1931, Corning's primary reason for employing J. F. Hyde (the first organic chemist hired by this specialty inorganic chemical company) was concern that new transparent organic polymers like polymethacrylate might challenge the traditional markets for Corning glass.[19] Hyde was given the task of investigating the possibility of producing a polymer–glass material, an organic-inorganic hybrid, in the hope that such a material might combine the heat and chemical resistance of glass with the versatility and ease of processing of plastics. As he familiarized himself with inorganic silicon chemistry Hyde encountered Kipping's extensive work. He recognized that the siloxanes, with their inorganic backbones of alternating silicon and oxygen atoms and organic silicon-bound side groups, might prove just such a hybrid.

Physical and Chemical Properties

The Si-O main chain of PDMS is often compared to the analogous C-O main chain of organic polyethers. However, there are significant structural differences between siloxanes and polyethers, and these differences give PDMS very different chemical and physical properties. The lower electronegativity of Si (χ^{Si} =1.9) versus that of C (χ^{C} =2.55) or O (χ^{O} =3.44) gives the Si-O bond a much more polar nature.[20] Pauling calculated that as much as 51% of the Si-O bond strength may be due to its ionic character, versus 22% for the C-O bond.[21] In addition, it has long been postulated that the Si-O bond exhibits an incomplete overlap of the vacant low energy 3d orbital of silicon with the p orbital of oxygen (a partial dπ-pπ linkage), as well as a normal covalent σ bond. This pseudo double bonding can not exist in the C-O bond, since carbon has no vacant d orbital. It is generally believed that the observed Si-O bond is shorter than the sum of the covalent bonding radii of silicon and oxygen as a consequence of this partial double bonding. Theoretical calculations have raised some doubt as to the validity of this structural theory, but have yet to supply a better one.[22] Regardless, an unusual structure and highly ionic nature result in Si-O bonds having ~30% greater bond dissociation energy (452 kJ/mol) than C-O bonds (346 kJ/mol).[23]

While in aliphatic ethers the C-O-C bond angle is found to be around 111˚ (± 4), the Si-O-Si bond in silicones is both wider (nominally 143˚) and more deformable with reported values of from 105˚ to 180˚.[24] As noted above, the Si-O bond is highly polar and this facilitates lone pair delocalization from negatively polarized oxygen to the vacant d orbitals of positively polarized silicon. The small divalent oxygen of the Si-O-Si bond can therefore easily donate or withdraw electrons to/from silicon orbitals allowing the silicone main chain oxygen atoms to assume either sp^3 or sp hybridization. The energy barrier to bond linearization has been found to be <0.8 kJ/mole.[25] As a consequence oxygen atoms are very nearly free to move from side to side in the PDMS molecule, thereby allowing PDMS to form compact coils while still maintaining a characteristically high degree of conformational randomness (high entropy of fusion). The equilibrium flexibility of the Si-O-Si bond also largely determines the low melting point (T_m = -40˚C) of PDMS.[26]

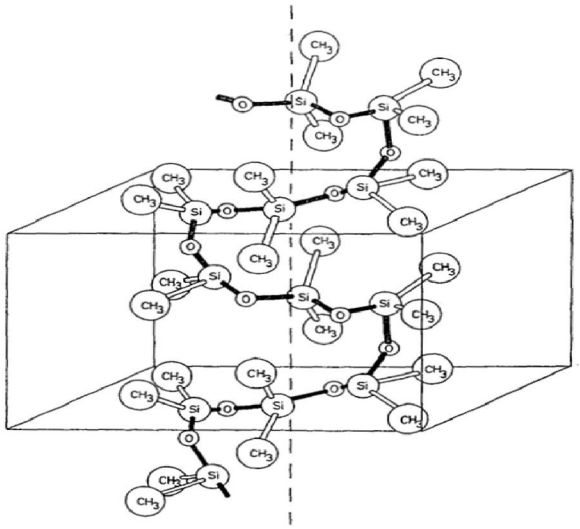

Figure 1. Three dimensional PDMS structure.
(Adapted from reference 32)

The Si-O bond is also longer (1.63 Å) than the C-O bond (1.42 Å).[28] Greater bond length and wider bond angle allow for greater spatial separation of side groups along the siloxane chain than is possible in polyethers. The resulting lack of steric hindrance accounts for a low activation energy for rotation of methyl side groups around backbone

silicon atoms (~2.5 kJ/mol). An analogous rotation of pendant methyl groups around carbon in a polyether requires >11 kJ/mol. The PDMS chain can therefore easily change its spatial arrangement by rotations around its skeletal bonds. This dynamic flexibility is reflected in the low glass transition temperature of PDMS (T_g ~ -125˚C), when compared to analogous hydrocarbon elastomers like polyisobutylene (T_g ~ -70˚C) or natural rubber (T_g ~ -72˚C). In fact, PDMS has the lowest T_g of any common polymer.[29]

The combination of nearly free side group rotation around the main chain (dynamic flexibility) and easy deformability of PDMS chain bonds (equilibrium flexibility) results in the unusual overall flexibility of the PDMS macromolecule. In solution this flexibility allows siloxane chains to readily adopt an energetically favorable coiled helical conformation that, places the maximum number of methyl groups on the macromolecular surface. The outward facing methyl groups interact only weakly with those on adjacent chains and act to shield the strongly polarized Si-O backbone bonds, thus minimizing inter-chain interactions.[30] As a result, though it has a main chain similar to the typically high surface energy silicates, PDMS exhibits the low surface energy more typical of organics. The surface free energy (or surface tension) of PDMS (γ_s) at 20˚C is ~20.4 mJ/m^2 and is comprised of a dispersive component (γ_s^d) of 19.5 mJ/m^2 and a specific component (γ_s^{sp}) of <1 mJ/m^2.[31] This low surface free energy, and the small polar (specific) component, makes PDMS strongly hydrophobic. For PDMS, the critical surface tension of wetting is also low at only 24 mJ/m^2. Thus, PDMS will not only wet most surfaces, it will also wet itself; and it forms films with good coverage and release properties.[32]

In the bulk, due to the weak interaction of PDMS chains, the space between chains is high and the flow of molecules past each other involves small frictional forces. As a result, PDMS has a lower and less temperature dependent viscosity than hydrocarbons. At room temperature the 26 kDa PDMS used in this work has an advertised viscosity of 1,000 centiStoke (0.98 Pa · s). A comparable polyether, such as polypropylene oxide, exhibits a higher viscosity at about one sixth this molecular weight.[33] The weak inter-chain interaction that causes high chain separation in PDMS

also gives it a higher free volume than hydrocarbons. This high free volume results in high compressibility. The α, ω-hydroxy$PDMS_{26k}$ used in this study has a reported free volume of ~25% and a compressibility of 7.36% at 1,000 atm.[33, 34] High free volume also accounts for the high solubility and diffusion coefficients of gases such as oxygen and nitrogen in PDMS. This polymer is even permeable to water vapor, in spite of the fact that liquid water does not wet its surface. In addition, low chain-chain interaction and a lack of conduction electrons make PDMS a good electrical insulator. Typically, PDMS oils have a volume resistivity ($10^{15}\ \Omega \cdot$ cm) and a dielectric strength (15 kV/mm) similar to those of commonly used mineral oil, while also being much more fire resistant.[35]

Thermal stability in air is one of the most useful properties of PDMS. This polymer does not undergo thermal oxidation below ~205˚C, while polyethers commonly oxidize before reaching 150˚C.[36] The high Si-O bond energy in the main chain results in a high activation energy for homeolytic cleavage. Also, the positively polarized main chain silicon atoms withdraw electron density from methyl side groups making them less susceptible to radical attack. Thus, the methyl groups of PDMS are thermally and oxidatively more stable than the methyl groups of comparable hydrocarbons. However, the large silicon atom and polar nature of the Si-O bond do make the PDMS main chain susceptible to heterolytic cleavage by nucleophilic attack. The Si-O bond will hydrolyze in the presence of strong acids and bases. The reversible condensation reactions (eqs 8 and 9) by which the molecule is formed illustrate this susceptibility. Nevertheless, under normal environmental conditions PDMS is, for the most part, chemically inert. This inertness and its hydrophobicity make PDMS highly biocompatible.

Most chemical reactions of PDMS occur at chemically functional molecular side or end groups. Of particular importance to this work is the silanol group. The same structural and ionic properties that stabilize and strengthen the backbone Si-O bonds also stabilize and strengthen the Si-O-H bonds of silanol end groups. The difference in electronegativity between Si-O ($\chi^{Si\text{-}O} = 1.54$) and O-H ($\chi^{O\text{-}H} = 1.24$) bonds is small as is the difference in their bond energies (ΔH^0 Si-O = 452 kJ/mole, ΔH^0 O-H = 467 kJ/mole). Therefore, silanol is almost as likely to act as an acid as it is to act as a base, though it is

not likely to act as either. The Si-OH acid dissociation constant is only on the order of ~10^{-7}, and the basicity of PDMS is also low, since the high affinity of Si for electrons causes the free electron pairs of silanol oxygen to have low activity.[37, 38] As a consequence, PDMS end group silanol is an equally poor proton donor and acceptor. This is exemplified by the facility with which hydroxy PDMS chain ends hydrogen bond to form an intramolecular catalyst during homofunctional polycondensation (eq 12). This facility also allows silanols to easily form intermolecular hydrogen bonds, and physical interactions between hydroxy PDMS and other hydroxy containing species are high.

Silicone Elastomer

History and Synthesis

Polydimethylsiloxane elastomer formation is one of the most common uses of linear PDMS. To this point, the discussion of the properties of PDMS has focused on the properties of linear PDMS chains. In this form, lower MW PDMS (<5 kDa) finds many uses in products as diverse as lubricants, foodstuffs and cosmetics. However, PDMS in the 5-500 kDa molecular weight range is generally employed in silicone rubber synthesis.[39] It is when this higher MW PDMS is crosslinked that PDMS finds its greatest utility.

After he first synthesized polyethylphenylsiloxane [PEPS], Hyde subjected his product to heating. The phenyl side groups of PEPS are much more resistant to oxidation than the ethyl groups. At 200˚C some of the ethyl side groups on the PEPS chains will oxidize to form oxygen bridges between adjacent chains. By this crosslinking method Hyde produced the first siloxane based polymeric solid. This resin would later be named Dow Corning 900A.[40, 41] The resin had many desirable glass-like qualities such as high temperature stability, chemical resistance and electrical resistivity. Before heating, the resin was also as easily molded as any of the then available thermosetting organic polymers. It seemed that Hyde had indeed found a plastic-glass. However, he also noted that as PEPS heat cured it went from being a viscous liquid to a weak, sticky, flexible gum to a soft resin.[42] It was the rubber-like properties of the partially cured product that Hyde and other early researchers found most intriguing.

By the late 1930's, vulcanized natural rubber had been in widespread use for close to a century. Over that time its use had continually increased as it became an essential element in the industrial production of a progressively larger range of finished products. Its use expanded dramatically in the early twentieth century as the automobile and airplane gained wide acceptance. Initially, during the First World War, Germany failed to recognize how dependent its industry and military were upon imported rubber. A supply-cutting British blockade quickly made the extent of that dependence apparent and fostered the first large scale synthetic rubber project. The output of that project, methyl rubber, was both qualitatively inferior to, and much more expensive than, natural rubber.[43] The project was curtailed at war's end, but it left a lasting impression of the new-found industrial importance of rubber. By the Second World War, rubber was considered a strategically critical material by all combatants.

Though natural rubber is a product of a tree native to the South American rain forest, a highly contagious leaf blight (also native to the South American rain forest) makes large scale plantation based cultivation of the rubber tree impossible in the western hemisphere. To survive in the New World rubber trees must grow widely and (in the industrial sense) inefficiently dispersed in the rain forest. By the late nineteenth century demand for rubber began to outstrip the supply from wild rubber trees. Though numerous attempts were made from that time through the 1940s to establish plantations in Central and South America, all were wiped-out by leaf blight. Only in Southeast Asia were the climate and lack of indigenous leaf blight found to combine to make large scale rubber cultivation possible.[44]

British interests began to establish rubber plantations in Malaysia, Indonesia and Sri Lanka in the late 1890's. During the nineteenth century almost all rubber came from South America, but since the 1920's 80 - 95% of natural rubber has come from these Southeast Asian sources.[45] The industrial indispensability and supply vulnerability of natural rubber funded not only the failed Central and South American plantations, but also fueled a vigorous scientific effort to develop useful synthetic rubbers. During the

first half of the twentieth century the governmental, industrial, and academic organizations of many nations invested great amounts of time, effort, and money in order to make large scale production of synthetic rubbers a reality. In the United States, though much basic research had taken place, little actual investment was made in industrial synthetic rubber production until 1942. At that time, Japanese aggression had cut-off U.S. access to Far East rubber prompting the U.S. government to fund a crash program to construct 51 industrial scale manufacturing plants essential to synthetic rubber production. The production of synthetic rubber (commonly called government rubber, or GR) in the U.S. went from 231 tons a year in 1941 to 70,000 tons a month in 1945 and remained a government monopoly well into the 1950's.[46] Hyde and Dow Corning had only hoped to produce a glassy plastic. Instead, they found that they had unexpectedly happened upon a new rubber at almost exactly that time when the U.S. most desperately needed synthetic rubber.

Though Hyde's polyethylphenylsiloxane [PEPS] resin was somewhat flexible, its "rubbery" properties did not begin to compare with those of natural or synthetic hydrocarbon rubbers. The Grignard synthesis gave a mixture of low molecular weight PEPS and heating these to form a resin gave a poorly controlled degree of crosslinking. When fully heat cured Dow Corning 900A exhibited only the slight elasticity common to spar varnishes. Like the phenolic and drying-oil varnishes, it would find use as a binder for fiberglass cloth based electrical insulation. Though very expensive, the new fiberglass/silicone-varnish composite was found to be oxidatively stable to higher temperatures than fiberglass/organic-varnish composites. During the war this new high temperature (180˚C upper operational limit) Class H insulation made it possible to design smaller, lighter electrical equipment, and to make the then current designs more durable.[47] The slight elasticity of this composite also made it a useful gasket material for the glass lenses of searchlights on naval vessels. These lenses often shattered when large caliber shipboard cannons fired. Organically based natural and synthetic rubbers and resins could not stand the high temperatures generated by these arc lights, while non-elastic gasket materials could not insulate the glass lenses against the shattering vibration.[48] The fiberglass/900A composite could do both.

Much of the silicone research conducted during the 1940's focused on the development of silicone elastomers in the hope of replacing natural or synthetic rubbers. At that time, the quality that scientists most often sought to reproduce was rubber's defining ability to recover from large deformations quickly and forcibly. Since organic rubber chemists had the most experience in this type of work, they were most often employed in silicone rubber research. As a result, silicone elastomer science became something of a subspecialty within the then long established field of rubber science. The lessons and terminology of the rubber industry were soon applied to silicone rubbers. Crosslinking of PDMS is not generally referred to as polymerization, but rather as the vulcanization or curing of a rubber. Mixing liquid PDMS and other reactants is not usually referred to as polymer melt processing, but instead as rubber compounding. The compounded material is not said to consist of elastomer, filler, crosslinker and catalyst, but is instead said to consist of base rubber, reinforcing agent, vulcanizing agent, and accelerator. Even in current silicone research the unusual unit phr (parts per hundred parts of rubber base) is frequently encountered. Nevertheless, the chemistry of semi-organic silicone rubber is not the organic chemistry of other rubbers. Silicone rubber chemistry owes far more of its development to general advances in polymer chemistry than it does to specific advances in rubber chemistry.

The first recognizably elastic silicone rubber did not become available until nearly the end of World War II. Earl Warrick joined the new Dow Corning company in 1943. Prior to that, he had been working in a Corning fellowship funded research group at the Mellon Institute. In the early 1940's plastics from peroxide based free radical polymerization first became available. By 1944 Warrick had adapted this technique to the controlled crosslinking of PDMS to produce the first silicone based rubber with properties approaching those of natural rubber.[49] Warrick employed benzoyl peroxide $(C_6H_5COO)_2$ to oxidize methyl groups on adjacent PDMS chains to form $SiCH_2CH_2Si$ crosslinks (eq 13).

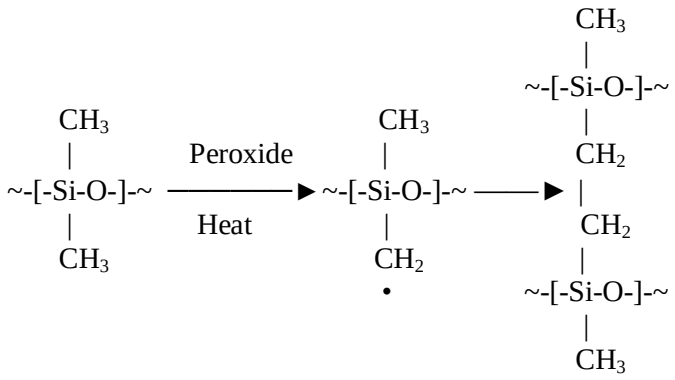

(13)

The PDMS/peroxide mixture must be heated above 100˚C to decompose the peroxide and liberate the oxygen radicals that accomplish the methyl crosslinking. This thermal crosslinking (vulcanizing) reaction is one form of a number of High Temperature Vulcanization [HTV] reactions used in silicone rubber production. Beginning late in 1944 Warrick's HTV reaction was used to create the temperature resistant silicone rubber gaskets needed to seal the superchargers required for the high altitude operation of B-29 bombers.[50] Peroxide HTV cure is still used in the production of a number of silicone elastomers.

Condensation Cure RTV

Room Temperature Vulcanization [RTV] based crosslinking of PDMS produces ~10% of all silicone rubber.[51] A commonly employed RTV cure proceeds by the polycondensation of hydroxy terminated PDMS and silicon-alkoxide in the presence of a tin catalyst. This alkoxy cure reaction has been known since the mid 1950's, and was the crosslinking reaction employed in most of the work of this study.[52] This reaction can be implemented as a two part system [RTV-2] in which one part consists of a rubber base material that must be mixed with a separate part containing a curing agent. Or, it may be implemented as a one part system [RTV-1] in which the rubber base and curing agent come premixed but do not react until removed from their sealed packaging. Condensation cure RTV-1 systems are used as general construction sealants, as formed in place gaskets, and as adhesives; while condensation cure RTV-2 systems are widely used in molding, mould making, and encapsulation. In the last decade, condensation cure RTV-2 systems have become popular for the production of microfluidic devices by soft lithography. In either one or two part systems the base rubber mixture is usually liquid to paste like in

consistency. It generally contains PDMS that has a MW between 5 and 500 kDa with a viscosity of between 100 and 20,000 cP.[53] Much of the work presented here involved an RTV-2 system that employed α,ω-hydroxyPDMS$_{26k}$ as a base rubber, polydiethoxysiloxane [ES-40] as a crosslinking agent, and dibutyltindiacetate [DBTDA] as a catalyst.

An idealized example of the alkoxy condensation cure is the reaction of hydroxy terminated PDMS with tetraethylorthosilicate [TEOS] in the presence of DBTDA catalyst. First, a small amount of water must activate the low concentration (0.05-0.5 wt %) catalyst by hydrolyzing a tin to acetate bond, thus forming a tin hydroxide and liberating volatile acetic acid (eq 14).

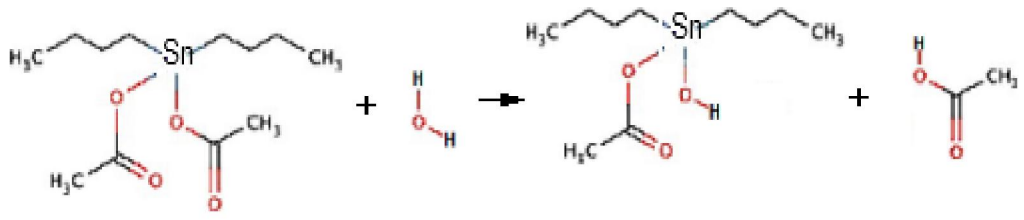

(14)

The activated catalyst then forms a Sn-O-Si complex with TEOS by hydrolyzing a silicon-alkoxy bond and eliminating a volatile ethanol (eq 15).[54, 55]

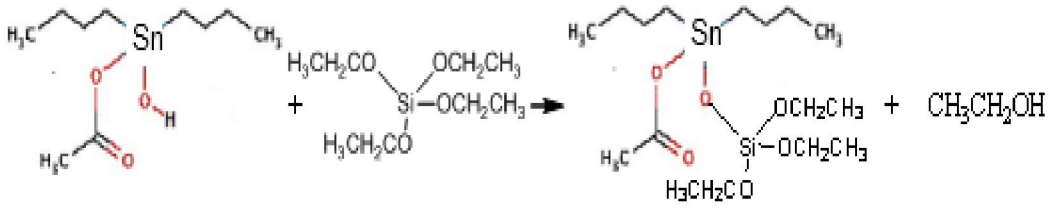

(15)

The catalyst/TEOS complex then transfers hydrolyzed TEOS to the hydroxy end group of a PDMS chain while extracting a proton from the group to regenerate the activated catalyst (eq 16).

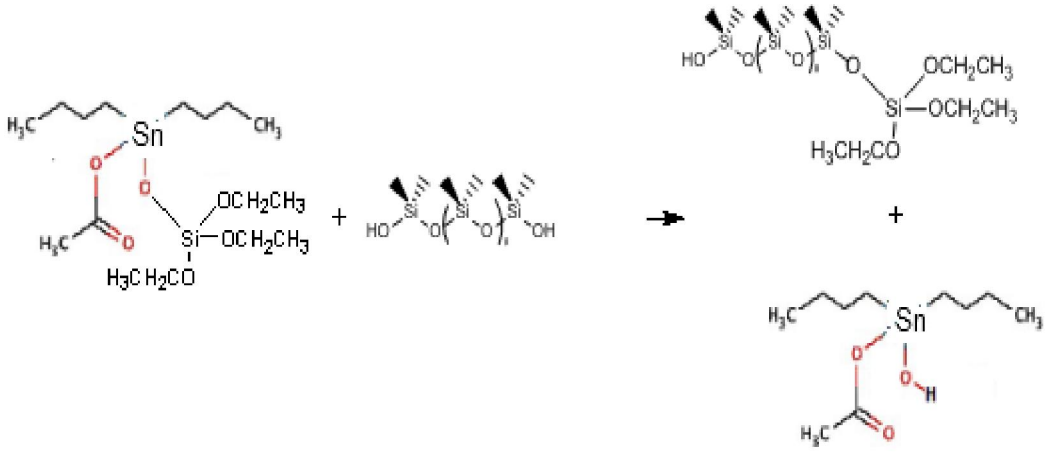

(16)

The regenerated catalyst may then complex with either unhydrolyzed TEOS or with one of the three remaining silica-ethoxy groups of the TEOS now bound to PDMS. In either case the resulting complex then reacts with the hydroxy end groups of other PDMS chains, until all of the PDMS hydroxy end groups have been consumed. In the ideal, each TEOS molecule ultimately forms siloxane bonds with four PDMS molecules and each PDMS molecule forms siloxane bonds with two TEOS molecules. The volatile acetic acid and ethanol diffuse out of the polymer leaving an idealized three dimensional network structure (Figure 2) in which flexible PDMS molecules are bound to each other by rigid O-Si-O (silica) linkages.[56]

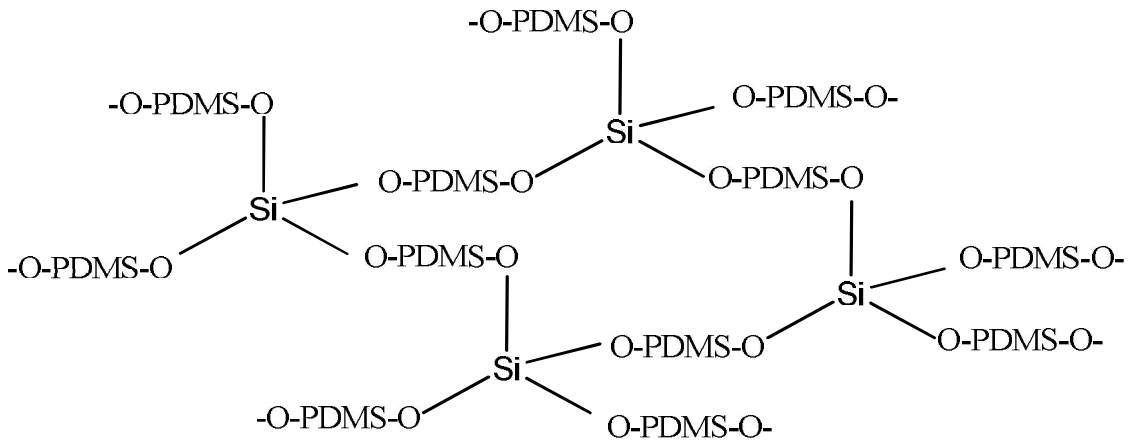

Figure 2. Idealized TEOS crosslinked PDMS rubber network.

In real applications, more TEOS is used than is needed to bind the available PDMS hydroxy groups. This is done, in part, in order to limit the possibility of any chain forming a cyclic by binding both reactive end groups to a single TEOS molecule. The molar excess of TEOS and miniscule quantity of catalyst statistically ensure that the hydroxy end groups of a given PDMS chain are most likely to encounter two different catalyst/TEOS complexes. Also, it has been shown to be progressively more difficult to successively hydrolyze each ethoxy group of a silicon-alkoxy compound like TEOS.[57] The excess of TEOS and its progressively increasing resistance to hydrolysis tends to ensure that initially each of the complexes encountered by a given hydroxy terminated PDMS molecule is most likely to contain a TEOS that has only been hydrolyzed once. Thus, early in the reaction sequence, the reaction mixture is found to predominantly contain PDMS chains that are end-capped by triethoxy groups (Figure 3).

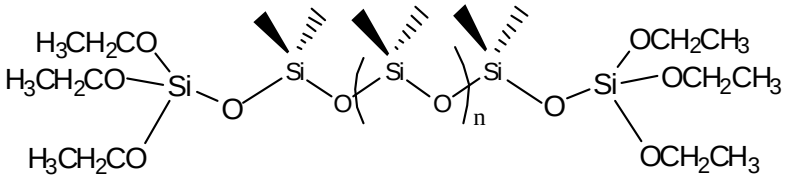

Figure 3. TEOS end-capped PDMS molecular intermediate.

In this mixture unhydrolyzed TEOS is still in high concentration, and it is also the easiest species for the catalyst to hydrolyze for both energetic and steric reasons. Thus, the activated catalyst regenerated by the formation of end capped PDMS is most likely to complex with unhydrolyzed TEOS (eq 15). However, at this point in the reaction, all of the hydroxy-PDMS has been end capped and no hydroxy groups remain to react with this newly formed DBTDA/TEOS complex, therefore the reaction stops. A number of common storable one part RTV sealants consist of just this type of liquid reaction mixture sealed in a waterproof container.

When the container is opened the mixture is exposed to atmospheric moisture and the reaction continues. Water absorbed from the air forms alkoxy-silicon-hydroxides by hydrolyzing the silicon-alkoxy bonds of TEOS in the same manner that a small amount of water had initially hydrolyzed tin-acetoxy bonds to activate the catalyst. At reaction

resumption, unhydrolyzed TEOS remains the most likely species to react with water due to the same concentration and energetic considerations that were earlier found to make unhydrolyzed TEOS most likely to complex with catalyst (eq 17).

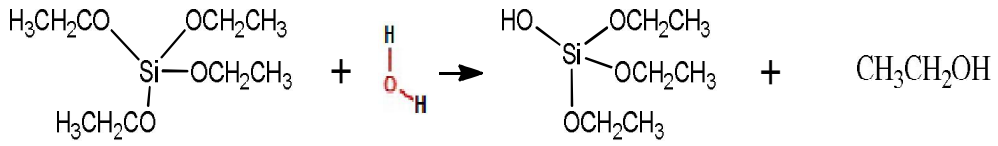

(17)

The resulting hydroxide may then react with the already present catalyst/TEOS complex to polymerize the TEOS and regenerate the activated catalyst (eq 18).

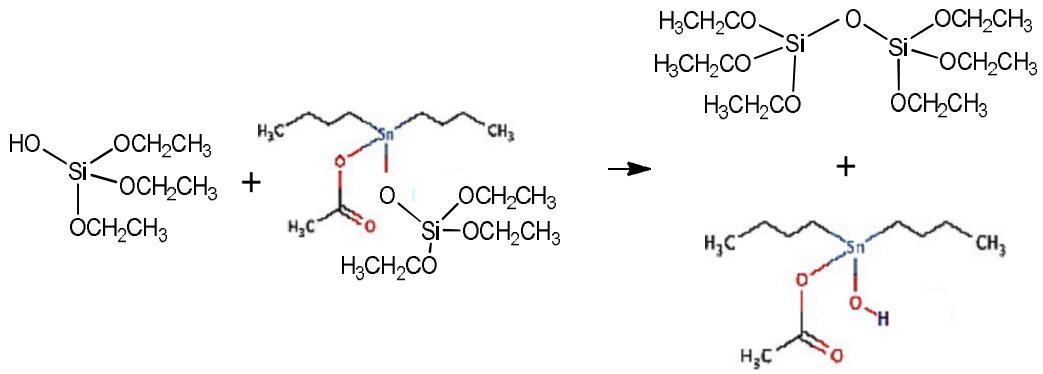

(18)

Or these hydroxylated species may polymerize TEOS by condensing with each other (eq 19).

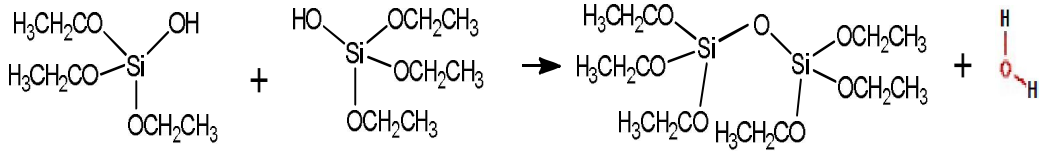

(19)

The reaction with the catalyst-TEOS complex (eq 18) is, however, the far faster reaction. The hydrolysis of TEOS by slowly diffusing absorbed water vapor (eq 17) is the rate limiting process in this type of cure. As a result, at this point in curing the hydroxylated species is seldom in high enough a concentration for the homocondensation reaction (eq 19) to occur.[58, 59]

As the reaction progresses the concentration of unhydrolyzed TEOS decreases. Activated catalyst or water then become more likely to complex with or hydroxylate an ethoxy group on the available triethoxy structures (including the triethoxy groups end-capping the PDMS molecules). The resulting products may then condense into larger silicon-oxygen linked structures containing diethoxy groups. In turn, as the concentration of the triethoxy containing compounds drops, catalyst and water become more likely to complex or hydroxylate an ethoxy group on the available diethoxy structures. Ultimately, the TEOS becomes fully hydrolyzed and condenses to form many nano-domains of amorphous silica distributed throughout the elastomer network. Under moderately acidic to basic conditions the catalyzed condensation reaction (eq 18) is favored and the silica forms dense nano-domains by nucleation. Under highly acid conditions (pH $\leq$2.5) with abundant water the hydrolysis reaction (eqs 17) is favored and more diffuse silica nano-domains form by homocondensation (eq 19).[60]

Unlike the ideal PDMS rubber structure depicted earlier (Figure 2), where a single silicon atom acted as a binding center for four PDMS molecules, the actual condensation cured polymer is much more complex. While it is possible that any two PDMS chains in the rubber might be bound to each other by one or two silicon atoms, the use of a molar excess of crosslinker makes it far more likely that they will be connected by binding centers composed of crosslinker derived silica nano-domains. In such a structure, each of the silica nano-domains acts as a binding center for a random number of polymer chains. PDMS chains that are bound to a common silica nano-domain by their near ends may be bound to either common or different silica nano-domains at their far ends. Individual chains may also form loops by having both ends bound to the same nano-domain. Finally, as the reaction proceeds, the reaction mixture becomes progressively more viscous, and the free movement of reactants becomes progressively more constrained. Thus, it may take a very long time for an alkoxy condensation RTV rubber to fully cure and unreacted/unbound species may persist in seemingly cured material.[61]

Physical and Chemical Properties

The physical properties of the resulting PDMS based polymer networks have much in common with the properties of straight chain PDMS. This is not too surprising when one considers that a typical alkoxy condensation cure silicone rubber, such as G.E. RTV 162, consists of as much as 80% by weight PDMS.[62] The thermal properties of RTV 162 (T_m ~ -43˚C, T_g ~ -125˚C) are so close to the values for the linear polymer that it appears that crosslinking alters neither the equilibrium nor the dynamic flexibility of the PDMS chains to any great degree.[63] In air RTV 162 has an indefinite service life at 204˚C and a useful lifetime of hundreds of hours at 260˚C.[64] Pyrolytic degradation of PDMS rubber does not occur below 400-450ºC. Most PDMS based silicone rubbers remain flexible and usable from - 50˚C to 250˚C. In comparison, vulcanized natural rubber becomes inflexible below - 35˚C, and softens to uselessness above 100˚C.[65] Silicone elastomers can withstand exposure to ozone and hot oils that would rapidly deteriorate a naturally based rubber. Ozone resistance is especially important in electrical applications. The electrical properties of a silicone rubber like RTV 162 (dielectric strength = 18 kV/mm and volume resistivity of $3x10^{15}$ Ω·cm) compare well with those of natural rubber (dielectric strength = 18-24 kV/mm and volume resistivity of $1x10^{15}$ Ω·cm).[66]

Figure 4 graphically compares many of the properties of silicone rubber with those of natural and some synthetic rubbers. For these common properties, silicone based rubber is about as good, and in many cases better than, natural or synthetic alternatives. For applications where extreme temperature or chemical stability is of paramount importance, silicone rubbers are often the material of choice. However, compared to natural and synthetic organic rubbers, the production of silicone rubbers is energy intensive and hence expensive. Only when the special properties of silicone elastomers are required are they employed. Currently only about 1% of world-wide rubber demand is met by silicone rubber.

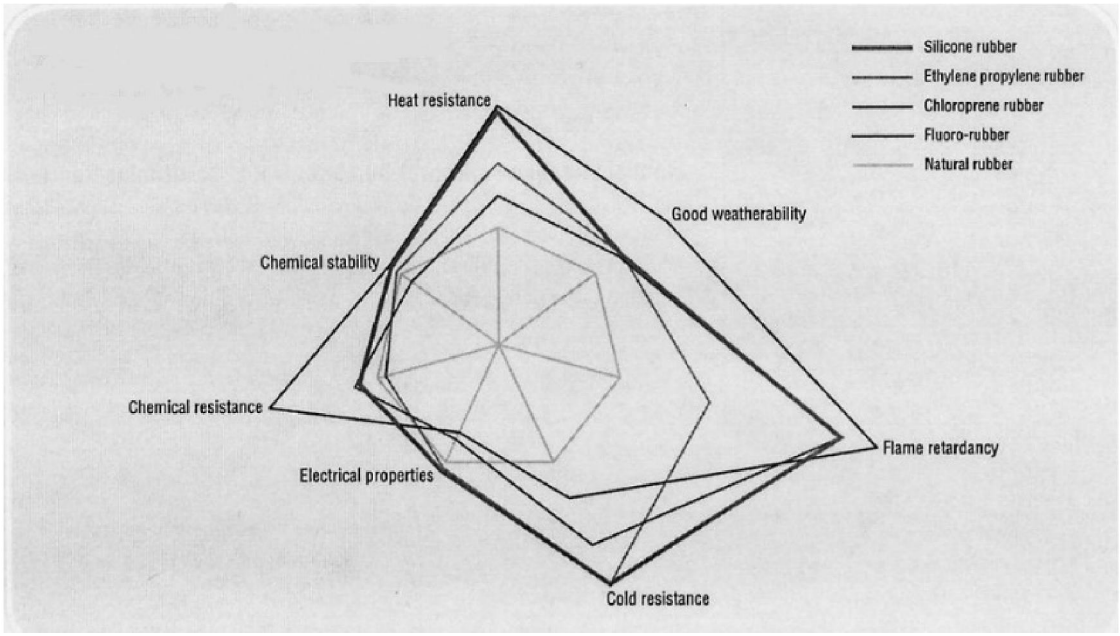

Figure 4. Comparison of useful properties of various elastomers.
(Reprinted from ref. 67. Copyright 2005 Shin-Etsu, Inc.)

Apart from high cost, silicone rubber's one other failing is a lack of mechanical strength. PDMS crosslinked in an RTV condensation cure is typically a gum like substance that exhibits a tensile strength of <0.5 MPa, a Shore durometer A hardness of ~20, and a Die B tear resistance that is so negligible as to be immeasurable by this standard method. This gum is in fact a very high viscosity liquid (~20,000 cP). It will flow if left in a tipped container for several weeks.[68] This low strength is less of a problem in an elastomer than one might expect. Unprocessed natural rubber gum is also a weak, thick, sticky fluid. Natural rubber requires sulfur crosslinking (vulcanization) to improve strength. For example, ACS#1, a specified vulcanized natural rubber formulation, exhibits a tensile strength of ~6 MPa, a Shore A hardness of 52, and a Die B tear resistance of 53 kN/m. The addition of a structural filler like carbon black will further reinforce vulcanized natural rubber. A common conveyor belt made of ACS#1 reinforced by carbon black has three times the tensile strength, 20% greater hardness, and over twice the tear resistance of ACS#1 alone.[69] While crosslinking alone provides little strengthening, silicone rubber can also be reinforced with filler. Addition of a structural filler to condensation cured PDMS gum increases tensile strength to 6 MPa, Shore

hardness to 23, and tear resistance to 0.25 kN/m making it almost as strong as unfilled vulcanized ACS#1.[70]

Fumed Silica

History and Synthesis

By the mid nineteenth century rubber manufacturers were aware that adding fillers, such as ground charcoal, to uncured natural rubber would improve mechanical properties (stiffness, hardness, wear resistance, etc.) of the cured product.[71] Thus it is not surprising that, when weak elastomers based on PDMS were first produced in the early 1940's, rubber scientists would attempt to employ organic rubber fillers to improve mechanical properties. Carbon black, an excellent structural reinforcing filler for natural and synthetic organic rubbers, was found to give little reinforcement to silicon rubbers. Various ground minerals, such as calcium carbonate, calcium silicate, and the finely ground quartz used in Dow Corning Compound #4, were also tested with somewhat better results. Not until after the war, however, would the best reinforcing filler for silicon rubbers become widely available.

In the 1930's the German firm Degussa (now part of Evonik Industries) developed the "German Channel Black" process for the production of carbon black. For many years it was recognized that carbon black provided the best mechanical reinforcement to natural and synthetic organic rubber products, such as tires. The then standard carbon black production method, the "Channel Black" process, burned natural gas, but at that time little natural gas was available in Germany. Oil was in somewhat better supply, and as a result Degussa developed a process that burned vaporized oil. In addition to using a more readily available raw material, the Degussa process was also found to produce a better quality (smaller particle) carbon black in higher quantities than could be realized by the standard Channel Black process.[72]

With the outbreak of the Second World War, a British blockade once again curtailed German imports of natural rubber and most imports of oil. Though a small amount of oil was available from Romanian fields, much of Germany's wartime fuel oil

came from a synthetic fuels program based on the hydrogenation of coal. This program also supplied the starting materials for Germany's wartime production of synthetic rubber (BUNA). However, the synthetic fuel oil did not prove to be a good feedstock for Degussa's German Channel Black process. In addition, usable BUNA rubber required even more carbon black reinforcement than natural rubber. In order to avoid burning scarce oil to manufacture filler, Degussa began to investigate the possibility of using other compounds as rubber reinforcing fillers.

Fumed Silica Nanoparticles [FSN] were first synthesized by the German chemist Harry Kloepfer at Degussa AG in 1941. Kloepfer had lead the Degussa team that developed the German Channel Black process, and while working on that project he had conceived the idea of producing a "white filler" by the high temperature flame hydrolysis of silicon tetrachloride (eqs 20 a-c).[73]

$$2H_2 + O_2 + SiCl_4 \xrightarrow{>1000^\circ C} SiO_2 + 4HCl \qquad (20a)$$

$$2H_2 + O_2 \longrightarrow 2H_2O \qquad (20b)$$

$$SiCl_4 + 2H_2O \longrightarrow SiO_2 + 4HCl \qquad (20c)$$

In this process vaporized silicon tetrachloride is entrained by dry air or oxygen and fed to a hydrogen fired burner (eq 20a). In the high temperature (1,000-2,000˚C) flame of the burner water vapor from combustion (eq 20b) reacts in the gas phase to hydrolyze silicon tetrachloride to silicon dioxide (eq 20c). This silicon dioxide vapor rapidly combines to form angstrom-scale silica nucleation particles. While still at a high enough temperature to fully sinter, these nucleation particles grow by coagulating with other nucleation particles and/or silicon dioxide vapor to form spherical amorphous silica primary particles 5 - 50 nm in diameter. During the late stages of primary particle growth some Si-O moieties at the surface of these primary particles fail to completely condense with other Si-O structures in the particle leaving incompletely bound oxygen at the silica

surface. In order to fulfill valence the incompletely bound oxygen abstracts a proton from surrounding water vapor, thus forming some silanol on the primary particle surface.[74]

As the primary particles move to regions where the burner flame is below the melting point of amorphous fumed silica (~1,300ºC) colliding primary particles fuse (coagulate with only partial sintering) into three dimensional branching "string of pearl-like" aggregates of a few tens to a few hundred nanometers in size.[75] As these aggregates cool further the silanols on their surfaces weakly hydrogen bond them together into even larger agglomerates of aggregates. These agglomerates vary in size from about a micron to a few hundred microns in size.[76] The scale of fumed silica structure (nucleation particle, primary particle, aggregate, and agglomerate) varies over six decades of magnitude. However, the coalescence and aggregation processes are normally so complete that one rarely, if ever, sees the smallest (nucleation or primary) particles individually; and the tendency for aggregates to hydrogen bond is so great that fully unagglomerated aggregate structures are only observed under special circumstances. The gas phase pyrogenic chemical reaction takes place in about a hundredth of a second, and the entire reaction, from the silicon tetrachloride feed to the agglomerated fumed silica product, occurs in about one tenth of a second.[77] By slightly varying the reactor dwell time, temperature, or reactant concentration; both the size and size distribution of primary particles and aggregates can be, within limits, well controlled. The gaseous HCl is easily removed from the production stream leaving a very pure amorphous silica product (Figure 5).

Physical and Chemical Properties

To the eye, fumed silica appears as a fine white powder with a slight bluish tinge. Though the primary particles that comprise the powder have the structural density of silica, (ρ_{pp}) = 2.2 g/cm^3, the particle density of the agglomerated powder (ρ_{aggl}) is much lower at ~0.05 g/cm^3. The powder packs loosely and contains >97% air by volume.[78] Fumed silica contains so much air that Kloepfer thought of it as airborne silica and coined the name Aerosil® to describe it. Degussa has been offering it under that trade name since 1943. A number of other firms including Cabot, Wacker, Shin-Etsu, Dow

Corning, and Momentive Performance (G.E.) also produce pyrogenic silica commercially. In 2001 worldwide demand for fumed silica was 200,000 tons and ~60% of that demand was from silicone rubber production.[79]

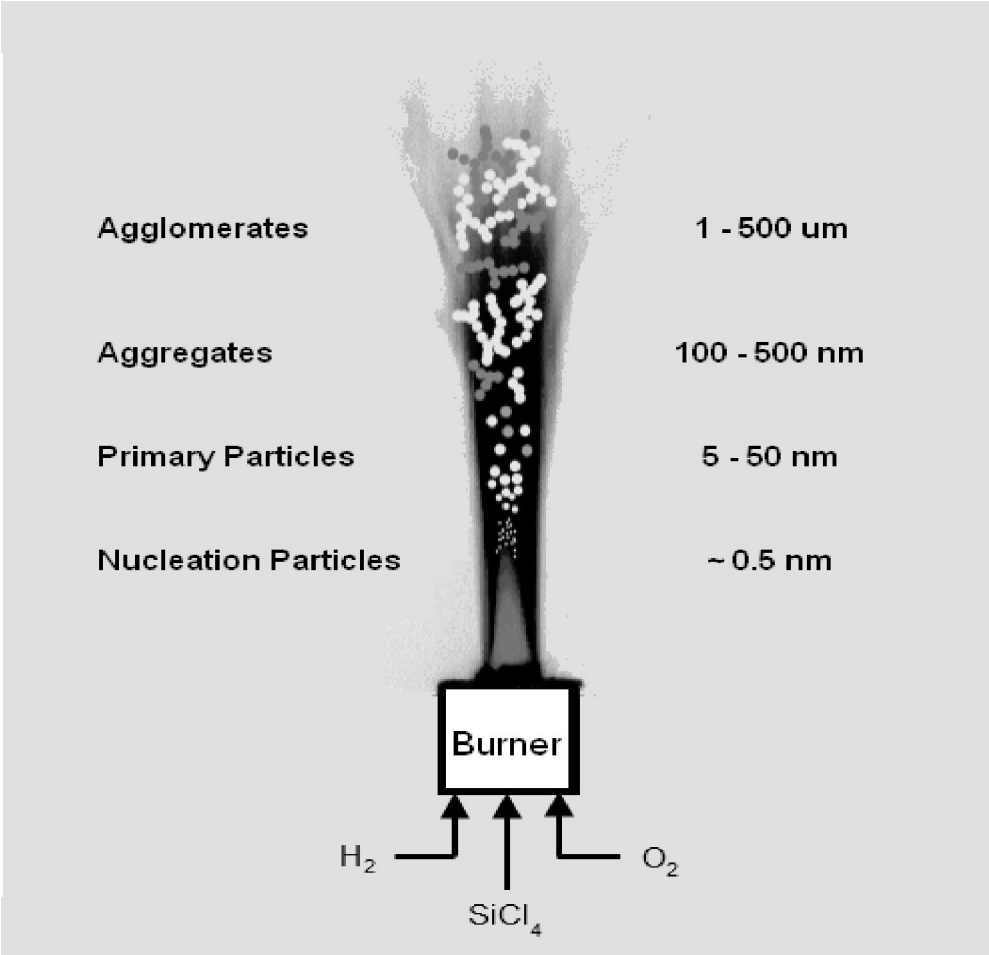

Figure 5. Fumed silica, pyrolytic formation and levels of structure.

The small primary particle size of fumed silica aggregates gives them remarkably high specific surface areas. Evonik Degussa offers Aerosil® with primary particle diameters that range from 50 to 5 nm and corresponding surface areas that range from 90 to 380 m^2/g. As might be expected, the BET (Brunauer-Emmit-Teller) specific surface area of fumed silica increases as the primary particle diameter decreases; but, somewhat unexpectedly, as the specific surface area increases the primary particle size distribution also decreases. The current study employed Aerosil® 300 that has a surface area of 300

±30 m^2/g, and is composed of primary particles 7 ±1 nm in diameter (d_{pp}).[80] An ideal spherical 7 nm diameter primary particle has a surface area of 154 nm^2, a volume of 180 nm^3, and a mass of 3.95 X 10^{-19} g. Such an ideal primary particle is comprised of roughly 4,000 silicon dioxide molecules. If unaggregated, a powder made up of these ideal primary particles would have a specific surface area of 390 m^2/g. The spherical distortion and overlap of fusing primary particles that is required to form the linear branching fumed silica aggregates of Aerosil® 300 reduces the surface area by ~23%.

The low density of fumed silica arises from the fractal nature of these aggregates. In non-fractal structures the mass of a particle varies in proportion to its size raised to the third power (i.e., mass varies with volume). Analogously, in fractal structures the mass of a particle varies in proportion to its characteristic size raised to the power of its mass fractal dimension (D_f). D_f is always less than three and therefore serves as a measure of how well a fractal object fills a spherical volume defined by the object's characteristic size. Thus, it represents a fractal object's non-integer, fractional dimensionality. A long thin object would have a characteristic size equal to its length and a D_f approaching 1, since the object occupies only a small fraction of the 3-dimensional spherical space defined by the object's length. On the other hand, a solid sphere of the same characteristic size would have a D_f of 3, because it occupies all of the same 3-dimensioal space. Mass fractal dimensions above or below 2 describe more closed or open structures respectively.[81] By SEM and TEM Aerosil® 300 aggregates have been found to be between 20 and 200 nm in characteristic size (d_{aggr}). By x-ray and neutron scattering these aggregates have been found to have a D_f of ~1.86.[82] These highly fractal aggregates are incapable of fitting closely together. Instead, by hydrogen bonding where they come in contact, aggregates combine into coarse scaffold-like agglomerate structures that span and loosely enclose air filled voids. These agglomerates are typically one to several hundred microns in size (d_{aggl}), but are weak enough that larger agglomerates can be broken apart by finger pressure. An exact analytical description for fumed silica agglomerates is difficult due to their dynamic instability and wide variation in size and structure. However, the mass fractal dimension of these agglomerates can be estimated

from the ratios of the average agglomerate and primary particle sizes and densities (eq 21).[83]

$$\frac{\rho_{aggl}}{\rho_{pp}} = \left(\frac{d_{aggl}}{d_{pp}}\right)^{D_f - 3} \tag{21}$$

For Aerosil® 300 agglomerates, using the values given above, and assuming an average agglomerate diameter of 100 µm, eq 21 gives a mass fractal dimension of ~2.61. Thus, while Aerosil® 300 is highly fractal at the aggregate level (D_f ~1.86), it is only slightly fractal at the agglomerate level.

As with its agglomerates, Aerosil® 300 aggregates also defy exact description. The three dimensional randomly branched linear aggregate structures are too variable. However, knowledge of the primary particle makeup and approximate aggregate structure does make an average description possible. Assuming the maximum dimension (d_m) of an average Aerosil® 300 aggregate is 100 nm, and knowing that the radius of gyration (R_g) of fumed silica aggregates has been found to be $R_g \sim 0.69(d_m/2)$.[84] Then the R_g for an average Aerosil® 300 aggregate is ~34.5 nm. Fractal mathematics gives an expression (eq 22) for the number of primary particles (N_{pp}) in such a fractal aggregate.[85]

$$N_{pp} = k\left(R_g / r_{pp}\right)^{D_f} \tag{22}$$

In Aerosil® 300 the radius of a primary particle ($r_{pp} = d_{pp}/2$) is ~3.5 nm. The geometric lacunarity factor, k, has a value of ~1.65 for fumed silica aggregates, and D_f is the mass fractal dimension of 1.86 noted above. Using these values the number of primary particles (N_{pp}) in the average Aerosil® 300 aggregate is ~116. Being composed of 116, spherical, 7 nm diameter primary particles this average aggregate should have a surface area (reduced by 23% to account for distortion due to aggregation) of ~13,756 nm^2, a volume of 20,880 nm^3, and a mass of ~ 4.59 X 10^{-17} g. Each of these primary particles

makes approximately 2.2 sintering contacts with other particles to form linear branching aggregates.

At a scale of 1 to 10 nm the surface of fumed silica is smooth and non-porous.[86, 87] The fumed silica surface is composed of siloxane (Si-O-Si) and silanol (Si-OH). The silanols may take a number of forms. If a silanol is widely separated (>3Å) from other silanols on the silica surface, then it is termed a "free" silanol. If two silanols are adjacent (<3Å) and are capable of sharing a hydrogen by hydrogen bonding, then they are referred to as "vicinal" silanols Lastly, if two hydroxy groups are bound to the same silicon atom then this is termed a "geminal" silanol (Figure 6).[88] By reaction with lithium alanate and other methods fumed silica has been determined to have between 2 and 3 silanol groups per square nanometer of surface. Aerosil® 300 has an advertised silanol group density of

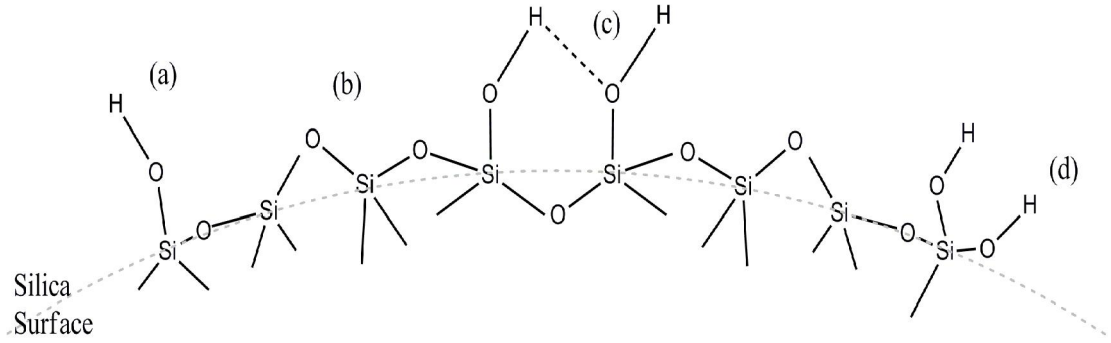

Figure 6. Fumed Silica, molecular surface structures (a) free silanol (b) siloxane (c) vicinal silanol showing H bonding (d) geminal silanol

2.2 SiOH/nm^2.[89] Of these silanols IR studies at elevated temperature have shown that ~18% are hydrogen bridged vicinal silanols, and the rest are mostly free. The geminal type is rare.[90] The average Aerosil® 300 aggregate described above with a surface area of 13,756 nm^2 can therefore be calculated to have ~30,263 silanols on its surface, of which ~24,816 are free silanols.

The large number of free silanols per aggregate and the ease with which they hydrogen bond is the source of the fumed silica agglomerate structure. Of the nearly 25,000 free silanols present on the average aggregate, IR examination before and after selective conversion with hexamethyl disilazane revealed that ~27% become involved in

interaggregate hydrogen bonding.[91] The average Aerosil® 300 aggregate is therefore agglomerated with other aggregates by the hydrogen bonding of ~6,700 silanols on its surface to silanols on the surface of other aggregates (Figure 7). The average energy of each of these hydrogen bonds has been found to be ~11.7 kJ/(mole silanol).[92] It follows that the 6,700 agglomerating silanols on an average Aerosil® 300 aggregate hydrogen bond the aggregate to agglomerate with an energy of ~1.3 X 10^{-16} Joules.

This large number of easily hydrogen bonded surface silanols also makes fumed silica strongly hydrophilic. At 23˚C surface free energies (γ_s) as high as 77 mJ/m^2 have been reported for fumed silica. Thus, at 23˚C fumed silica has a surface free energy that is only slightly higher than that of water (73 mJ/m^2).[93] Similar surface energies allow individual and pairs of free silanols, as well as vicinal silanols, to hydrogen bond water molecules to the silica surface (Figure 8). This physically bound water is termed free

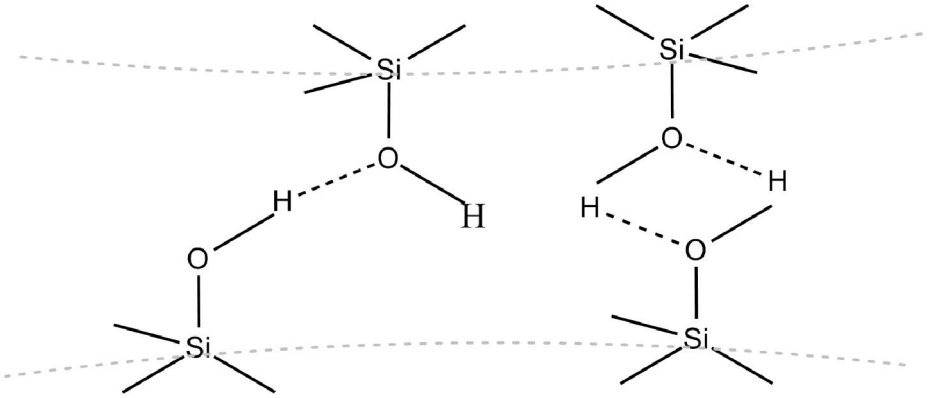

Figure 7. Fumed Silica, interaggregate hydrogen bonding (agglomeration).

water, since it may be relatively easily removed from the silica surface by moderate (<250˚C) heating. From the factory Aerosil® 300 is advertised as having a free water content of <1.5 wt%. Therefore, an ideal average Aerosil® 300 aggregate with the calculated mass of 4.59 X 10^{-17} g (p 31) should have a maximum of 6.89 X 10^{-19} g of water adsorbed on its surface. Dividing this value by the molecular weight of water and multiplying by Avogadro's number reveals that on delivery the average Aerosil® 300 aggregate has ~25,900 water molecules bound to its surface. Interestingly, from the calculations above for agglomerated powder the average Aerosil® 300 aggregate surface

should display roughly 24,500 silanols (free and vicinal) that are not already occupied by interaggregate hydrogen bonding (agglomeration). Thus it appears that, as supplied, all of the available surface silanols of Aerosil® 300 could be hydrogen bound to water.

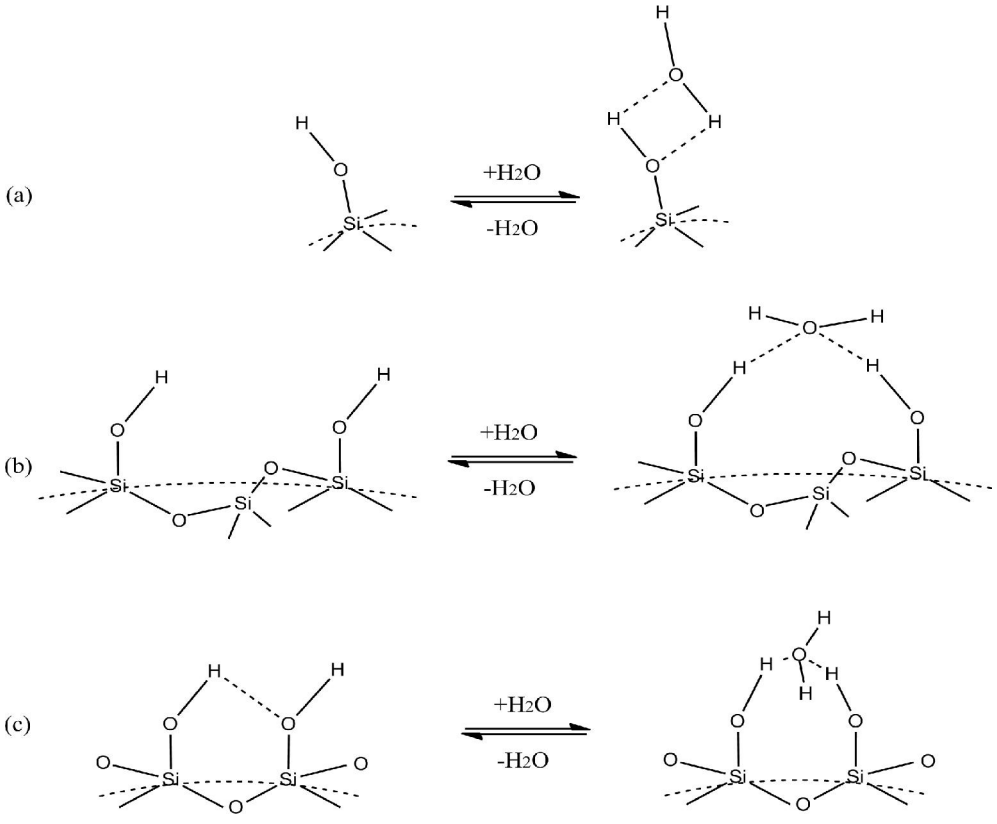

Figure 8. Fumed Silica, surface bound water configurations:
(a) free silanol (b) multiple free silanol,
(c) vicinal silanol.

Compounding

Compounding Fumed Silica with PDMS to create a reinforced elastomer is reported in the literature as early as 1947, though the first patent application mentioning such a mixture was not made until mid 1949.[94, 95] The techniques used in FSN/PDMS mixing grew out of those developed for compounding organic rubbers. Much as the most finely divided and evenly distributed forms of carbon black were found to provide the best mechanical reinforcement of organic rubbers, the most finely divided and evenly distributed forms of silica were found to provide the best mechanical reinforcement of

silicone rubbers. However, it quickly became apparent that, while compounding mixtures of fine carbon black and natural rubber is not easy, it is even more difficult to mechanically mix FSN and PDMS.

Industrially, for silicone rubber production, such compounding typically involves combining 8 – 30 wt% FSN with PDMS. This is most often accomplished by the slow addition of a portion of the desired quantity of FSN to PDMS in a fast cycle Banbury mixer, dough mixer, or extruder. The mixture is then transferred to a stainless steel two roll mixing mill where the remaining FSN is added even more slowly and the melt is mixed for long periods. Judging the exact milling times for any given compound is considered a fine art, but for batch work 5-15 minutes of fast cycle mixing during the addition of a quarter of the desired amount of filler followed by 15-45 minutes of addition of the remaining FSN during a further 30-90 minutes of high shear roller mixing are not uncommon.[96] Degussa warns in their literature that the low shear rate (γ = tip speed/wall gap) dispersion of propellers or stirring blades (common tip speeds = 1.5 – 6 m/s at a tip to wall gap 0.06 m, γ = 25 – 100 /s) provides far too little shear for fumed silica compounding. Degussa even considers the high shear rate dispersion (γ =300-400 /s) of saw tooth dissolvers to be only minimally adequate for mixing low surface area Aerosil® solutions. For high surface area fumed silica, such as the Aerosil® 300 employed in this study, Degussa suggests equipment that can generate very high shear rates (γ >2000 /s) such as high intensity mills, sand mills, media mills, and the aforementioned roller mills.[97]

Compounding FSN and PDMS is an expensive and time consuming operation. It can be modeled as a combination of several processes.

- Incorporation
- Adsorption
- Dispersion
- Distribution

Incorporation

Incorporation involves surrounding the powdered filler with polymer. This is accomplished by applying shear forces both to fold the PDMS matrix around the FSN agglomerates, and to force the polymer into the air filled agglomerate voids. Industrially this is referred to as wetting-in. The ease with which a polymer will wet a filler decreases in proportion to the difference in their solubility parameters. PDMS and Fumed Silica have Hildebrand Solubility Parameters of 7-7.5 and 14-18 $(cal/cm^3)^{½}$ respectively, and are therefore quite difficult to blend.

Incorporation is also difficult because the addition of filler increases mixture viscosity. This phenomenon was first addressed by Einstein in his hydrodynamic analysis of 1906 (eq 23).[98] He postulated that dilute solutions ($solute \rightarrow 0$) of ideal, uniform, wettable, non-interacting spheres have a higher intrinsic viscosity (η) than that of the pure liquid (η_o) by an amount proportional to the volume fraction (φ) of the mixture occupied by the spheres.

$$\eta = \eta_o (1 + 2.5\varphi) \tag{23}$$

While working to describe viscosity in carbon black filled rubber compounds in the late 1930's, Guth and Gold virally expanded this expression to accommodate higher filler concentrations and to compensate for some filler-polymer interactions (eq 24).[99]

$$\eta = \eta_o (1 + 2.5\varphi + 14.1\varphi^2) \tag{24}$$

This equation provides a good model for the viscosity of Newtonian fluids containing particles of micron scale and above in the dilute solution regime (φ = 0 – 10 vol %), but at higher filler concentrations, or for non-spherical particles, or for particle smaller than a micron, or particles that interact strongly with solvent or other particles it consistently underestimates viscosity.[100]

Neither the Einstein nor the Guth-Gold model takes into account the large surface area of nanoparticles or the filler-polymer and filler-filler interactions that this area

engenders. In the late 1950's Krieger and Dougherty sought to address these limitations by introducing an effective filler volume fraction term (φ_{eff} = filler vol. / (filler vol. + initial PDMS vol. – Penetrated PDMS vol.)) to compensate for polymer-filler interactions, and a maximum filler volume fraction term (φ_m) to account for the percolation based filler- filler effect of solution solidification at high volume loadings (eq 25).[101]

$$\eta = \eta_0 K \left(1 - \frac{\varphi_{eff}}{\varphi_m}\right)^{-2.5\varphi_m} \tag{25}$$

K is related to the Guth-Gold viral expansion (eq 24) of the pure liquid viscosity (η_o) and has a value of between 0.88 and 1, and φ_m is generally the maximum volumetric random close packing fraction for spheres, $\varphi_{rcp} = 0.64$.

By percolation theory at solid volume fractions above φ_{rcp} a solution ceases to be a liquid and its viscosity must be modeled as a non-Newtonian function of shear rate.[102, 103] Until PDMS has penetrated into the FSN agglomerates the agglomerates maintain a powder density of 0.05 g/cm^3, or equivalently a specific volume of 20 cm^3/g. Thus a 14 wt% solution of newly introduced Aerosil® 300 in α, ω-hydroxyPDMS$_{26k}$ has an effective volume fraction φ_{eff} = (0.14(20 cm^3/g)/ (0.14(20 cm^3/g) + 0.86(1.02 cm^3/g))) = 0.77, and since this exceeds φ_m the mixture is a solid. Even if only half of this mass of FSN is added (a 7 wt% solution) the initial φ_{eff} = 0.61 is only slightly below φ_m and eq 25 predicts that the solution will have a viscosity similar to that of cold lard (~125 Pa· s).

For full incorporation (wetting) PDMS must penetrate the dry silica agglomerates. At full penetration the effective volume of the agglomerates should be reduced to the actual volume of the solid silica aggregates of which the agglomerates are composed. Pure amorphous silica has a specific volume of 0.45 cm^3/g. Therefore, a 14 wt% solution of fully wetted silica in PDMS should have a φ_{eff} = (0.14(0.45 cm^3/g)/ (0.14(0.45 cm^3/g) + 0.86(1.02 cm^3/g))) = 0.068 and by eq 25 a viscosity ~20% greater than that of the pure

polymer. In the mid 90's Bohin, et al., proposed a model for the capillary driven penetration of PDMS into spherical silica agglomerates against viscous resistance.[104] By this model, without mixing, full wetting of Aerosil® 300 by α, ω-hydroxyPDMS$_{26k}$ should require <3 hours. Other authors believe this model greatly underestimates the time required, and give wetting periods for this type of mixture of from one to two weeks.[105, 106]

Adsorption

Adsorption of PDMS on fumed silica nanoparticles has received a great deal of attention in the last several decades. Central to the understanding of this process is the concept of "Bound Rubber" borrowed from traditional organic rubber compounding. In mixes of un-crosslinked elastomer base and filler at room temperature (RT), bound rubber (BR) is defined as that elastomer that can not be extracted from the mixture by a good elastomer solvent. It is generally expressed as a percent ratio of the masses of attached rubber and filler, or as a bound rubber mass per mass of filler, rather than as a weight percent. A sample containing equal masses of bound rubber and binding filler is usually said to contain a gram of bound rubber per gram of filler (1 g/g), or to be composed of 100 phr (100 parts filler per hundred parts of rubber base), rather than as being 50 wt% bound rubber. In a compound of FSN in PDMS melt, bound rubber is the PDMS that remains attached to the fumed silica when a good solvent ceases to be capable of extracting any further PDMS.

The nature of the polymer-filler interaction that results in the binding of PDMS to fumed silica in the polymer melt is of particular importance, since this interaction has long been believed to also be responsible for much of the mechanical reinforcement provided by FSN to cured PDMS elastomers.[107] Initially, due to the strong degree to which the room temperature addition of even small quantities of fumed silica mechanically reinforces a silicone melt, it was believed that covalent bonding between filler and PDMS might be occurring.[108] The elimination of FSN silanols had been shown to eliminate the formation of BR, so this was deemed the binding group on silica. It was conceivable that hydroxy terminated PDMS might covalently bond to fumed silica by the

condensation of end groups and surface silanols. However, such condensation reactions were not observed to occur below 150ºC, while PDMS bound rubber was known to form at RT.[109] Furthermore, there was no obvious analogous reaction by which trimethyl terminated PDMS might also covalently bond to FSN. Yet, trimethyl terminated PDMS could easily be shown to form BR with fumed silica. Nor, were any alterations in the IR spectra indicative of covalent bond formation ever observed for mixtures of FSN and PDMS.[110] In addition, while no good solvent alone would extract bound rubber from these mixtures; it was found that toluene under an ammonia atmosphere could remove intact bound PDMS. Further, it was also found that, independent of reaction temperature, a dilute solution of trimethylchlorosilane could also fully desorb unaltered bound PDMS from FSN.[111, 112] Over time this accumulated evidence, and the lack of any evidence to the contrary, has lead to the abandonment of any theory that PDMS chains become covalently bound to the silica surface during BR formation.

While the hydrogen bonding of PDMS to fumed silica had initially been considered to be of only minor importance, by the 1980's it was widely accepted that this physical adsorption process caused the formation of BR in these mixtures.[113, 114] Transverse magnetic proton relaxation responses under NMR indicated that some parts of the adsorbed polymer chains were solidly bound to the filler while other parts retained the liquid response of the bulk polymer.[115] From the ratio of solid to liquid relaxation response and the nature of linear polymers it was concluded that PDMS chains bonded to silica intermittently along their length leaving intervening randomly sized loops and tails exposed to the free bulk polymer. It was postulated that hydrogen bonding occurred between silanol hydrogen on the fumed silica surface and PDMS main chain oxygen atoms.[116, 117] This model has also been found to be consistent with later Small Angle X-ray and Shallow Angle Neutron studies of the FSN/ trimethyl terminated PDMS interface and it currently remains the most widely accepted description.[118]

Within the last decade, however, doubt has been cast on the nature of the bond between PDMS and silica. In 2002, from a computerized semi-empirical Quantum Chemical interpretation of data from Inelastic Neutron Scattering and Diffuse

Reflectance Fourier Transform Infrared experiments conducted on FSN/PDMS mixtures, Barthel and Nikitina concluded that only weak hydrogen bonding occurred during PDMS adsorption on fumed silica. They further concluded that the main contribution to adsorption came from the interaction of permanent and induced Si-O dipoles on the silica surface, in the silica core, and on the PDMS siloxane backbone.[119] In contrast the following year, from a comparison of Molecular Dynamics simulations and Wide Angle X-ray Scattering data, Tsige et al. concluded that the only possible interaction during adsorption is between PDMS end groups (hydroxy or methyl) and FSN silanols.[120] Most recently, using a Quantum Chemistry based Molecular Dynamics simulation that correctly predicted the results of Quasi-Elastic Neutron Scattering experiments, Smith et al. concluded that the FSN/PDMS interaction is due solely to Van der Waals dispersion forces with no contribution from hydrogen bonding.[121] Currently, resolution of the nature of the interaction by which bound rubber forms in FSN/PDMS mixtures awaits further advancements in instrumentation and modeling.

Starting in the late 1980's Cohen-Addad et al. began measuring the bound rubber masses remaining in a series of solvent extracted mixtures of FSN and PDMS. These mixtures were of increasing age and contained either hydroxy or trimethyl terminated PDMS with any one of several different molecular weights, along with FSN with any one of several different specific areas and concentrations. After extensive solvent extraction, BR content was established by elemental analysis, and was found to correlate well to variations in the proton relaxation function of PDMS obtained by NMR of the same samples.[122] Experimentally, it was found that the equilibrium value for the maximum (saturation) quantity of bound rubber per unit mass of fumed silica , Q_r^l, in a given mixture was proportional to the square root of the molecular weight, M_p of the bound polymer (eq 26).

$$Q_r^l = \beta_m M_p^{0.5} \tag{26}$$

The proportionality constant, β_m, (eq 27) was found to depend on: the number of available silanols per gram of fumed silica (specific surface area (A_T) of fumed silica

divided by the area occupied by each silanol on that surface (σ_e)), the average molecular weight of a chain monomer (M_m = 74 g/mol for PDMS), Avogadro's number (Â), and factors to account for chain stiffness (ε) and polymer bridging of particles (μ_a).

$$\beta_m = (A_T(M_m)^{0.5}) / (\hat{A}\varepsilon(1+\mu_a)\sigma_e) \tag{27}$$

The dependence on the square root of polymer MW (eq 26) makes sense if it is assumed that in the adsorbed polymer (as in the bulk polymer) the chains obey a Gaussian distribution in which any chain containing N skeletal bonds is on average swollen by $N^{0.5}$ other chains. Where the adsorption points on a chain can be represented by the random flight of a particle that collides with a plane, then the probability function for the chain's r_c^{th} return to the plane occurring at the N_b^{th} bond can be mathematically modeled by eq 28.

$$\nu_c\left(r_c, N_b\right) \propto \frac{r_c}{N_b - r_c} \frac{\left(N_b - r_c\right)!}{r\left(N_b/2\right)!\left(\left(N_b - 2r_c\right)/2\right)!} \frac{1}{2^{N_b - r_c}} \tag{28}$$

Because of the large numbers involved, eq 28 can be presented in a more convenient form by eq 29.

$$\nu_c\left(r_c, N_b\right) \propto r_c\left(N_b - r_c\right)^{-3/2} e^{-\left(r_c^2/2\left(N_b - r_c\right)\right)} \tag{29}$$

For an assumed Gaussian chain distribution, the maximum value of this expression will be ‹r_c› the mean number of contact points that the Gaussian chain can make with a plane.[123] When eq 29 is solved for its maximum value it is found that the mean number of contact points is equal to the square root of the total number of skeletal bonds found in the chain (eq 30).

$$\nu_c(r_c, N_b)_{max} = \langle r_c \rangle = N_b^{0.5} \tag{30}$$

In an average calculated over all contacts and skeletal bonds, the number of FSN/PDMS bonds per chain (μ_c) is therefore (eq 31)

$$\mu_c = \varepsilon N^{0.5} \tag{31}$$

The term ε is introduced to account for chain to silica bonds that are unable to form due to geometrical restrictions imposed by chain stiffness (for the highly flexible PDMS molecule it has a value close to one), and $N = 2N_b$ reflects the fact that that two chain bonds are associated with each PDMS monomer unit. The average silica surface area occupied by a chain (σ_c) is then simply a product of the number of silica/siloxane bonds per chain (μ_c) and the average silica surface area occupied by an individual silanol (σ_e). Here, since there can only be one bond per monomer unit, N can also be expressed as a ratio of polymer (M_p) and monomer (M_m) molecular weights (eq 32).

$$\sigma_c = \mu_c\sigma_e = \varepsilon N^{0.5}\sigma_e = \varepsilon\sigma_e(M_p/M_m)^{0.5} = \varepsilon\sigma_e(M_p)^{0.5}/(M_m)^{0.5} \tag{32}$$

The number of chains bound to a specific amount of fumed silica is then the specific silica surface area divided by the surface area occupied by a single chain (eq 33).

$$A_T/\sigma_c = A_T(1/(\varepsilon\sigma_e(M_p)^{0.5}/(M_m)^{0.5})) = A_T(M_m)^{0..5}/\varepsilon\sigma_e(M_p)^{0.5} \tag{33}$$

From which it follows that the maximum mass of polymer bound to a specific amount of fumed silica (Q_m) is the product of the specific number of bound chains and the mass of a single chain (eq 34).

$$Q_m = (A_T(M_m)^{0..5}/\varepsilon\,\sigma_e(M_p)^{0.5})\,((M_p)/\hat{A}) = (A_T(M_m)^{0..5}/\hat{A}\,\varepsilon\,\sigma_e)\,(M_p)^{0.5} \tag{34}$$

The actual specific saturation mass Q_r[1] is usually smaller than Q_m. As the concentration of FSN is increased the number of chains that bridge particles also increases, and the total number of chains bound only to any individual mass of silica decreases. The relation between these actual and ideal values was later found to depend upon the specific amount of polymer initially in the mixture, Q_i (eq 35).

$$Q_r^l = Q_m (1 - (Q_m/4Q_i)) \quad (35)$$

The polymer/filler dependent concentration factor that modifies Q_m in eq 35 is equivalent to the $1/(1+\mu_a)$ bridging term of eq 27. If $1/(1+\mu_a)$ is introduced to eq 34 to compensate for the fractional reduction in bound rubber due to bridging explicitly described by eq 35, then eq 34 becomes identical to β_m (eq 27) and Cohen-Addad's original empirical equation (eq 26) is theoretically derived from only the assumptions of one polymer-silica bond per monomer unit and Gaussian chain behavior.[124] Equation 26 has been empirically verified for uFSN of various surface areas mixed with hydroxy and methyl terminated PDMS and other siloxane compounds in further work by Cohen-Addad, and numerous other investigators.[125, 126, 127, 128]

From his data Cohen-Addad also produced an empirical model to describe the kinetics of PDMS adsorption on fumed silica (eq 36).

$$Q_r(t) = Q_r^l - (Q_r^l - Q_r(0)) \exp(-(t/\tau)^{0.5}) \quad (36)$$

Here, as before, Q_r^l is the saturation value of adsorbed PDMS (g/g of fumed silica). $Q_r(t)$ is the specific amount of PDMS adsorbed at a time, t, after the end of mechanical mixing, while $Q_r(0)$ is the specific amount PDMS discovered bound to the FSN right after the materials are first combined. The τ term describes the characteristic adsorption time of the process.[129] At RT τ was found to have values ranging from hundreds of hours to years.

Cohen-Addad initially rationalized the slow kinetics of adsorption by attributing it to the diffusively driven random collision of a particle with an absorbing screen and the excluded surface that results when that collision leads to adsorption. He thought that the experimentally derived dependence of adsorption on the square root of time was suggestive of a Fickian diffusion process that can be modeled by $\partial Q_r(t)/\partial t \propto 1/(Dt)^{0.5}$, while the progressive effect of surface exclusion on diffusion rate could be expressed as

the difference between the maximum amount of adsorbed material and the material adsorbed at a given time ($Q_r^l - Q_r(t)$). Combining these relations and defining the Fickian diffusion constant D as $1/\tau$ gives eq 37.

$$dQ_r(t)/dt = 2(Q_r^l - Q_r(t))/ (t/\tau)^{0.5} \quad (37)$$

Integrating eq 37 from 0 to t regenerates eq 36.[130] Only two variables remain undefined in eq 37, the bound polymer at the end of mixing, $Q_r(0)$, and the time constant, τ.

Like saturation bound rubber, experimental values for the bound rubber right after mixing, $Q_r(0)$, were also found to vary in proportion to the square root of polymer molecular weight. Thus, the distribution of PDMS chains could be assumed to be Gaussian and the maximum amount of bound rubber immediately after mixing could be described in the same manner as the saturation value by eq 38.

$$Q_r(0) = B_o M_p^{0.5} \quad (38)$$

Here B_0 is always smaller than B_m, but it can be a significant fraction of the larger saturation constant. Thus, the value of $Q_r(0)$ can also be a significant fraction of Q_r^l. For mixtures initially containing 20 wt% FSN in PDMS with MW of 43k to 300k, the bound rubber at the end of mixing was found to be 24 - 50% of the saturation value.[131] Like the saturation value for bound rubber, the amount of rubber bound at the end of mixing was also found to exhibit a dependence on the specific amount of polymer initially in the mixture (Q_i). However, while adsorption to the $Q_r(0)$ value is rapid, adsorption to saturation (Q_r^l) takes far longer.

Overall, the rate of adsorption from just after mixing to saturation showed a strong dependence on end group functionality with hydroxy terminated PDMS being adsorbed about an order of magnitude more quickly than trimethyl terminated. Cohen-Addad attributed this to an anchoring effect from the formation of strong double hydrogen bonds between hydroxy PDMS end groups and silica surface silanols. These anchors are in turn believed to facilitate the bonding of PDMS siloxane units and silica

surface silanols. For example, for the α, ω-hydroxyPDMS$_{26k}$ used in this work with a 14 wt% FSN loading at room temperature, Cohen-Addad's data indicates a τ value of ~450 hours. Thus, at room temperature, for such an experimental mixture to adsorb 99% of its saturation level of bound PDMS should require an adsorption time of about a year. For a similar mixture containing trimethyl terminated PDMS to achieve 99% bound rubber saturation should require nearly 10 years. The adsorption rate also showed a strong dependence on temperature with faster adsorption occurring at higher temperatures. From Cohen-Addad's data, at 70ºC the hydroxy terminated PDMS experimental mixtures employed in this study should attain 99% saturation in ~2 weeks. If trimethyl terminated PDMS is substituted, then mixtures processed at 70ºC should achieve 99% saturation in about a year rather than the 10 years observed at ambient. Higher filler concentration or lower MW polymer were also found to increase the time needed for saturation.[132]

It is remarkable that relatively simple relations such as eqs 26 and 36 were not found earlier. The delay is best explained by the long time intervals required for FSN/PDMS mixtures to achieve bound rubber saturation. Most adsorption processes are limited by the rate at which the adsorbed species can diffuse to the adsorbing surface. Such diffusion, and hence adsorption, usually occurs in fractions of a second to at most a few hours. At room temperature, the meaningful examination of bound rubber formation in FSN/PDMS mixtures requires adsorption times of from months to years. The relations that describe the adsorption of PDMS on fumed silica went unrecognized for so long largely because it was unsuspected that the process of adsorption might occur over such long periods of time.

The mechanism that causes such extended adsorption times is still being hotly debated. In commonly used mixtures of PDMS and FSN the concentration of silica (<30 %wt) is low enough that (assuming Bohin's wetting model) each silica particle should be surrounded by polymer molecules in far less than the observed saturation time. In addition, larger polymer chains should diffuse more slowly and therefore form BR more slowly than small chains, but the rate of BR formation has been found to increases with polymer MW. Therefore, in these mixtures the diffusion of polymer chains in the melt is

unlikely to be the factor that limits adsorption. In the very late 1990's, recognizing the unexplained slow kinetics of adsorption, Cohen-Addad proposed that water on the silica surface acts as a poison to the adsorption process. In this model the low energy displacement of water from free silanols on the silica surface results in rapid adsorption to the "just after mixing" value. Further adsorption to the saturation value requires the much slower displacement of much more strongly bound water from vicinal silanols (see Figure 8.).[133]

At roughly the same time, Levresse proposed a competing model that attributes the slow adsorption to a combination of two factors. First, as the amount of bound polymer increases adsorption slows, because fewer silanols remain available for further adsorption. Fewer silanols are available both because silanol/polymer bonding has made some unavailable, and because the bound chains have obscured some unbound silanols. Secondly, over time, the increasing amount of bound polymer causes steric crowding at the polymer/filler interface making it progressively more difficult for free chains to get close enough to the surface to form bonds. This model differs from the excluded surface effect that Cohen-Addad's model addressed in that Levresse considers the silica and surrounding polymer as a dynamic system of continually forming, breaking, and reforming low energy bonds. The resulting slow rearrangement eventually allows the largest number of polymer molecules to form bonds to surface silanols while still allowing each polymer molecule to assume its lowest energy configuration (where each bound molecule has formed $(N)^{0.5}$ bonds with the surface). In Levresse's view, the enormous number of intermediate configurations that the polymer molecules could assume in the process of achieving this state causes the slow adsorption kinetics.[134] Another significant difference from the Cohen-Addad model is that Levresse symbolically expressed adsorption in terms of concentration and reaction order in a manner more familiar to chemists. At this time, neither the Cohen-Addad nor the Levresse model has been conclusively proven.

Dispersion

Dispersion is the process by which the fumed silica powder is reduced to nano-particulates suspended in the polymer melt. Before dispersion the fumed silica powder consists of agglomerates from one to several hundred microns in size. As noted earlier (Figure 5), when at its most reduced, fumed silica has been found to consist of nanometer scale primary particles physically sintered together into linear branching aggregate structures 50 - 500 nm in size.[135] Dispersion therefore consists of breaking the hydrogen bonds that assemble the aggregates into weak agglomerates. This reduction is accomplished by applying hydrodynamic shear forces to overcome interaggregate cohesive forces.

Recently, from TEM and energy resolved fragmentation analysis of low pressure impact data for fumed silica, it was shown that for every three sintering contacts that primary particles make while forming an Aerosil® 200 aggregate that aggregate will in turn make a single contact with another aggregate while forming an agglomerate.[136] On average Aerosil® 200 is comprised of primary particles 12 nm in diameter that combine to form aggregates ~120 nm in size.[137] Equation 22 can be used to determine that an average Aerosil® 200 aggregate is comprised of 60 primary particles (N_{pp}). These primary particles have been found to form aggregates by sintering to (coordinating with) between 2 and 3.3 neighboring particles. Applying the experimentally determined ratio of agglomerate to aggregate contacts it follows that an average Aerosil® 200 aggregate makes ~45 contacts with neighboring aggregates in order to become part of a larger Aerosil® 200 agglomerate.

The impact data also revealed that the cohesive energy by which an Aerosil® 200 aggregate is bound to other aggregates to form an agglomerate is ~1.1.X 10^{-16} J. (This reported experimental result is in close agreement with the theoretical calculation made earlier in this work (p 32) that revealed an average agglomeration energy of 1.3 X 10^{-16} J/aggregate for Aerosil® 300.) Thus, each of an Aerosil® 200's 45 agglomerating contacts has a mean inter-particle energy of 2.4 X 10^{-18} J. To remove an aggregate from the agglomerate therefore requires energy greater than this cohesive contact energy. This

energy, if applied at an average distance of half the diameter of an average Aerosil® 200 aggregate (60 nm) from the agglomeration contact and spread over half of the surface area of that aggregate (10,500 nm^2) can be supplied by a shear stress of ~3800 Pa. Such a shear stress (τ) must come from the high shear rate (γ) mixing of the surrounding viscous (η) polymer ($\tau = \eta\gamma$). At the shear rate Degussa suggests for Aerosil® 200 (~2000 /s), a shear stress of at least 3800 Pa can be generated for any siloxane with a viscosity of over 1.9 Pa·s. In experimental work involving Aerosil® 200 compounded in vinyl terminated PDMS, Schaer et al. reported the reduction of some of the fumed silica powder to aggregates around 100 nm size.[138] However, it was also found that much of the fumed silica remained in agglomerate structures clustered around one micron or twenty microns in size. Since the 1000 /s shear rate in Schaer's work was applied to a polymer with a viscosity of η = 1.5 Pa·s, the hydrodynamic shear stress generated in these experiments (1500 Pa) was less than half that needed to fully separate aggregates from agglomerates. So, the lack of complete dispersion is not surprising. In earlier work involving Aerosil® 300 in PDMS under a similar shear stress, Bohin et al. observed even less dispersion.[139] Being composed of aggregates having both a larger surface area and more primary particles, Aerosil® 300 would be expected to require an even higher shear force for full dispersion than does Aerosil® 200, so again the lack of full dispersion in these experiments is not surprising.

Such strong interaggregate cohesive forces make complete dispersion difficult. Initially, shearing forces are exerted over the relatively large surface areas of agglomerates (~10^{-8} m^2), and are therefore concentrated over the relatively small interaggregate hydrogen bonding regions (~10^{-15} m^2). These concentrated shear forces causes the rapid bulk rupture of large agglomerates due to dry cohesive failure between some of the aggregates within the agglomerates.[140] However, rupture quickly ceases as the size of the resulting agglomerate fragments approaches a micron. Further dispersion is then believed to occur by the slow erosion of smaller particles from these micron scale fragments. This erosion can be due to cohesive failure between aggregates that are wetted by polymer, or it may result from adhesive failure at the boundary between wetted and dry aggregates. In either case, full dispersion to aggregate sized particles depends on the

incorporation (wetting) of FSN by PDMS. In typical industrial equipment this requires high shear rate mixing over time periods of at least a significant fraction of an hour.

Distribution

Distribution is the homogenous spread of dispersed FSN throughout the PDMS matrix. The greatest impediment to distribution is the viscosity of the mixture, especially when sufficient filler is present to cause the mixture to gel into a solid. In the earlier discussion of "incorporation" it was calculated by eq 25 that a fully incorporated 14 wt% solution of Aerosil® 300 in α, ω-hydroxyPDMS$_{26k}$ should have a viscosity only 20% greater than that of the liquid PDMS alone. However, such mixtures are typically found to be soft solids. There are several reasons for this disparity.

First, for the purpose of agglomerate formation, the volume fraction occupied by fumed silica aggregates can be considered far greater than the volume occupied by the bulk silica of which they are composed. This consideration arises from the application of Flory-Stockmayer gelation (mean field percolation) theory. In the early 1940's these researchers were involved in developing a theoretical explanation for the existence of solvent swelled polymeric gels that were known to be composed of solid polymer molecules that occupied only small fractions of the bulk gel volume. Flory and Stockmayer proposed that the small volume of solid matter in these solid materials could be explained by the formation of space spanning polymeric networks. They showed that at a given time in a liquid polymerization mixture any free molecule had a roughly equal probability of occupying not only its actual spatial volume, but any equivalent volume within a spherical region defined by rotating the molecule three dimensionally around the center of its longest dimension. Thus, for the purpose of network formation, the volume effectively occupied by the molecule could be considered the volume of this sphere. Further they demonstrated that, for polymers with reactive end groups, when the volumetric fraction occupied by these spheres exceeded the maximum possible volume occupied by randomly close packed spheres (φ_{rcp} = 64%), then the probability that polymer molecules would link with adjacent molecules, thus forming a polymeric network, was high.[141, 142] Much like the steel framework of a skyscraper, such space-

spanning continuous network structures could form solids even if their molecular subunits occupied only a small fraction of the volume of the bulk material.

In the case of fumed silica, the effective aggregate volume is a function of the distance the aggregate can span when forming a network by agglomerating with other aggregates. This aggregate volume is defined as a spherical volume with a radius equal to the average aggregate radius of gyration ($V_{aggr} = (\pi/6)(2R_g)^3$). When some number of aggregates (N_{aggr}) with this volume (V_{aggr}) occupies the random close packing volume fraction for spheres ($\varphi_{rcp} = 64\%$) of some larger volume (V_{tot}), then those aggregates can form an interconnected percolation network (eq 39).

$$\varphi_{rcp} V_{tot} = N_{aggr} V_{aggr} \tag{39}$$

Rearranging this equation, the number density of aggregates of spherical gyration radius, R_g, required to randomly closely pack some volume is then given by eq 40.

$$N_{aggr}/V_{tot} = \varphi_{rcp}/V_{aggr} = \varphi_{rcp}/((\pi/6)(2R_g)^3) \tag{40}$$

Where the number of primary particles (N_{pp}) in an aggregate of gyration radius, R_g, is given by (eq 22, p 31), the actual volume of filler in the aggregate is given by ($N_{pp}V_{pp} = N_{pp}(\pi/6)(2r_{pp})^3$). The product of this actual filler volume per aggregate and the number density of these aggregates that are required to randomly close pack a volume is the critical fraction of a volume ($\varphi_{v,c}$) that must be physically occupied by this filler in order to form a gelled percolation network (eq 41).[143]

$$\varphi_{v,c} = N_{pp} V_{pp} \left(\frac{N_{aggr}}{V_{tot}} \right) = k \left(\frac{R_g}{r_{pp}} \right)^{D_f} \frac{\pi}{6} (2r_{pp})^3 \left(\frac{\varphi_{rcp}}{\left(\frac{\pi}{6} \right) (2R_g)^3} \right) = \varphi_{rcp} k \left(\frac{r_{pp}}{R_g} \right)^{3-D_f} \tag{41}$$

Using values calculated earlier (pp 30-31), the critical volume fraction for fully dispersed (unagglomerated) Aerosil® 300 aggregates is ~7.8 vol%, and the volume effectively

occupied by an average Aerosil® 300 aggregate is around 8.2 times that of the volume of the silica it contains. Thus, at 7.8 vol% Aerosil® 300 has the effective volume fraction of spherical random close packing, 8.2(0.078) = φ_{eff} = 0.64 = φ_{rcp}, and by the Krieger-Dougherty viscosity relation (eq 25) a mixture of 7.8 vol% Aerosil® 300 in α, ω-hydroxyPDMS$_{26k}$ should be a solid. The experimental mixtures used in the current work, for example, contained from 5.9 to 7.6 vol% filler and might therefore by eq 25 be expected to have viscosities ranging from that of Blackstrap Molasses (~10 Pa· s) to 20% above that of un-homogenized peanut butter (~300 Pa· s). However, typically all such mixtures are found to be harder waxy solids.

The initial structure of fumed silica is a second reason for the solidity of these mixtures. The percolation based critical volume relation (eq 41) assumes that small particles in a liquid must link-up to form a solidifying network. When first introduced to polymer, however, the fumed silica already exists as an agglomerate network with an effective volume greater than φ_{rcp} and by the Kreiger-Dougherty viscosity relation (eq 25) such a mixture should be solid. So long as mixing leaves the agglomerate network largely intact ($\varphi_{eff} \geq 0.64$) the mixture should remain solid. For experimental (5.9 to 7.6 vol% filler) mixtures of Aerosil® 300 in PDMS the dispersion of uFSN agglomerates to near aggregate size (average characteristic size 100 nm) would be required before a mixture might liquefy. If the average characteristic size of the dispersed particles was even 200nm, equation 41 would predict a solid mixture based on a critical volume (φ_{vc} = 3.5 vol%) below that of the silica in the mixtures.

The final reason for higher than expected viscosity in these mixtures is the adsorption of polymer by filler. When immersed in polymer, the volume fraction (φ_v) occupied by an adsorbing filler increases in proportion to the volume of polymer adsorbed on its surface. The polymer immobilized on the filler surface increases the filler volume, because it physically behaves more like solid filler than like fluid matrix. From the earlier discussion of polymer adsorption on silica (pp 40 - 45) it can be calculated that the mass of α, ω-hydroxyPDMS$_{26k}$ adsorbed on Aerosil® 300 ($Q_r(t)$) varies from 0.25 (g/g) right after mixing to 0.85 (g/g) at saturation. The average thickness of the PDMS

layer bound to the silica surface (h) can be calculated from the volume of bound PDMS (bound rubber mass ($Q_r(t)$) divided by the polymer density ($\rho \sim 980$ kg/m^3)) and the surface area ($A_T = 300$ m^2) of the fumed silica which it coats (eq 42).[144]

$$h = Q_r(t) / (A_T \rho) \tag{42}$$

Thus, the thickness of the layer of α, ω-hydroxyPDMS$_{26k}$ adsorbed on Aerosil® 300 varies from a low of 0.85 nm right after mixing to a maximum of 2.89 nm at saturation. Eggers and Schummer developed an empirically derived factor (β) that describes the ratio of the effective volume fraction of fractal aggregates coated in bound rubber (φ_{sbr}) to the effective volume of uncoated aggregates (φ_v) in order to correct for the increase in filler volume due to adsorbed polymer. This factor was found to depend upon: primary particle volume (V_p), bound rubber volume per primary particle (V_{br}), the average number of other particles adjacent to (coordinated with) a primary particle in the aggregate ($C_N = 2.2$ to 3.3), and a correcting term for the interpenetrating bound polymer at the sintered junction of primary particles. Further, they found that all these factors could be expressed in terms of bound polymer thickness, h, and primary particle diameter, d_p (eq 43).[145]

$$\beta = \frac{V_p + V_{br} - c_N \Delta V}{V_p} = 1 + 6\left(\frac{h}{d_p}\right) + 12\left(\frac{h}{d_p}\right)^2 + 8\left(\frac{h}{d_p}\right)^3 - c_N\left(3\left(\frac{h}{d_p}\right)^2 + 4\left(\frac{h}{d_p}\right)^3\right) \tag{43}$$

From this expression it can be calculated that the volume fraction occupied by the coated filler in the experimental mixtures should be from 2.5 to 9.2 times that of the filler alone. Therefore, for example, just after mixing 5.9 vol% of Aerosil® 300 in α, ω-hydroxyPDMS$_{26k}$ (the lowest filler concentration employed in this work) should occupy a minimal effective volume fraction of 14.8 vol% due to the polymer adsorbed on the filler surface, and because this exceeds the mixture's critical volume of 7.8 vol% the mixture would be expected to be solid. Hence, any of the experimental admixtures would also be expected to be solid.

Compounding Techniques

Since compounding FSN and PDMS is essential to the production of silicone rubbers, many techniques have been employed over the decades to reduce the time and energy it requires. One of the earliest methods was the simple addition of solvent to reduce the viscosity of the FSN/PDMS mixture. Unfortunately, due to the disparity in their solubility parameters, it is quite difficult to find a good solvent for both fumed silica and PDMS. Where nonpolar organics are typically good solvents for PDMS, polar compounds are required to solvate fumed silica. If only the polymer is solvated, then large visible clumps of silica are found unevenly dispersed throughout the mixture. This occurs not only because of solvent induced phase separation but also because of a reduction in viscosity dependent shearing by the thinned polymer. Solvating only the filler is found to result in much the same type of mixture once the solvent is removed. Neither approach leads to filler that is well dispersed and distributed throughout the polymer matrix.[146] Silicone elastomers made from solvated mixtures are seldom found to be much stronger than crosslinked PDMS alone. Currently, the addition of solvents is seldom practiced in FSN/PDMS compounding. However, solvents are sometimes employed when fumed silica is used as filler for other polymers such as PMMA or epoxy resins.[147]

In the mid 1950's manufacturers began replacing a percentage of the high molecular weight polymer in FSN/PDMS compounds with lower molecular weight PDMS oils by pre-wetting the filler with oil. When adsorbed, the lower molecular weight silicone oil shields silanols on the filler surface rendering the FSN more hydrophobic, thus easing later mixing with the hydrophobic high molecular weight polymer.[148] The lower molecular weight oils also have lower viscosity and when mixed with higher molecular weight polymer act to reduce the overall viscosity of the compounding solution. This method is still being employed, and tubes of RTV-1 sealants that have been thinned by the addition of 20 -30 wt% short chain PDMS are quite common. There are several drawbacks to this approach. First, the shorter chains are less elastic and crosslink to form less flexible rubbers. Second, the shorter chains interact less strongly with filler and form less robust elastomer networks of lower strength. Sometimes nonreactive low

molecular weight PDMS is used to thin process mixtures. In this case the polymer acts as a plasticizer that swells the network, but does not participate in crosslinking. It does, however, form bound rubber reducing the filler-filler and filler-HMW polymer interactions thereby reducing the reinforcing effect due to filler.[149] Its inclusion also reduces the concentration of higher molecular weight PDMS, thereby reducing overall crosslink density with a consequent reduction in material strength. In addition, depending on the environment in which it is used, the low molecular weight species may over time leak or leach from the elastomer reducing its elasticity and shrinking its volume. Nevertheless, in situations where high strength silicone rubber is not required, pre-treatment of filler with low MW silicone oil facilitates compounding cheaply and effectively.

Early in the 1960's manufacturers began to offer fumed silica treated with compounds that reduce silica surface activity. The first of these, Aerosil® R972, was produced by treating just synthesized Aerosil® 150 with dimethyldichlorosilane (DDCS) in a fluidized bed at elevated temperature (Figure 9.). The DDCS reacts with ~70 % of the Aerosil® surface silanols, and thereby converts the hydrophilic untreated FSN to a hydrophobic treated form (tFSN). Since, like PDMS molecules, the treated fumed silica presents a surface covered in hydrophobic methyl groups, tFSN and PDMS compound easily. Boonstra et al. reported, that for mixtures containing 28 wt% high surface area (345 m^2/g) fumed silica in vinyl terminated PDMS, compounding time could be reduced from 41 minutes for untreated FSN to 9 minutes for fully treated (no unreacted surface silanols) FSN.[150]

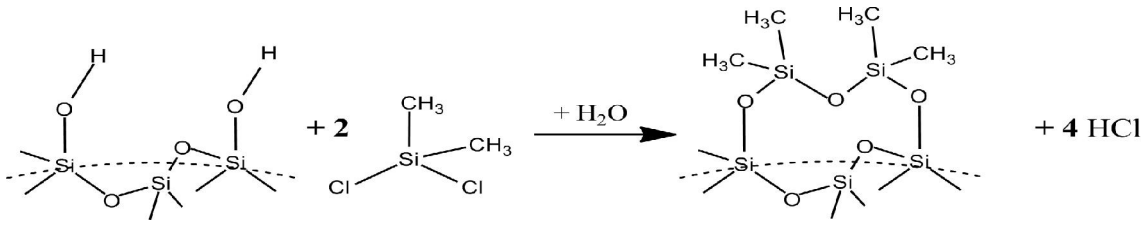

Figure 9. Hydrophobic treatment of fumed silica with DDCS

Unfortunately, the reduction in surface silanols caused by treatment also reduces particle-particle and particle-filler interaction and therefore, for equal filler loading, generally leads to a lower strength elastomer than compounds of untreated FSN and PDMS. While rubbers containing Boonstra's fully tFSN mixtures had about the same tensile strength as equivalent mixtures containing untreated FSN, they were also ~20% less resistant to tear and 40% softer (Shore A). In fairness, however, it should be noted that these rubbers also exhibited 75% greater elongation before break. In addition, rubbers in which treatment incompletely converted FSN surface silanols (30-50%) were shown to have both improved tensile strength and tear resistance when compared to rubbers filled with untreated FSN. However, reducing the degree of surface treatment increases compounding difficulty, thereby proportionally negating the processing advantage gained from treatment.

The reduction in particle-filler interaction that contributes to the observed reduction in strength also reduces the ability of fully tFSN to adsorb polymer and thereby all but eliminates any increase in effective particle volume fraction (eq 43) due to bound rubber. Since this lowers the effective volume of the filler, this allows rubber manufacturers to incorporate much more treated than untreated fumed silica in their compounds without exceeding the critical percolation volume for gelation. Rubbers with these higher treated filler loadings often have mechanical strength even greater than that of rubbers containing lesser amounts of untreated FSN. In addition, these high tFSN loaded PDMS compounds are typically easily processed viscous liquids, rather than difficult to handle waxes and gels. This strength and process-ability comes, however, quite literally, at a price. In comparison with other fillers, uFSN is expensive to produce ($2 – $4 /kg). Functionalizing its surface makes its production even more expensive ($5 - $10 /kg), and using larger quantities of this more expensive treated filler makes silicone rubber production very expensive indeed. Nevertheless, tFSN eases and accelerates the compounding of PDMS and fumed silica to such a degree, and (at high filler loadings) so improves elastomer mechanical strength, that it is the preferred filler for high molecular weight PDMS compounds such as liquid silicone rubber. Degussa and many other

manufacturers currently offer fumed silica with surfaces modified by a variety of chemical species.

Over the years a number of other compounding methods that utilize non-fumed forms of silica, such as precipitated silica and silica gel, have been employed to facilitate silica filled silicone rubber production; but, with a single exception, they are outside the scope of this work. In the 1980's Mark et al. began employing a sol-gel technique to form silica in situ during silicone rubber curing in order to avoid the problems encountered when compounding ex situ formed fumed silica and PDMS.[151] To accomplish silica synthesis during curing the tin catalyzed hydrolysis/condensation of a molar excess of TEOS with hydroxy terminated PDMS was employed. This reaction has been described in great detail in the "Silicone Rubber Synthesis" (pp 18-23) section of this document. Therein it was noted that one reason for using a molar quantity of TEOS in excess of that needed to crosslink the PDMS in this reaction was a desire to limit the possibility that the two reactive ends of a dihydroxy PDMS molecule might condense with one TEOS molecule and form a cyclic. Another, more important, reason is that when the excess hydroxylated TEOS molecules homocondense during this reaction they form nano-scale silica structures that chemically link the polymer matrix.

Electron microscopy and small angle x-ray scattering experiments have shown that, when formed during PDMS crosslinking, silica derived from excess crosslinker precipitates via spinodal decomposition to form a bi-continuous array of PDMS and silicate polymers with interpenetrating domains on a scale of 5nm. Increasing phase incompatibility during crosslinker polymerization is believed to induce phase separation in the polymer pre-gel that subsequent gelation locks into a spinodal morphology. [152, 153] Silicone rubber filled with 8 wt% of silica that was formed in situ during curing has been shown to have a reduced stress (modulus) at rupture: 5% greater than an equivalent rubber containing 20 wt% ex situ treated fumed silica, 60% greater than an equivalent rubber containing 10 wt% ex situ untreated fumed silica, and 130% greater than an equivalent silicone rubber containing no filler at all.[138, 154, 155]

Study Specific Background

Disappearing Silica

This work was initially motivated by a desire to replicate the work of Ogoshi et al.[156] and Inagi et al.[157] in order to compare their results with those in the then as yet unpublished work of Chakrabarty et al.[158] Each of these studies involved AFM imaging of condensation cured PDMS elastomers filled with FSN. Each utilized admixtures of 26 kDalton (M_n) hydroxy terminated PDMS containing approximately 14 wt% uFSN or tFSN that had been crosslinked by polydiethoxysiloxane (PDES) in a condensation reaction catalyzed by Dibutyltin diacetate [DBTDA]. There were, however, significant differences between the processing methods employed by Ogoshi/Inagi and those employed by Chakrabarty. Further, there were also significant differences in their results.

Ogoshi and Inagi reported that they first mechanically hand mixed PDMS and uFSN over a period of two hours, while Chakrabarty reported that he had combined these components in a SpeedMixer™ operating at 2,700 rpm for four cycles of one minute each. To samples of these admixtures each researcher then added PDES in molar multiples of the quantity needed to crosslink the available hydroxy-PDMS along with a small amount (0.3 - 0.5 wt%) of DBTDA catalyst. Ogoshi produced reaction mixtures with 4 and 14 times the stoichiometrically required quantity of crosslinker, while Inagi produced mixtures with 4, 14 and 28 times the required crosslinker. Chakrabarty produced like mixtures, and additional mixtures containing 35, 45 and 60 times the required crosslinker. Ogoshi and Inagi reported vigorously stirring their reactant mixtures for ten minutes, while Chakrabarty reported that he "speed mixed" his reactants for a total of six minutes. Ogoshi and Inagi then used their mixtures to dip-coat glass cover slips, while Chakrabarty used his mixtures to spin-coat glass cover slips. All researchers cured comparable samples for 72 hours at either ambient or 100ºC. All researchers examined their cured coated glass cover slips by AFM using similar protocols.

Ogoshi found that, while untreated fumed silica nanoparticles were visible in phase contrast AFM images of cured films under hard tapping ($A_{sp}/A_0 = 0.6$) in samples containing 4 times the required crosslinker cured at either ambient or 100ºC, they were

only visible in samples containing 14 times the required crosslinker that were cured at ambient. No nanoparticles were observed in samples containing 14 times the needed crosslinker cured at 100ºC. Inagi also observed a lack of phase image visible nanoparticles only in14x samples cured at 100ºC. He further observed that phase AFM showed nanoparticles in samples containing 28 times the needed crosslinker at ambient cure, and that, far from disappearing after 100ºC cure, the particles in the 28x film were even more clearly resolved. Inagi also extended this work to elastomers containing

Table 1. Nanoparticle Detection by AFM on Filled PDMS Elastomer Surfaces

Cross Linker	Silica	Cure	Ogoshi	Inagi	Chakrabarty
4x	uFSN	100°C	visible	visible	visible
		RT	visible	visible	
	tFSN	100°C		visible	none
		RT		visible	
14x	uFSN	100°C	none	none	sharper
		RT	visible	visible	
	tFSN	100°C		none	
		RT		disappearing	
28x	uFSN	100°C		sharper	sharper
		RT		visible	
	tFSN	100°C		faint	none
		RT		faint	
35x	uFSN	100°C			faint
		RT			
45x	uFSN	100°C			none
		RT			
60x	uFSN	100°C			faint
		RT			
	tFSN	100°C			none
		RT			

treated fumed silica nanoparticles. He found that, just as with uFSN materials, treated fumed silica nanoparticles (tFSN) could be observed in 4x samples regardless of cure, and could not be observed in 14x samples at 100ºC cure. In samples containing tFSN at 14x crosslinker and low concentration catalyst cured at ambient however, he reported that phase AFM displayed nanoparticles for about the first 24 hrs of cure, after which time

they were no longer visible. In addition, he found that the particles visible in samples containing tFSN and 28x crosslinker were less clearly resolved than in similar samples containing uFSN, and that higher temperature cure did not improve their resolution. Chakrabarty similarly observed the crosslinker concentration dependent phase image AFM detect-ability of uFSN on 100ºC cured PDMS elastomer surfaces. However, he found that nanoparticles were detectable at 35x crosslinker and below, and then disappeared at 45x only to reappear again at 60x. Table 1 summarizes these results.

Admixture Softening/Liquefaction

While attempting to replicate the work of these earlier researchers it was unexpectedly discovered that some aged uFSN/PDMS admixtures could be induced to liquefy by high shear mixing. The opposite behavior, hardening over time, is so common in uFSN/PDMS admixtures that it has been named crepe (or creep) hardening. Two reports of the softening over time of PDMS/silica admixtures were found in the literature and theoretically each relies on Cohen-Addad's adsorption work (pp 40-46). Both studies were predominantly rheological. DeGroot and Macosko, working with well-filled (14.4 vol %) mixtures of Aerosil®130 in low to moderate M_n (9-140 kDa) PDMS, examined the change over time of elastic/storage shear modulus [G'] measured at a single frequency (0.1 rad/s), and the corresponding change over time of bound rubber. Selimovik, Maynard and Hu, working with lower concentrations (5.3 - 8 vol %) of precipitated silica in lower M_n (5 - 35 kDa) PDMS, similarly examined the variation of elastic moduli, G', over time, but they did not examine any related variations in BR. They did, however, measure the corresponding viscous/loss [G"] shear moduli of the aged mixtures, and they measured both storage and loss moduli over a range of frequencies (0.1 - 300 rad/s).

Both studies found that, unlike initial BR formation ($Q_r(0)$), the initial storage modulus [G'(0)] of each mixture was independent of polymer M_n and increased in proportion to filler, not polymer, concentration. Selimovik et al. further found G'(0) to be, like that of any elastic gel, both frequency independent and much larger than the

initial loss modus [G"(0)]. From these discoveries both studies concluded that the initial strength of the PDMS/silica gum stock admixtures was due to the existence of space spanning silica-silica particle networks.

Like BR formation ($Q_r(t)$), both studies observed that the elastic modulus [G'(t)] of these admixtures slowly changed over time at a rate and to a degree that increased with the concentration, C_i, and molecular weight, M_n, of polymer employed. However, unlike the asymptotic increase characteristic of BR formation, G'(t) was found to asymptotically decay, and both studies found this decay occurred (like BR formation) over periods of days to months. Degroot and Macosko's work further showed that G' decreased approximately in inverse proportion to the observed extent and rate of BR formation. These similarities lead both studies to posit that the age related weakening of these admixtures was due to the slow adsorptive formation of BR with a consequent gradual deterioration of the original strengthening filler-filler network.

The Selimovik group further reported that, like G', the viscous moduli [G"] of their mixtures also decayed over time to an extent and at a rate that increased with polymer C_i and M_n. However, they found that the viscous moduli decreased to a lesser degree and at a slower rate than the elastic moduli so that, while initially G'>G", over time the elastic modulus became smaller than the viscous. All their mixtures were observed to liquefy at, or shortly after, the time that G" exceeded G'. As might be expected from the dependency of G' and G" on M_n and C_i , the modulus at crossover was also found to decay in inverse proportion to BR formation at a rate and to an extent that increased as did the polymer M_n and C_i. Thus, within the range of polymer M_n and C_i investigated any given combination of polymer and filler was found to require a specific period of time after mixing (during which, by eq 36, a specific quantity of bound rubber would form) before it would liquefy. In addition, beginning around the crossover point G" was found to assume the linearly increasing dependence on frequency characteristic of viscous fluids. Selimovik's group therefore further postulated that at modulus crossover BR formation eliminated the initial reinforcing silica-silica structure of the gum stock leaving a nearly Newtonian fluid mixture of polymer coated filler particles well dispersed

and distributed in a polymer matrix. In contrast, DeGroot and Macosko proposed that the destruction of the initial strengthening silica-silica network was from particle separation due to the contraction of polymer chains attached to multiple fumed silica particles. They believed that a higher concentration of filler enhanced this effect by reducing particle separation, and that longer aging periods enhanced this effect due to the adsorptive creation of more bridging chains.

Experimental

Materials and Equipment

The choice of materials and equipment was generally limited to those employed in the earlier work being replicated. Initially, the same untreated fumed silica nanoparticlulate (uFSN) donated by SiTech that had been used in Ogoshi's and Inagi's work was employed. However, as the stock of that material was depleted, the functionally equivalent untreated fumed silica, Aerosil® 300, that was used in Chakrabarty's work was substituted. This Aerosil® 300 had been obtained from Evonik/Degussa and stored for several years in a large sealed Tupperware® container. A few experiments were conducted with hexamethyldisilazane treated fumed silica (tFSN, Cab-o-sil TS530 HMDZ, BET surface area 200 m^2/g) that was generously provided by Quantum Silicones, Midlothian, VA. Fumed silica was oven dried at 120ºC for at least 2 days before use. α, ω-hydroxy-terminated poly(dimethyl siloxane),(DMS-S31, $HO(Me_2SiO)_nOH$, M_n = 26 kDa, ν = 1000 cSt), and poly(diethoxy siloxane), (PSI-021, $(SiO(OEt)_2)_n$, ES40, M_n = 134.2 Da with 40-42 wt% equivalent SiO_2) were obtained from Gelest Corp., Tullytown, PA. Dibutyltin diacetate (Cat No. 29,089-0, DBTDA) was purchased from Aldrich Chemistry. Solvents such as hexane and cyclohexane were Fischer Brand reagent grade. THF for GPC analysis was HPLC spectral grade.

All PDMS, uFSN, ES40, and BDTDA masses used in pre-mixtures and reaction-mixtures were measured by electro balance. Though ES40 and catalyst were dispensed using appropriately sized disposable tipped Eppendorf automatic μL pipettes, the quantity of these reactants was determined by mass, not by volume. All masses for bound rubber determination by solvent extraction and all initial TGA sample masses were also determined by electro balance.

Most mechanical mixing was accomplished in a Hauschilde & Co. KG built FlackTek DAC 150 FV SpeedMixer™. Speed mixed samples were contained in Parkway Plastics translucent polypropylene mixing cups with white polypropylene screw on lids. Cups were of either 1 oz. or 3 oz volume (30 or 90 mL). Some mechanical mixing was also carried out with a Cannon Instruments electric overhead mixer operating at 1550 rpm with a 3 cm diameter 5 bladed disk impeller.

Dip and spin coatings were made on 1½ x 22 x 44 mm Corning microscope slide cover slips (Cat No. 2940-224). A few coatings were made on slightly larger 1½ x 24 x 50 mm Fisher cover slips. In order to remove surface contaminants, all cover slips were briefly flamed with a propane torch then allowed to cool to ambient shortly before coating. Spin coating was achieved in either an Eppendorf mini-spin desktop centrifuge or in an SPS-Europe POLOS Spin 150. During curing dip coated cover slips were held upright by small (15-25 mm) rubber or plastic laboratory stoppers/septa. Spin coated cover slips were laid flat during curing. All coated cover slips were placed in Fisher Brand aluminum weighing dishes (Cat No. 08-732-106), and loosely covered by inverted disposable 50 mL polypropylene beakers during cure.

Poured plaques of cured material were produced in either standard 9.5 cm diameter culture (Petri) plates or in smaller 5.1 cm diameter plates. Some samples were also poured and cured in a 7.9 cm diameter PTFE pan resembling the bottom of a culture plate. A number of poured samples were produced in Lab-Tek® II Chamber Slides™ (Model 154461) consisting of a 4.8 cm long by 2 cm wide by 2 cm deep chamber

divided into two 2.4 X 2 X 2 cm wells adhesively mounted and sealed to the surface of a glass microscope slide.

To achieve crosslinking polymer samples were cured either in ambient air, or at 100ºC in a Lindberg/Blue Model MO1420A heated mechanical forced air oven. Fumed silica was dried, and pre-reaction compounds of FSN and PDMS were heated, in a Fisher Scientific Model 506G Isotemp Oven. Solvent solutions containing FSN and bound PDMS solids were separated from free PDMS using a Fisher Scientific Marathon 21000R centrifuge. Extracts and extracted gels were dried in a Thermo Electro NAPCO Model 5831 vacuum oven.

Atomic Force Microscopy (AFM) imaging was conducted on a Veeco Instruments DI-3100 with a Veeco Nanoscope V controller and Veeco RTESPW cantilevers (part: MPP-11100-W) having nominal spring constants in the range of 20 N/m-80 N/m. Some AFM imaging was accomplished on an Asylum Research MFP-3D using an Olympus AC240TS cantilever with nominal spring constant in the 0.7-3.8 N/m range. A scan rate of 1 Hz was used for all AFM imaging.

Optical microscopy utilized both a low power Nikon SMZ-1500 and a higher power Nikon Eclipse LV-100.

Gel Permeation Chromatography (GPC) was performed on a Viscotek GPC max with a TDA 305 triple detector array and a THF solvent feed of 1 mL/min.

Infra Red adsorption (FTIR) examination was conducted on KBr plates in a Nicolet Magna-IR 760 with an attached FT-Raman module. Attenuated Total Reflectance infra red (ATRIR) examination was conducted with a Nicolet iS10 with a smart iTR module and both Germanium and Diamond crystal sample stages. IR data collection, analysis, and display were accomplished with a Thermo Scientific OMNIC software package.

Dynamic Light scattering (DLS) data was collected on a Malvern Zetasizer nano SZ90 and analyzed using the Malvern Zetasizer software package. DLS samples were contained in 10 x 10 x 45 mm polystyrene sizing cuvettes, DTS0012.

Thermogravimetric analysis (TGA) was performed using a TA Instruments TGA-Q500 at a heating rate of 20^{o}C per minute in a nitrogen atmosphere.

Compositions

Initially, sample compositions were dictated by those employed in the earlier work. The earlier researchers reported their experimental results in terms of the supplied molar multiples of the quantity of crosslinker needed to react with the available dihydroxy PDMS end groups in a sample(4x, 8x, etc.), and the % by weight of uFSN (-14) in the sample. The molar multiples of crosslinker used in a sample were calculated from the ratio of the moles of Si-O in the crosslinker to the moles of Si-OH in the hydroxy PDMS being crosslinked. Gelest reported that their ES40 crosslinker contained SiO_2 equivalent to 40 – 42 wt% of total crosslinker mass. In this polycondensation reaction the SiO_2 moiety was the crosslinking agent providing 2 moles of Si-O- per mole of SiO_2. Since hydroxy terminated PDMS provides 2 moles of Si-OH per mole of PDMS, the molar multiple of crosslinker in a sample was easily calculated from the sample molar ratio of ES40 SiO_2 to PDMS (eq 44).

$$\text{Mult}(x) = (0.41(\text{mass ES40})/\text{MW } SiO_2) \,/\, (\text{mass PDMS}/\text{MW PDMS}) \qquad (44)$$

The actual masses of reactants used by each researcher were obtained from the Supporting Information available for Ogoshi's[159] and Inagi's[160] work, and from Chakrabarty's work and laboratory notes.[157, 161] These values are presented in Table 2. Samples in this table are identified by a molar crosslinker multiplier and filler concentration naming convention similar to that employed by the earlier researchers. Early in this work this naming convention was adopted in order to facilitate the comparison of experimental results. This table also displays the molar multiple of

crosslinker in each sample as calculated by eq 44. The calculated multiplier values were found to vary somewhat from the values indicated by sample name.

By common convention, the weight % of filler in a sample could refer to either the mass ratio of filler to reactants (eq 45).

$$wt\% = (uFSN/(uFSN + PDMS + ES40))100 \quad (45)$$

Or else it could refer to the mass ratio of filler to product (eq 46).

$$wt\% = (uFSN/(uFSN + PDMS + 0.4(ES40)))100 \quad (46)$$

The earlier researchers, however, appear to have expressed this value as the mass ratio of filler to non filler in the reactant mixture (eq 47).

$$wt\% = (uFSN/(PDMS + ES40))100 \quad (47)$$

Table 2 also lists the values of wt% uFSN for all samples calculated by eq 47. All earlier researchers reported an uFSN value of 14 wt% for all samples; though, as Table 2 shows, even by eq 47 there was some deviation from this value. In Ogoshi's and Inagi's work no modifications to uFSN content were made to maintain a 14 wt% composition as crosslinker mass, and hence total non-filler reactant mass, increased. As a result, their reactant mixtures contained a progressively lower wt% of uFSN for each increase in crosslinker. Chakrabarty, on the hand, did so compensate, and (since the envisioned work would require replicating samples with as much as 60 times the required crosslinker) his compositional protocol was adopted for the current work. Though by eq 47 the "-14" samples in both Chakrabarty's and this work contained ~14 wt% uFSN, it must be noted that by the more generally understood definitions of wt% (eq 45) the reaction mixtures contained ~12.2 wt% uFSN and the cured elastomeric products (eq 46) contained from 12.3 to 14.1 wt% uFSN.

Table 2. Sample Compositions

Old Name	26k PDMS	ES40	Multiple Si-O/Si-OH	uFSN	uFSN (PDMS+ES40)	uFSN (PDMS+uFSN)	ES40 (PDMS+uFSN+ES40)	New Name
	g	g	mole/mole	g	%	wt% pre-mix	wt% reactants	
Ogosi/Inagi								
4x-14	8.7	0.21	4.3x	1.35	15.2	13.4	2	26k-13.4-2.0
14x-14	13.8	1.07	13.8x	2.16	14.5	13.5	6.3	26k-13.5-6.3
28x-14	15.1	2.56	30.1x	2.11	12	12.3	13	26k-12.3-13.0
Chakrabarty								
4x-14	5	0.104	3.7x	0.710	13.9	12.4	1.8	26k-12.4-1.8
14x-14	5	0.363	12.9x	0.751	14	13.1	5.9	26k-13.1-5.9
28x-14	5	0.727	25.8x	0.802	14	13.8	11.1	26k-13.8-11.1
35x-14	5	0.908	32.3x	0.827	14	14.2	13.5	26k-14.2-13.5
45x-14	5	1.170	41.6x	0.869	14.1	14.8	16.6	26k-14.8-16.6
60x-14	5	1.560	55.4x	0.920	14	15.5	20.9	26k-15.5-20.9
WBD Addnl								
8x-14	5	0.208	7.4x	0.729	14	12.7	3.5	26k-12.7-3.5
11x-14	5	0.303	10.8x	0.742	14	12.9	5.0	26k-12.9-5.0
12.5x-14	5	0.330	11.7x	0.746	14	13.0	5.4	26k-13.0-5.4
40x-14	5	1.040	36.9x	0.850	14.1	14.5	15.1	26k-14.5-15.1
40x-16	10	2.340	41.6x	1.930	15.6	16.2	16.4	26k-16.2-16.4
40x-17	10	2.340	41.6x	2.130	17.3	17.6	16.2	26k-17.6-16.2
40x-20	5	1.170	41.6x	1.270	20.6	20.3	17.1	26k-20.3-17.1
40x-28	5	1.170	41.6x	1.740	28.2	25.8	14.8	26k-25.8-14.8

Later, a decision was made to abandon the multiples of crosslinker and eq 47 based wt% names in favor of a more accurate and descriptive, naming convention. In order to allow for the future use of non 26 kDa PDMS it was decided that the first term in the new sample name should refer to the molecular weight of the PDMS in the sample. In this study the first term in the name of the vast majority of samples was 26k. Much of this work was concerned with the difficulties encountered when mixing PDMS and uFSN and a knowledge of the wt% of filler in pre-reaction admixtures was deemed both significant and useful. Therefore, it was decided that the second term in a sample name should represent the wt% of filler present in the pre-mixture of filler and polymer before the addition of crosslinker (eq 48).

$$wt\% = (uFSN/(PDMS + uFSN))100 \quad (48)$$

For the experimental mixtures derived from Chakrabarty's compositional protocol this value was found to vary from a low of 12.4 wt% for a 4x crosslinker pre-mixture to a high of 15.5 wt% for a 60x pre-mixture. In addition, a third term was included to express the wt% of crosslinker in a sample reaction-mixture (eq 49).

$$wt\% = (ES40/(uFSN + PDMS + ES40))100 \quad (49)$$

This value was found to vary from 1.8 wt% to 20.9 wt% in the 4x to 60x experimental range of crosslinker concentrations.

If some mass basis for PDMS were assumed terms 2 and 3 would allow one to generate masses for all of the reactants in a sample, and term 1 would allow for the determination of the multiple of PDMS-required crosslinker in the sample. A typical sample name by this convention might be "26k-14.2-13.5" representing a sample containing hydroxy terminated PDMS with a number average molecular weight of 26 kDa, a pre-reaction mixture mass based filler weight percent of 14.2, and a reactant-mixture mass based crosslinker weight percent of 13.5. The equivalent sample name by the older admittedly more compact, but less accurate, naming convention would be "35x-14." Additional terms were added to sample names as needed to describe variations in sample processing conditions. Frequently, for the purpose of comparison, references to both the "old" and "new" names of a sample have been made in this study.

Procedures

Mixing

At least two phases of mixing were required for elastomer synthesis. First, it was necessary to combine PDMS and uFSN to obtain a well dispersed, homogenous pre-mixture. Next the process required the blending of crosslinker and catalyst with this pre-

mixture to produce the final curing reaction-mixture. A number of techniques were attempted to achieve this mixing.

Mechanical Hand Mixing of pre-reaction solutions consisted of the slow addition of a known mass of uFSN over a period of 2 hours to a beaker containing a known agitated mass of hydroxy terminated PDMS. In different experiments, mixtures were agitated by a variety of stirring devices including: a glass stirring rod, a manual mechanical eggbeater, an electric eggbeater, an overhead laboratory stirrer with a 5 blade disc impeller, and a counter top electric blender. Subsequent blending of pre-mixtures with appropriate amounts of crosslinker and catalyst (0.2 - 0.5 wt% reactants) was attempted for 10 minutes with whatever device had been used to produce the pre-mixture.

Solvated Mechanical Hand Mixing was similar to Mechanical Hand Mixing. However, during the slow addition of uFSN to PDMS, small quantities of Hexane were also added. The quantity of solvent added at any time was that amount just sufficient to render the pre-reaction mixture liquid enough that visible mixing of reactants was maintained. Generally, the total mass of solvent required was ~25% greater than that of the sum of the PDMS and uFSN masses. Agitation was effected by an overhead laboratory stirrer with a 5 blade disc impeller operating at 1550 rpm. Subsequent 10 minute blending of pre-mixtures with appropriate quantities of crosslinker and catalyst was also by overhead stirrer. Depending on the quantity of crosslinker added and the time between the two mixing steps it was sometimes necessary to add slightly more solvent during the production of solvated curing reaction-mixtures to compensate for evaporation.

High speed mixing was accomplished using a Hauschilde & Co. built FlackTek DAC 150 FV SpeedMixer™. This is a dual asymmetric centrifugal mixing device. Within the unit a cylindrical mixing cup, tipped at ~30˚ from the vertical, is positioned at the end of a horizontal arm. In operation this horizontal arm is rotated in a clockwise direction at speeds as high as 3,500 rpm, while the cup is simultaneously rotated counterclockwise around its own cylindrical axis in the tipped plane at one third of the

arm speed. Rotation of the cup centrifugally forces contained material to move towards the cup wall, while rotation of the arm centrifugally forces contained material to move towards the bottom of the cup. In combination these forces move materials in complex patterns that cause high shear mixing through sharp directional changes and countercurrent flows. Comparison to other mixing methods is difficult since the SpeedMixer™ has neither a rotating impeller nor an impeller-to-wall gap from which a shear rate, and hence a shear stress may be calculated. FlackTek claims that the compounding of as much as 25 wt% fumed silica in silicone oil (a process that by other methods can take hours) can be accomplished by the SpeedMixer™ in less than a minute.[162] In this work it was found that the SpeedMixer™ could successfully mix 12.4 – 17.5 wt% Aerosil® 300 and α, ω-hydroxyPDMS$_{26k}$ in 3 - 5 minutes.

Chakrabarty's High Speed Mixing protocol was followed during some early experiments.[157, 160] Hydroxy-terminated polydimethylsiloxane (5 g), and calculated quantities of unmodified fumed silica nanoparticles were placed in mixing containers with screw tops. The containers were placed in the Flacktek SpeedMixer™ and mixed at 2700 rpm for 60 s. This mixing process was repeated 4 times with 10 second pauses between mixing cycles. Calculated amounts of ES40 and 0.5 wt% DBTDA catalyst were then added to the nanoparticle/PDMS pre-mixtures, and blended 6 times at 2700 rpm for 60 s, again with 10 second pauses between mixing cycles, to produce reaction-mixtures.

Standard Heated Speed Mixing soon replaced Chakrabarty's method. In this procedure first, a disposable 1 oz. polypropylene mixing cup and corresponding lid were tared. (The lids of these cups were found to contain white foamed polyethylene sealing discs, and these discs were removed before taring.) The glue holding these sealing discs in place was also removed by wiping the interior of the caps with acetone soaked paper towels. Failure to remove sealing discs and glue was found to lead to sample contamination by melted material during processing.) A pre-mixture consisting of 5g of 26 kDa hydroxy terminated PDMS and the calculated mass of uFSN required by the sample was then placed in the cup. (The limitation to 5g of polymer was initially imposed by the size of the cup and the low density of uFSN. The small cups were incapable of

containing the volume of filler required by samples containing a greater mass of polymer. Later, larger 3 oz. cups were used allowing for samples containing up to 15 g of polymer.) The lid was tightly screwed on the cup and it was placed in the SpeedMixer™. Experimentally, a number of rotational speeds were used in sample production; however the vast majority of samples were mixed at 3,500 rpm for 1 minute. (The restriction to 1 minute of mixing was a function of the mixer design. The speed mixer could not be set to mix for periods longer than 1 minute at a time.) The cup was then removed from the mixer and opened. Fumed silica and PDMS adhering to the sides of the cup were scraped-off with a spatula and deposited in the waxy mixture in the bottom of the cup. The cup was then resealed and returned to the speed mixer. Mixing and scraping was repeated once followed by one additional mixing cycle. Primary mixing of pre-mixtures consisted of a total of three one minute 3,500 rpm mixing cycles interrupted by 2 scrapings. In some experiments slower mixing speeds and/or more mixing cycles were used.

The sealed cup containing a waxy solid sample of pre-mixture was removed from the SpeedMixer™ and placed in a glassware drying oven. The pre-mixture was then subjected to process heating at 110-115 ºC for 2½ hours. At the end of that time, the cup was returned to the SpeedMixer™ and the still solid pre-mixture was subjected to secondary mixing consisting of 2 consecutive 1 minute mixing cycles at 3,500 rpm. The sealed cup, now containing a viscous liquid mixture of PDMS and fumed silica, was removed from the mixer and opened. Sample, cap, and cup were then tared together on a balance. A curable reaction-mixture was produced by adding to the viscous pre-mixture both a pre-calculated mass of ES40 appropriate to the sample and 0.3 wt% DBTDA catalyst. Addition of crosslinker and catalyst was accomplished on the balance using appropriately sized auto pipettes with disposable tips. The cup was then resealed and returned to the SpeedMixer™ and the reaction-mixture was subjected to a final mixing of 3 one minute cycles at 3,500 rpm. As with pre-mixture processing, in some cases slower mixing speeds and/or more mixing cycles were used. In addition, in some experiments process temperature and heating time were also varied.

Coating

Dip coating of cover slips was not completely described in any of the earlier studies. From a few surviving samples, one surviving picture, and current practice, it appeared that dip coated cover slips were produced so that they could be cured in an upright position. This was accomplished in this work by cutting a slit across the narrow face of a small rubber septa or stopper and placing it wide face down in an aluminum weighing pan. The cover slip to be coated was then held by the thin sides at one of its narrow ends and the opposite end was dipped in the reaction-mixture. The slip was then inverted so that the coated end faced up and the uncoated end was inserted in the slit of the stopper. The stopper served as a relatively wide base to hold the slip upright in the pan. Finally, an inverted 50 mL disposable polypropylene beaker was placed over the upright slip in the pan and the coated sample was then ready for curing. The inverted beaker served to keep airborne material from contaminating the sample, while still allowing the coating to cure.

Spin coating was initially accomplished by attaching the center of one side of a cover slip with double sided sticky tape to the axial post of an Eppendorf mini-spin desktop centrifuge. A drop of reaction mixture was then deposited on the center of the slip with a small spatula. The centrifuge lid was closed and the unit was set to spin the sample at 3,000 rpm for 30 seconds. Later, an SPS-Europe POLOS Spin 150 spin processor became available and, because of ease of cleaning, it replaced the Eppendorf unit. However, spin coating parameters remained otherwise unchanged. Spin coated cover slips were laid flat, coated side up, in aluminum weighing pans and covered with inverted 50 mL disposable polypropylene beakers for curing.

Pouring reaction-mixtures into flat bottomed glass Petri plates, covering with plate lids, and then curing yielded gross elastomer samples for bulk property determination. Initially, glass plates were chosen over more common polystyrene, because they could tolerate 100ºC curing without melting. However, it was found to be difficult to remove the cured PDMS rubber from glass, and later samples were poured into similarly sized PTFE plates. After curing the elastomer was easily peeled from these

plates. A series of small poured samples for AFM imaging were also produced in the wells of 2 chamber biological microscope slides. Enough material was poured into each well to fully cover its base area with a 1 - 2 mm deep coating of polymer, and an included loose cover was then placed over the coated wells. After curing an Exacto® type knife was run between well walls and enclosed samples, and the well walls were peeled away from their glass slide bases with a manufacturer supplied tool. To produce flat samples for AFM imaging an approximately 2 mm frame of material containing an edge effect meniscus of cured polymer was razor cut from each sample and removed.

Curing

Prepared dip coated, spin coated, and poured samples were either left loosely covered at ambient temperature on an open laboratory shelf, or placed in a heated forced air oven at 100ºC for 72 hours to cure. Samples poured to chamber slides were cured at 100ºC for 72 hours. Some samples were left for greater or lesser periods of time in order to establish the time needed for sample curing. In later experiments it was found that some samples only required 24 hours at ambient or 100ºC for curing, and many comparable samples were produced in this manner. For many samples (most notably those processed outside of standardized parameters) only an initial cure at room temperature was found to result in bubble-free elastomers. For these samples ambient curing for from a day to a week followed by 24 hrs at 100ºC was found to give good results.

Imaging

AFM imaging was performed wherever possible on elastomeric reaction products. Nanocomposite films on cover slips and in well plates were initially examined by TM-AFM employing a low set point ratio ($A_{sp}/A_o = 0.6$), generally considered “hard tapping”, as near-surface nanoparticles had been reported to be non visible under lighter tapping ($A_{sp}/A_o \geq 0.9$). However, it was found that successful imaging could be accomplished at a ratio of 0.8 and most imaging was conducted under this lighter tapping. AFM images were normalized to the same phase scale (z, deg). The phase scale was chosen to

optimize image quality and consistency with topographical images. All samples were scanned at a 1 Hz scan rate.

Optical Imaging was performed on a number of elastomer products. Some polymer film surfaces were examined at low power (20X - 100X) with a Nikon SMZ 1500 stereo microscope that employed an illumination system capable of projecting light through a transparent sample at slightly oblique angles to give high relief surface images. Images were captured by focusing a tripod mounted Canon Power Shot A650 digital camera through an eyepiece of the stereomicroscope. Some higher resolution images were obtained using a Nikon Eclipse LV-100 microscope with an attached Nikon DS-Fi1 digital imaging system. Very Low resolution (visual scale) images of materials were made with a variety of common consumer grade digital cameras from Canon, Sony and Kodak.

Mechanical Testing

Dog bone testing samples were cut from well-cured poured silicone elastomer films using a D412-C die. Samples were taken of both uFSN and tFSN filled elastomers containing a range of crosslinker concentrations (14x-60x). In addition, unfilled 14x crosslinked elastomer was also sampled. Three dog bones of each material were tested at ambient in a TA Instruments RSA3 dynamic mechanical analyzer with standard clamps. Tensile testing was carried out at a rate of 0.05 mm/s until rupture. The mean values and standard deviation of stress and strain at rupture for each set of 3 samples were calculated and these mean values (with SD error bars) were plotted as a function of crosslinker concentration for materials filled with untreated and treated silica filler.

Gel Phase Chromatography

Approximately 2 mL of Gelest supplied α,ω-hydroxyPDMS$_{26k}$ was passed through a 200 nm syringe filter to remove dust and separated into two 1 mL volumes. One volume was sealed and heated to 110ºC for 2.5 hours then allowed to cool to room temperature. The other volume was sealed and maintained at ambient. To each volume was added 20 mL of HPLC grade tetrahydrofuran, and both volumes were then vortex

mixed for three minutes. Two 1.5 mL samples were removed from each volume and placed in separate GPC vials. The instrument was set to sequentially inject 100 µL volumes (containing ~5 mg of polymer) of these samples into a THF solvent stream flowing at 1 mL/minute. The samples were arranged in the order unheated-heated-unheated-heated. Each sample was eluted for a 30 minute period. Though the instrument had been calibrated using polystyrene standards, it was not known if this calibration would be applicable to silanols. Therefore results were considered qualitative, rather than quantitative.

Infrared Adsorption

Infrared examination was of two types. Fourier Transform Infrared (FTIR) transmission spectroscopy was conducted by coating KBr plates with thin films of material and then scanning the coated plates 32 times over a range of 4,000 to 400 cm^{-1}. Attenuated Total Reflectance Infrared (ATRIR) spectroscopy was conducted for a like number of scans over an identical range, but material samples were smeared directly on the Germanium or Diamond sample stages of the instrument. Data collection and processing was computerized.

Two admixtures containing 14.2 wt% uFSN in PDMS were subjected to primary mixing, and thin films of the resulting wax were spread on KBr plates. The plates were examined by FTIR and separate samples of each mixture were also examined by ATRIR. The coated salt plates were then placed in an oven with the remaining un-plated admixtures and held at 112ºC for 2.5 hrs. The materials were removed from the oven, and the plates were allowed approximately 10 minutes to return to ambient temperature. During that time, small samples of the now heated bulk mixtures were removed for ATRIR and the remaining heated bulk mixtures were subjected to secondary mixing reducing them to viscous liquids. The now cool plated samples were then re-examined by FTIR and the equivalent small samples that had been process heated (but not secondary mixed) were examined by ATRIR. The plates were cleaned with acetone, coated with thin films of the viscous mixtures from secondary mixing, and again examined by FTIR. Viscous samples were also examined by ATRIR.

Dynamic Light Scattering

Small (0.5g) samples were collected after each of the three stages of pre-processing from uFSN/PDMS admixtures containing 13.8 and 14.2 wt% filler. Each sample was placed in a scintillation vial and solvated in an excess of fresh PDMS that had been passed through a 200 nm filter. The excess was calculated so that final solutions containing 1.4, 0.75, 0.28, and 0.14 wt% uFSN would result. Each sample was vortex mixed for 2 minutes and allowed to stand overnight, then vortex mixed for an additional 2 minutes the following day. Approximately 1 mL of each solution was transferred to a polystyrene sizing cuvette. Additional samples were produced by filling additional cuvettes with ~1 mL of each solution after passing it through a 200 nm syringe filter during transfer. A standard operating procedure for testing these mixtures on the instrument was constructed by entering published values for the required physical constants into the Zetasizer SOP wizard. Values for PDMS were entered for the dispersant phase, and values for fumed silica were entered for the material phase. The default values for solution temperature (25ºC) and sample equilibration time (120 sec.) were left unchanged. The default settings for positioning (seek optimum) and automatic attenuation (active) were also left unchanged. Data analysis was performed by the supplied General Purpose model. Initially testing was performed using the standard short duration (50 sec.) procedure; however later (in response to the analysis software) duration was increased to as much as 7500 seconds.

Thermal Gravimetric Bound Rubber Determination

Solvent extractions of known masses (~5 g) of uFSN/PDMS admixtures that had been removed at the various stages of standard pre-mixture processing (after primary mixing, after primary mixing and process heating, after primary mixing, process heating and secondary mixing) as well as samples processed under non-standard conditions were placed in tared, capped 50 mL polypropylene centrifuge tubes. Cyclohexane was added to fill each tube to the 45 mL mark. The tubes were sealed and the contents were extensively hand shaken and vortex mixed to disperse the contained admixtures in the solvent. The tubes were allowed to stand for approximately 24 hours and hand/vortex mixing was repeated. The tubes were then placed in a centrifuge and spun at 10,000 rpm

for an hour. At the end of that time, the supernatant was carefully decanted from each tube to a tared aluminum weighing pan in a manner that minimized precipitant disturbance. This extraction process was repeated three to four times on each sample. In some cases the solvent extracts from a given sample were combined so that only one TGA to determine the extract composition of that sample would be required. The aluminum pans containing solvent and unbound polymer were left in a chemical hood for several days to allow the majority of the solvent to evaporate. After the final extraction the small amount of solvent remaining in the centrifuge tubes containing fumed silica and bound rubber precipitant was also allowed to evaporate in a fume hood for several days. At the end of that time all aluminum pans and centrifuge tubes were placed in an oven at 60ºC under full vacuum for 3 days. Experiment had shown that after three days of such drying no further reduction in sample mass occurred indicating the fullest possible removal of solvent. After this all dried materials were carefully weighed.

Thermal Gravimetric Analysis of roughly 20 mg samples of the precipitates remaining in the centrifuge tubes after extraction and drying was performed. Samples in flame cleaned aluminum sample pans were ramp heated at 20ºC/min from ambient to 800ºC under a nitrogen atmosphere. The dried polymer extracts of these precipitates were also thermo gravimetrically analyzed in a similar manner to determine their filler content. The % loss of sample mass during TGA was considered to represent the PDMS content of the sample. The mass % remaining in the pan after testing was considered equivalent to the mass percent of uFSN in the sample. From % compositions and known masses the % recovery of the PDMS and uFSN in a sample were calculated.

Admixture Re-solidification

To each of three glass scintillation vials was added 2.6 g of one of the viscous liquid admixtures that had been used to determine Bound Rubber content. One vial contained a mixture processed at 110ºC for approximately 2.5 hrs that had been found to contain 0.61 g/g of Bound Rubber. Another was filled with a mixture processed for 24 hours at 80ºC that had been determined to contain 0.54 g/g of Bound Rubber; and a third vial was filled with a mixture processed for 72 hours at 60ºC that had been found to

contain 0.41 g/g of Bound Rubber. The meniscus of each sample was marked on the outside of each vial and an additional mark was made 3 cm above each meniscus mark. Each vial was then placed on its side and the time required for each solution to flow to the edge of the 3 cm mark was recorded. Vials were then returned to an upright position to allow the solutions to re-accumulate at the bottom. Measurements were repeated many times over a period of several weeks. A minimum of one day was allowed to elapse between consecutive measurements. It was believed that the low shear gravitational flow of this test would be unlikely to greatly disturb any formed or forming solidifying network structures within the material.

Results and Discussion

Mechanical Hand Mixing

In order to determine whether the mixing or coating process was responsible for the reported differences in earlier experimental AFM results, a number of attempts were made to employ the Ogoshi/Inagi mixing method followed by both dip and spin coating the mixed reactants onto glass cover slips. Unfortunately, it did not prove possible to "mechanically hand mix"[158, 159] the reactants as described and obtain a product that was sufficiently liquid that it could be used for either dip or spin coating. Compounding pre-reaction admixtures of uFSN and PDMS in the range of specified amounts was attempted a number of times using a variety of stirring devices including: a glass stirring rod, a manual mechanical eggbeater, an electric eggbeater, an overhead laboratory stirrer with a disc impeller blade, and a countertop electric blender. In each case, the pace of uFSN addition during pre-mixture production was slow enough that complete addition would require 2 hours. In each case, the addition of less than half the desired filler resulted in a dough-like mass that the stirring device could no longer mix. Any attempt to add more filler resulted in a mixture resembling thick cookie dough sitting in a bed of powdered sugar.

This behavior was found to be consistent with the Kreiger-Dougherty viscosity relation (eq 25). By this model (as calculated on p 37) due to the high specific volume of dry Aerosil®300 powder, the addition of as little as half (7 wt%) of the specified fumed silica would be expected to result in an initial PDMS/uFSN solution as solid as cold lard. Though Bohin's wetting theory would predict that the specific volume of the dry filler would have been substantially decreased by wetting-in during the 2 hour mixing period, the concomitant fast adsorption of polymer on filler to the just mixed values described by Cohen-Addad (eq 38) and a consequent increase in filler effective volume due to immobilized polymer, as described by Eggers and Schummer (eq 43), would be expected to result in a sufficiently large enough effective filler volume to maintain the admixture in a solid state. Effective filler volume reduction might have been expected due to dispersion during mixing, but it was unlikely that any of the various stirring devices employed were capable of exerting the high shear rate (2000/s) that the manufacturer considers necessary for Aerosil®300 dispersion (p 35). Hence, little break-up of the reinforcing silica-silica filler network might be expected from the mechanical hand mixing of these materials.

Several of the above pre-mixtures were further processed for high crosslinker concentration reactions. These reaction-mixtures were produced in the hope that the necessary addition of large amounts of low viscosity crosslinker would thin the overall mixture. Though somewhat lower viscosity reaction-mixtures did result, they were still found to be too thick to allow cover slips to be coated by dipping, and when spin coating was attempted they were found to be insufficiently adhesive to spread into films. Lacking samples, AFM imaging could not be performed.

Solvated Mechanical Hand Mixing

The two earliest researchers were contacted, but due to the passage of time they were unable to elaborate on the method(s) they had used to compound PDMS and uFSN. Though neither could definitively remember doing so, both agreed that they might have thinned their mixtures with hexane. In consequence, a series of PDMS/uFSN pre-mixtures were compounded suitable for producing elastomers with 1.8 - 20.9 wt% (4x -

60x) crosslinker. During blending sufficient hexane was added to these mixtures to render them pourable. The requisite hexane was added a small amount at a time during the 2 hours specified for uFSN addition. Continuous stirring during uFSN/hexane addition was accomplished by a laboratory overhead mixer with a disc impeller blade. Generally, a total mass of hexane 25% greater than the total sample mass of PDMS and uFSN was required to maintain a stir-able mixture. Subsequently, ES40 and DBTDA appropriate to the pre-mixture filler content and desired multiple of crosslinker were blended with these pre-mixtures, and the resulting reaction-mixtures were used to dip-coat and spin-coat glass cover slips. All cover slips were then cured at either room temperature or 100ºC for 72 hours. During curing the dip-coated slips were held upright using rubber stopper bases, while the spin coated slips were laid flat with their coated sides up. After dip coating the remainder of each reaction-mixture was divided between two Petri plates. Each plate was cured for 72 hours. One plate was cured at room temperature and the other was cured at 100ºC.

At the end of 72 hours regardless of cure temperature all glass cover slips were found unevenly covered by a fine but uneven film containing embedded granules. Granules varied in size from just visible to about a millimeter in diameter. Overall the coatings were translucent and visibly rough. Granular coatings were found on both dip and spin coated samples regardless of crosslinker content or curing temperature (Figure 10.). All coated cover slip samples were also found to be incompletely cured. Samples with low crosslinker content (1.8 - 11.1 wt%) were oily to the touch, while higher crosslinker content samples remained tacky and deformable. Two heat cured high crosslinker content (16.6 and 20.9 wt %) samples exhibited some small bubbles within the tacky elastomer, while similar samples cured at ambient did not. The combination of high surface roughness and sticky materials defeated all attempts to examine these dipped/spun films by AFM.

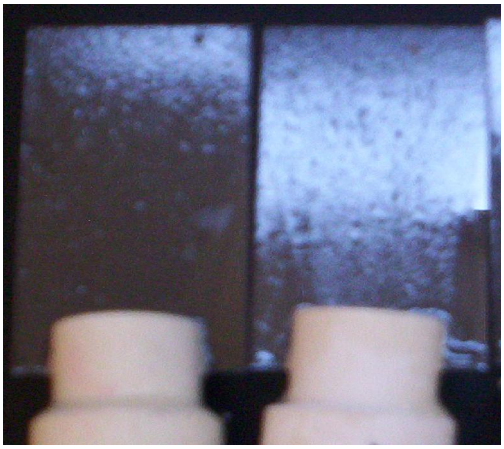

Figure10. Typical Solvated Hand Mixed Films

Solvated samples poured to plates were also found to be incompletely cured, though none remained the oily liquids found on the corresponding dipped cover slips. All poured samples cured to weak solids that would deform under finger pressure. Low crosslinker samples were somewhat softer than high crosslinker samples. All poured coatings were tacky. All plated samples contained numerous off-white inclusions. When compared to later samples all were found to be significantly more opaque. Thermally cured samples were found to contain numerous small bubbles.

The poor curing of these reaction-mixtures was worrying and, in order to eliminate the possibility that the age of the reactants contributed to the observed results, the solvated experimental mixtures were reproduced with newly obtained supplies of ES40, DBTDA, hexane, and hydroxy terminated PDMS that were first opened shortly before use. During this effort the supply of SiTech uFSN used by Ogoshi and Inagi (and in some experiments by Chakrabarty) was exhausted and further experiments were carried out using the similar uFSN, Aerosil® 300 (also used in some experiments by Chakrabarty). No differences in experimental results were observed when the fresh reactants or different filler were used.

It visibly appeared that the solvated reaction mixtures were thin enough to drain from the coated slips before cure leaving behind a large quantity of granular fumed silica agglomerates. The small polymer chain interaction (p 9), and hence relatively low

viscosity, of even higher MW PDMS would easily allow the oily uncured polymer to flow away under gravity or spin leaving thinly coated cover slips. The addition of thinning solvent would be expected to enhance polymer run-off. During such flow the surface silanols of untreated fumed silica nanoparticles in an admixture might be expected to adhere strongly to the underlying glass surface via hydrogen bonding. Hydrogen bonding would also be likely to cause uFSN aggregates in the draining PDMS to re-agglomerate with glass adherent uFSN resulting in the growth of more and/or larger granules. The large size and number of adherent granules that were observed may also have been a result of poor dispersion from the low shear rate (γ) mixing of the lower viscosity, thinned mixtures. For the mixers employed, the decrease in solution viscosity (η) that resulted from solvent thinning of the polymer would be expected to proportionately decrease the shear stress (τ) applied to the nanoparticle aggregates ($\tau = \eta\gamma$), and hence also decrease shear based agglomerate dispersion (p 47) to levels below that of even the poor dispersion observed in hand mechanically mixed un-thinned reaction mixtures. The large number of silanol groups on the surface of the glass bound fumed silica may then have competed with the remaining un-drained PDMS silanols for the quantity of crosslinker contained in the small amount of polymer/crosslinker solution left on the drained cover slips leading to incomplete PDMS cure even though the original solutions contained an excess of crosslinker. In this situation, the lower the initial concentration of crosslinker the lower would be the observed degree of cure as was observed.

In plated samples, unlike drained cover slips, the crosslinker to silanol ratio in each sample would remain constant, and complete cure in excess crosslinker would be expected. However, the large concentrations (over 50 wt%) of organic solvent employed, the hydrophobicity of PDMS, and the lack of the high shear force needed to disperse uFSN agglomerates might also be expected to partition the mixture into micro domains of solid hydrophilic uFSN agglomerates contained in a more hydrophobic PDMS/organic solvent matrix. Any water adsorbed on uFSN in these micro domains would be likely to hydrolyze any ES40 also present, and this hydrolyzed ES40 would then be most likely to condense with either the uFSN silanols or other hydrolyzed ES40 molecules within the

domain. In the fluid polymer phase this would lower the quantity of ES40 available to crosslink PDMS, but not to as great a degree as is believed to have occurred in coated cover slips. Therefore, somewhat less than complete curing might be expected. Growth of masses of silica in the polar micro domains might also be expected due both to the condensation reaction and physical agglomeration. Lastly, for thermally cured solvent thinned samples, a more rapidly solidifying matrix might be expected to trap bubbles of water, solvent, or alcoholic condensation byproduct vapors in the cured polymer. Room temperature cured materials would be less likely to contain such bubbles since slower curing polymer would be less likely to trap these materials, and at room temperature these materials would not be present as bubble forming vapors.

Chakrabarty High Speed Mixing

Having failed to produce useable samples for AFM imaging by either Hand Mechanical Mixing or Solvated Hand Mechanical Mixing, it was decided that Chakrabarty's SpeedMixer™ protocol followed by dip and spin coating might instead be employed to determine the processing variable(s) responsible for the observed difference in AFM results. Pre-mixtures of uFSN and PDMS in quantities appropriate to the production of reaction mixtures with 1.8 - 20.9 wt% crosslinker (4x - 60x) were therefore produced by Chakrabarty's protocol. Unfortunately, none of these pre-mixtures were observed to form the "highly viscous, whitish nanoparticle/PDMS dispersions" reported by Chakrabarty.[157] All pre-mixtures produced by this method were found to consist of dull, unevenly surfaced, opaque, friable waxes. In testing a sample admixture containing the lowest concentration of untreated fumed silica (12.4 wt%, see Table II) employed in Chakrabarty's work was subjected to 25 consecutive one minute speed mixing cycles at 2,700 rpm., yet remained a hard wax.

The solidity of these admixtures (like the solidity of the earlier mechanically hand mixed materials) was not surprising. By percolation theory (eq 41) Aerosil®300 aggregates form gel networks at a filler critical volume (φ_{cv}) of 7.8 vol% (p 50). Though the just mentioned extensively mixed low silica concentration compound (12.4 wt% = 5.9

vol%) contained much less than this critical volume of filler, that filler was introduced to the polymer as a powder with an effective volume fraction (0.71) much greater than that of spherical random close packing. Thus, the Krieger Dougherty viscosity relation (eq 25) would predict the observed solid admixture. Depending as it does on the properties (characteristic size and fractal dimension) of silica aggregates the percolation relation would only predict a liquid admixture if dispersive mixing had reduced the initial uFSN agglomerate structure to that of its constituent aggregates. Since this and the other Chakrabarty protocol admixtures remained solid after extensive mixing it is possible that, like earlier mechanical hand mixing, speed mixing alone could also not disperse Aerosil®300 agglomerates to the roughly 100nm size of Aerosil®300 aggregates.

Verbally the earlier researchers reported that they dried their fumed silica before use. On the chance that their silica drying had been less effective than that conducted in the course of the current work, a pre-mixture containing 14.2 wt% un-dried uFSN in 26k hydroxy PDMS was subjected to 10 consecutive SpeedMixer™ cycles at 2,700 rpm. At the completion of mixing the sample remained a solid wax. Chakrabarty's work also included the examination of a number of samples in which uFSN was replaced by hexamethyldisilazane (HMDZ) treated fumed silica. Thinking that the inadvertent use of tFSN might have resulted in the reported viscous pre-mixtures, an admixture containing the highest concentration of untreated filler reported in Chakrabarty's work was created using 15.5 wt% of treated fumed silica. A single 1 minute SpeedMixer™ cycle at 2,700 rpm sufficed to reduce this tFSN/PDMS pre-mixture to a highly viscous liquid.

As had been done for Hand Mechanical Mixing, two uFSN pre-mixtures for high crosslinker concentration (45x and 60x) reactions were produced by the Chakrabarty protocol in the hope that the addition of the large required amounts of low viscosity crosslinker during reaction-mixture production would thin the overall mixture. Though somewhat lower viscosity reaction-mixtures did result, they were still found to be too thick to allow cover slips to be coated by dipping. At best, the waxy reaction mixtures could be smeared onto cover slips, and samples so coated proved too rough for AFM imaging regardless of how they were cured. Spin coated samples containing 16.6 and

20.9 wt% crosslinker (45x, and 60x) were successfully produced and cured at both ambient and 100ºC. However, though numerous attempts were made to examine these films under AFM in both the Veeco and Asylum instruments at a number of tapping ratios from hard to soft and at a variety of phase angles, none resulted in usable images. One instrument operator thought that the light weight of the cover slips was allowing the sample to move while being imaged. To compensate one cover slip sample was taped to a heavier microscope slide, but this did not improve imaging. A small sample was also peeled from a cover slip using a razor and super-glued to a microscope slide, but this also did not improve imaging. In some cases the instrument operator believed the samples exhibited surface roughness beyond that which the instrument would tolerate. In other instances the operator believed that the material was so soft that penetration and stickiness made it impossible for the instrument to consistently detect a surface.

Heated Speed Mixing

Early Development

The primary obstacle to reproducing the earlier work appeared to be an inability to produce sufficiently liquid reaction-mixtures for dip and spin coating. In Chakrabarty's work it was noted that reaction-mixtures became significantly warmer during mixing due to frictional heating. Indeed, even though it did not liquefy, the sample mixed 25 times in the current work became so hot that it could not be comfortably handled. Thinking that warm uFSN/PDMS pre-mixtures might more readily form viscous reaction-mixtures, a sample containing 12.4 wt% fumed silica (-14% uFSN composition for a 4x reaction-mixture) in PDMS was mixed 4 times by Chakrabarty's high speed protocol to produce a characteristically lumpy surfaced, opaque, hard waxy compound. This material was then heated in an oil bath to 100ºC for 2 hours. At the end of that time the sole visible change was that the lumpy surface had acquired a glossy sheen. The sample was left at ambient overnight, and when examined the following day the still shiny surface was found to have self-leveled. Since no pre-mixture sample had yet been observed to self-level, it was thought that heating might have reduced the mixture viscosity to the point where flow might be observed over long periods. The mixture was returned to the oil bath and heated

to ~110ºC for from 2 to 3 hours, but when removed no further change was apparent. Serendipitously, it was decided to return this solution to the SpeedMixer™ for an additional 60 second mixing cycle at 2,700 rpm. Surprisingly, the remixed sample was found to have become a highly viscous, but slowly pourable, whitish liquid.

To this viscous pre-mixture were added 1.8 wt% of ES40 (4x composition) and 0.5 wt% of tin catalyst. The reaction-mixture was then mixed for six one minute cycles at 2,700 rpm. Dip coated, spin coated, and poured samples were then prepared from the reaction mixture and cured at either ambient temperature or 100ºC for 72 hours. At the end of that time, no sample was found much cured. The dip coatings resembled those of earlier solvated mechanically hand mixed samples. All dip coated slips were found unevenly covered by a fine translucent granular material embedded in a thin oily base. Spin coated samples were similar; but, because little material had remained on the cover slips after spin coating, they were much more sparsely covered in both oil and granular material. From earlier experience with uncured admixtures neither dipped nor spun samples were considered suitable for AFM imaging. Samples poured to Petri plates and cured remained slightly opaque viscous oils, but contained no inclusions or bubbles visible to the naked eye (Figure 11).

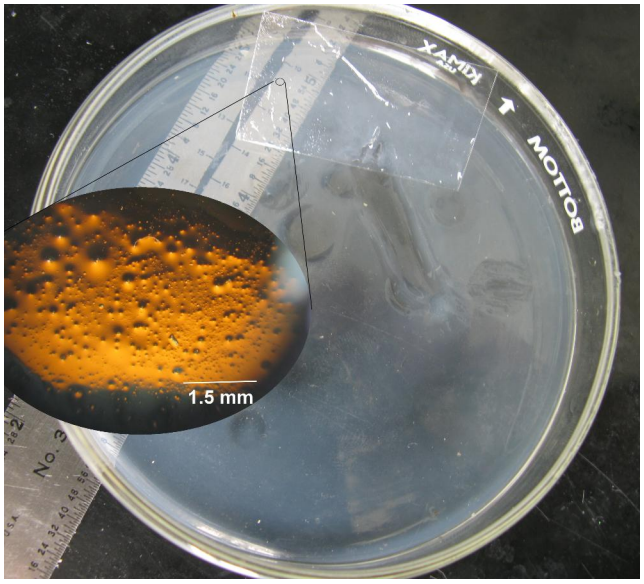

Figure11. Early low-crosslinker, non-curing Heated SpeedMixed™ reaction mixture (Inset – 20X image of cover-slip surface coated with same)

Remembering that plated samples of low-crosslinker "solvated mechanically hand mixed" reaction-mixtures had also failed to cure, while similar samples containing higher levels of crosslinker had been found somewhat better cured, a pre-mixture containing 13.1 wt % uFSN (14x-14 composition) was produced. Initial mixing was by Chakrabarty's high speed protocol (4 one minute cycles at 2,700 rpm). However, due to difficulty maintaining oil bath temperature, heat-processing consisted of an initial heating to 120ºC rather than 100ºC for 2 hours, and a secondary heating to 110ºC for 2 rather than 2 to 3 hours. Post heat-processing secondary-mixing was also different. A single one minute cycle at 2,700 rpm proved insufficient to cause a solid to liquid transition. Mixing for an additional 4 cycles at 2,700 rpm followed by 5 mixing cycles at 3,500 rpm was required to reduce the mixture to a barely pourable form. Appropriate quantities of ES40 and catalyst for this composition were added, and the reaction-mixture was mixed for an additional 6 cycles at 2,700 rpm. However, even with the thinning crosslinker and after this much mixing the material was visibly much more viscous than the earlier 4x reaction-mixture.

Two cover slips were dip coated with the new reaction-mixture and the remainder was poured into a Petri plate. The plate and one slip were cured for 3 days at 100ºC. The other slip was cured for the same period at room temperature. Though the earlier plated low-crosslinker mixture had spread and self-leveled to cover the bottom of the Petri plate, the current mixture was found to have only spread enough to cover a roughly circular area approximately 4.4 cm in diameter in the center of the 9.5 cm diameter plate. Visibly, the cured product was found to be slightly opaque and filled with a multitude of small bubbles. However, the product was also found to be a gratifyingly solid elastomer. Regardless of curing temperature, both cover slips were found coated with an identical, uneven, partially bubble filled, solid material. Visibly, these coatings were reflective and slightly opaque Viewed at an angle numerous granular inclusions could be discerned embedded in their surfaces (Figure 12). Though AFM imaging of these slips was attempted, no useable images were obtained.

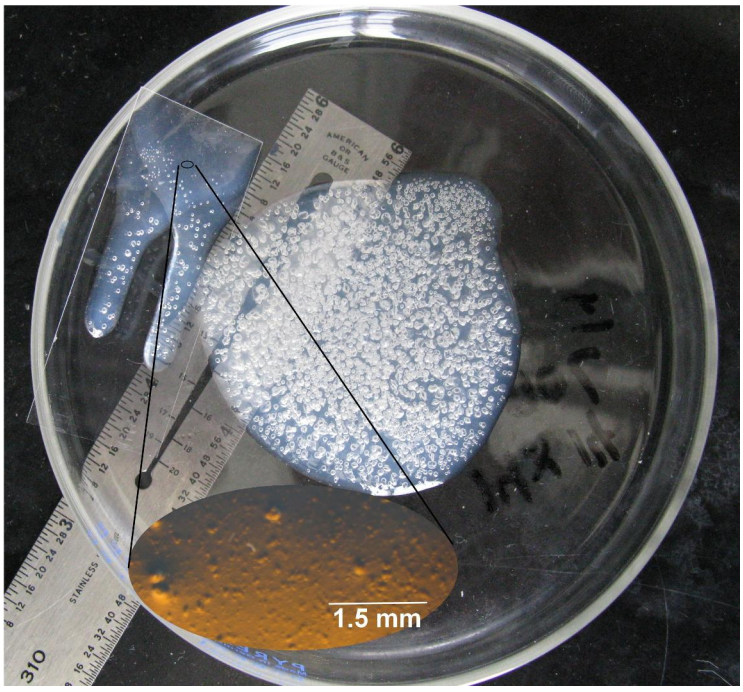

Figure 12. Early cured 5.9 wt% crosslinker elastomer
(Inset – 20X image of cover-slip surface)

Another pre-mixture of 13.1 wt% uFSN (nominally 14 wt%) in PDMS was prepared. Initial mixing consisted of 4 cycles at 2,700 rpm. Just one heating of the pre-mixture to 110ºC for 2.5 hours was made. To better control thermal processing a glassware drying oven was used in place of the oil bath. After heating only 2 secondary mixing cycles at 2,700 rpm were required to reduce the waxy solid pre-mixture to an opaque viscous liquid. ES40 to 5.9 wt% reactants (14x) and 0.5 wt% catalyst were added, and the reaction-mixture was subjected to 6 SpeedMixer™ cycles at 2,700 rpm. Two cover slips were dipped in the mixture and the remainder was poured in a Petri plate. One slip and the plated material were cured at 100ºC, and the other slip was cured at ambient. Due to an intervening 3 day weekend, all materials were cured for 4 days.

After curing, cover slips were found coated with a rough granular material embedded in a thin coating of solid, almost transparent polymer (Figure 13). Except for the lack of bubbles, these samples visibly resembled the coatings that had resulted from the just completed heated mixing experiment (Figure 12). Though repeated AFM imaging of these surfaces was attempted no usable images were obtained. The plated material was

found to have spread to cover the bottom of the plate with an approximately 2 mm thick, even layer of solid, bubble-free elastomer with a slight white (cloudy) appearance. This material was close in character to the "best" silicone elastomer which was desired for the undergraduate experiment that had in part motivated this study, so an effort was made to determine the processing conditions responsible for such even, translucent, bubble-free films of uFSN filled condensation cured silicone elastomer. This sample was considered the first example of such a material, and was designated "26k-13.1-5.9-p110C-2.5hr-c100-4d." The first three terms describing respectively, the sample polymer MW, pre-mixture filler wt%, and reaction-mixture crosslinker wt%. Terms 4 and 5 were added to describe the temperature (ºC) and duration (hrs.) of pre-mixture thermal treatment, and the last 2 terms were added to describe reaction-mixture curing temperature (ºC) and period (days).

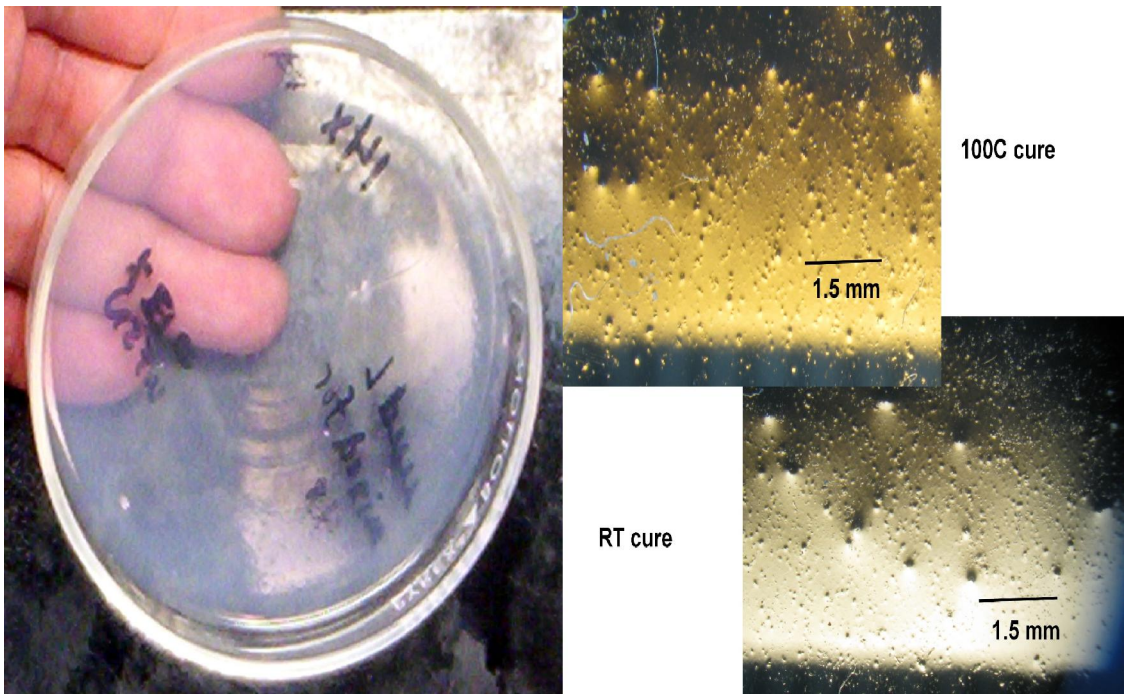

Figure 13. 26k-13.1-5.9-p110C-2.5hr-c100-4d and 20X images of coated Cover-Slips

Mixing Parameter

During the production of over 70 elastomeric samples, the rotational speed and number of SpeedMixer™ cycles were varied in order to determine optimal mixing

conditions. This experimentation revealed that primary mixing for 3 cycles at 3,500 rpm before process heating, and secondary mixing for two cycles at 3,500 rpm after process heating was sufficient to reduce the vast majority of pre-mixtures to a viscous liquid form. A further final mixing for 2 cycles at 3500 rpm after the addition of crosslinker and catalyst to the liquid pre-mixture was found to reliably produce curable reaction-mixtures. Figure 14 compares two 100X images of cured plated elastomers. One is of the just described first successful sample mixed at 2,700 rpm under a Chakrabarty-like protocol (Figure 13). The other is of a sample of identical composition mixed by this optimized 3,500 rpm protocol. The optimal protocol, using fewer, higher speed mixing cycles, was found to achieve much better dispersion and distribution of filler. Over time this 3,500 rpm protocol was adopted as the mixing parameters for a Standard Heated Speed Mixing protocol [SHSM].

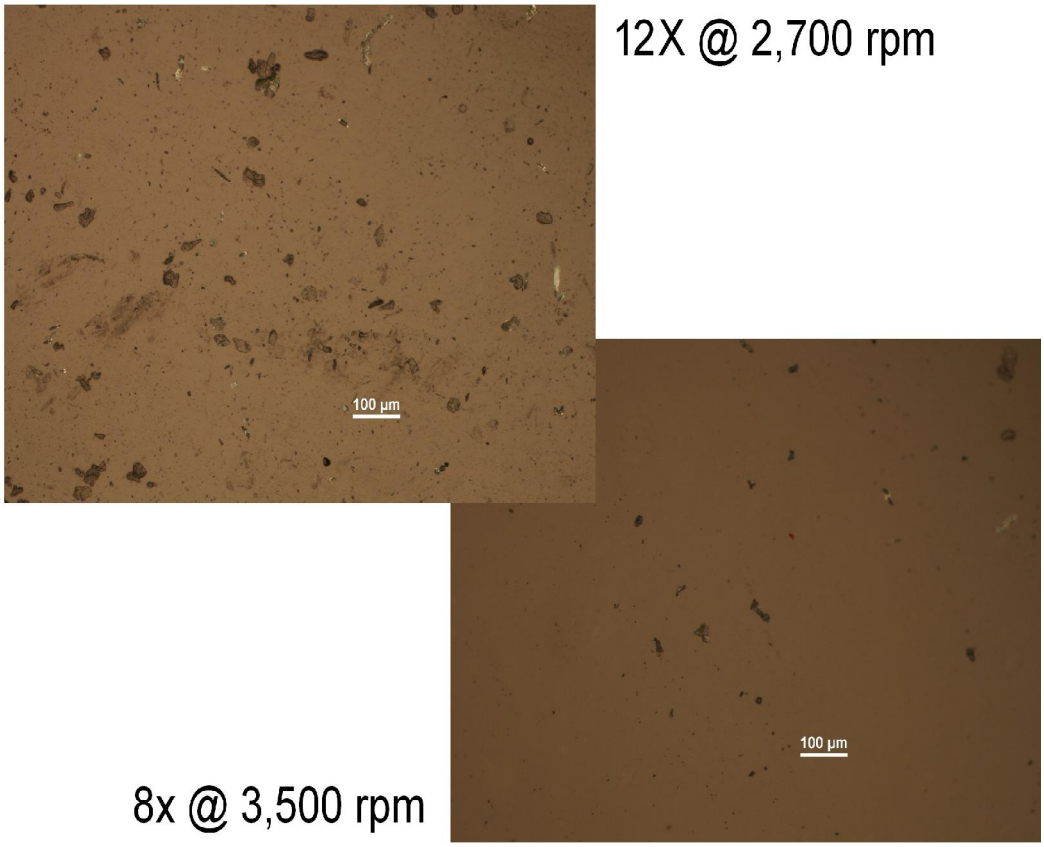

Figure 14. 100X images of plated 26k-13.1-5.9-p110C-2.5hr-c100-4d samples Mixed under Chakrabarty and Standard conditions

Minimal Crosslinker

After mixing conditions, the first processing variable investigated was low crosslinker concentration. Solvated mechanical hand mixing and the first heated SpeedMixer™ experiments had shown that little curing took place when 1.8 wt% (4x) of crosslinker was employed, while full curing to a solid material took place when 5.9 wt% (14x) crosslinker was used. Several reaction-mixtures containing 3.5, 5.0, and 5.4 wt% (8x, 11x, 12.5x) ES40, 0.5 wt% catalyst, and viscous SHSM pre-mixtures containing 12.7, 12.9, and 13 wt% (-14) uFSN respectively were produced. Most samples were process-heated for 2.5 hours at 113ºC, but one sample was accidentally processed at 118ºC. An additional reaction-mixture containing an unheated 12.4 wt% (-14) uFSN pre-mixture, 1.8 wt% (4x) crosslinker, and appropriate catalyst was also produced. All samples were cured at 100ºC for 72 hours.

Figure 15 compares several of the resulting elastomers. The majority of low crosslinker concentration samples (including the sample that was not process heated) were sufficiently uncured that finger pressure could permanently indent the material. At 5.0 wt% this deformability was small, and at 5.4 wt% no deformability was observed. For materials cured at 100ºC, none containing 5 wt% (11x) or less crosslinker and untreated filler were ever observed to fully cure into solid elastomers during the course of this investigation. However, a sample containing PDMS without filler was found to cure to a solid elastomer at 1.8 wt% (4x) crosslinker. From published values (pp 31 - 32) it was calculated that Aerosil® 300 presents 2.26×10^{-4} mole SiOH/g. For the examined reaction mixtures it can be determined that the ratio of reactive ES40 Si-O groups to the sum of fumed silica surface silanols and PDMS chain terminating silanols passes through 4 as the crosslinker concentration increases from 5 to 5.4wt% (3.94 @ 5 wt%, 4.26 @ 5.4 wt%). Such a ratio appeared to be the minimum crosslinker necessary for solid elastomer formation in these dried uFSN filled PDMS systems and likely indicates that silica silanols compete with siloxane silanols in the crosslinking reaction.

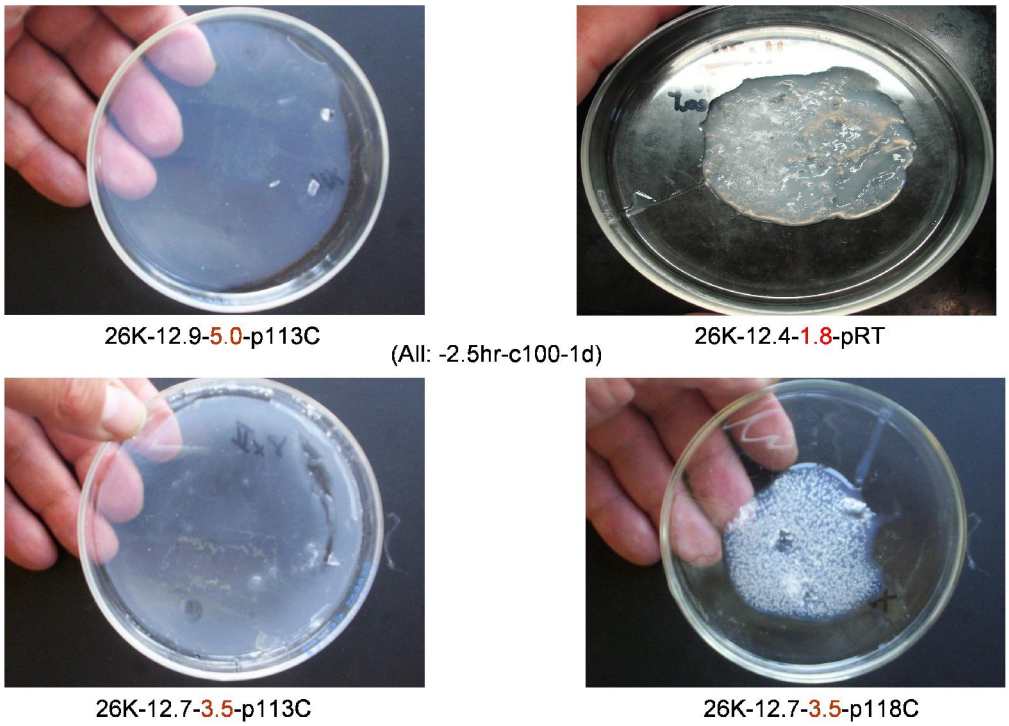

Figure 15. Effect of Low Crosslinker Concentration

Process-Heating Temperature

The samples containing pre-mixtures heat processed at ambient and at 118ºC were too thick to spread on the plate and when cured at 100°C both contained bubbles. The formation of bubbles in some of these finished elastomers indicated that bubble formation might be not just curing-temperature dependent as was observed during the production of films from solvated admixtures, but also process-temperature dependent. Accordingly, a series of cured samples containing pre-mixtures that had been heat processed over a range of temperatures was produced. Representative examples are shown in Figure 16. As had been noticed during the earliest heated speed mixing experiments reaction-mixtures were more viscous (based on a failure to spread) when their pre-mixtures had been heat processed at <110°C (Figure 16, pRT and p105C images). It was surprising however to find that otherwise identical reaction-mixtures were also more viscous (again based on failure to spread) when their pre-mixtures had been heat processed at temperatures above 115ºC (Figure 16, p117C and p120C images).

Though not readily apparent in these images, all of the poor spreading, higher viscosity reaction mixtures were also found to be bubble filled when cured. Extensive experimentation revealed that when cured at 100ºC only reaction mixtures containing pre-mixtures heat processed at temperatures between 110 and 115ºC yielded level, fully spread, bubble-free, finished elastomers. Pre-mixtures processed even a few degrees below 110ºC (Figure 16, 13.5 wt% crosslinker, p105C), or a few degrees above 115ºC (Figure 16, 11.1 wt% crosslinker, p117C) were found to be too viscous to self level (fully spread) and displayed some degree of bubble formation in the finished elastomer.

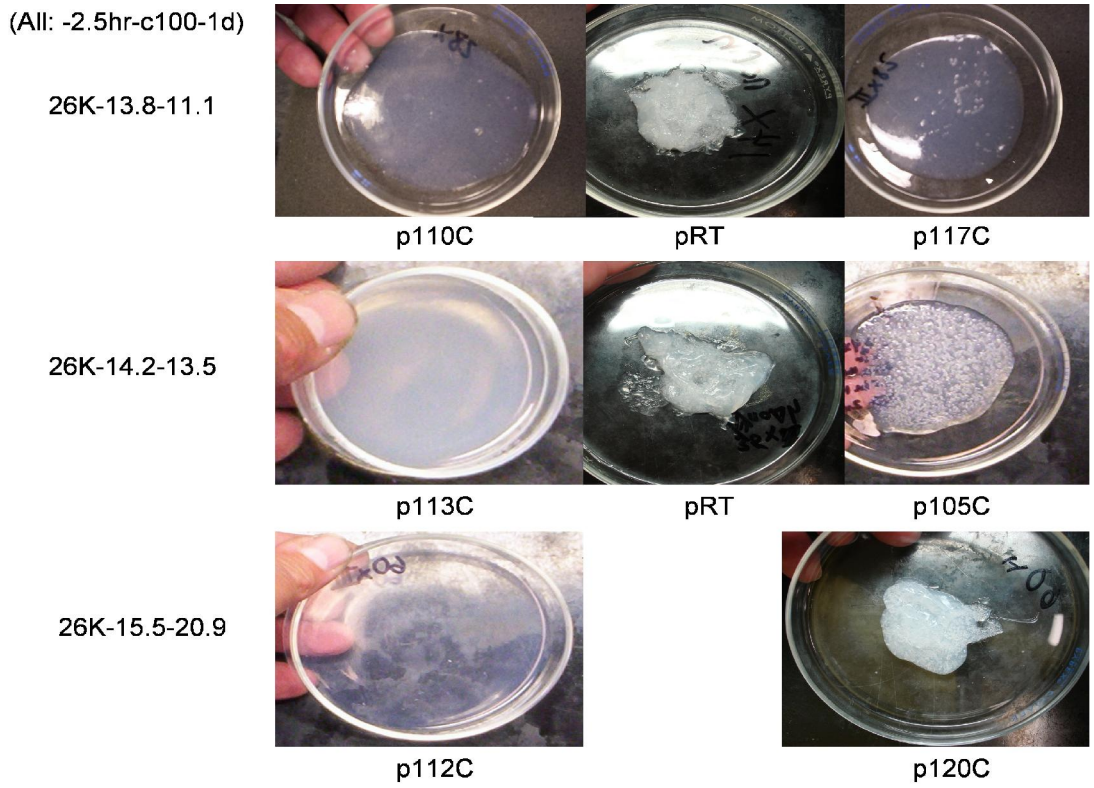

Figure 16. Effect of variable heat processing temperature.

Process-Heating Period

Bubble-free elastomer formation was also found to depend on the period of pre-mixture heating. Pre-mixtures heated processed at 110-115ºC for as little as half an hour above or below 2.5 hours were found to produce bubble-filled elastomers, while otherwise identical samples heat processed for 2.5 hours did not (Figure 17).

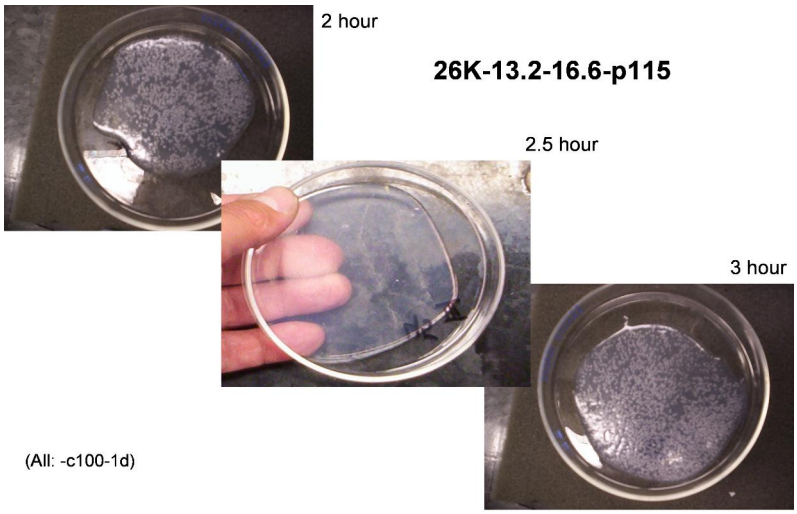

Figure 17. Effect of variable heat processing time.

It also did not prove possible to heat process admixtures at a lower temperature for a longer period (Figure 18, p105C-3hr) or at a greater temperature for a shorter period (Figure 18, p120-2hr) without also generating bubbles in the thermally cured product. Bubble-free materials of low crosslinker content could be produced regardless of heat processing period if pre-processing temperature was restricted to the bubble-free range (Figure 18, 1.8-p112C-3hr). However, like all other low crosslinker compounds, none of these mixtures cured to solid films.

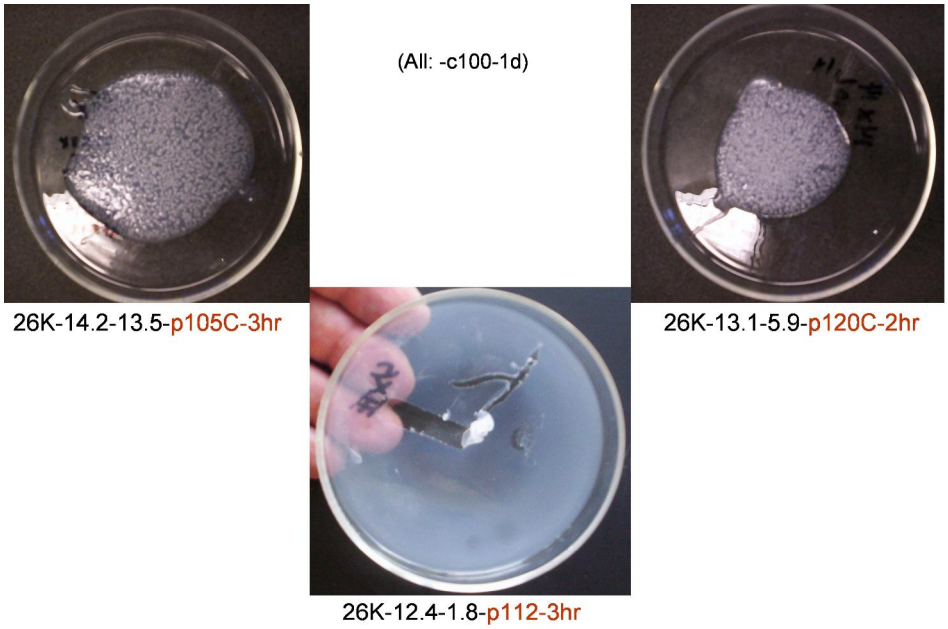

Figure 18. Effect of variable crosslinker heat processing time and temperature.

To summarize, for materials containing dried uFSN that were cured at 100ºC, solid polymers were only observed for samples containing over 5 wt% crosslinker, and translucent, bubble-free, even, polymer films were only observed for samples containing pre-mixtures heat processed at temperatures between 110 and 115ºC for 2½ hours (Graph A).

Graph A. % Cross Linker / Filler vs. 2.5 Hr. Process Temperature (100ºC Cure)

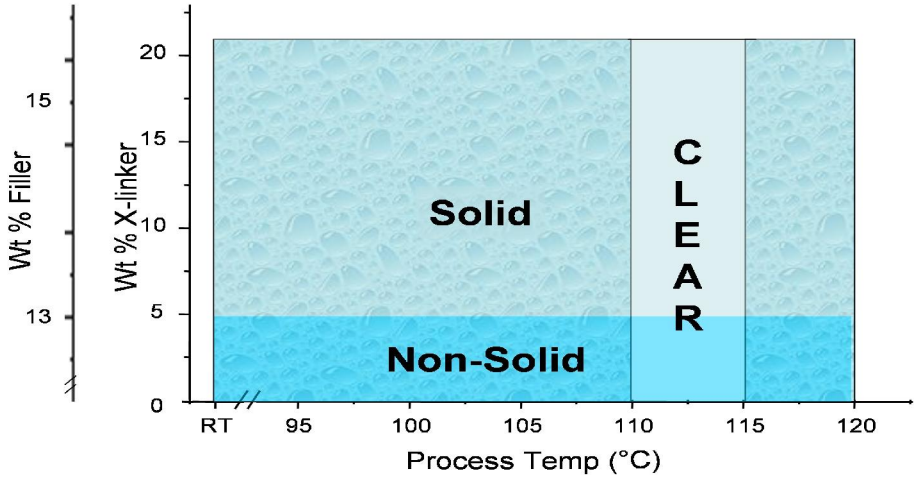

Curing Temperature

In confirmation of earlier observations for solvent thinned admixtures, bubble formation in finished elastomers containing heated, sheared viscous admixtures was also found to be curing temperature dependent. A range of reaction-mixtures containing pre-mixtures process heated over an ambient to 120ºC range for from 2 to 3 hours were all found to form bubble free films when cured for 24 hrs. at room temperature (Figure 19, cRT samples). However, all samples containing pre-mixtures thermally processed outside of the 110°C - 115ºC range formed thicker reaction-mixtures than those processed within this range (Figure 19, p105 and p120). When cured at either RT or 100ºC these thicker reaction-mixtures were found to fail to fully spread into even films. Samples of low crosslinker concentration materials cured at ambient, though free of bubbles, were not found to form fully solid elastomers, just as had similar samples cured at 100ºC (Graph B).

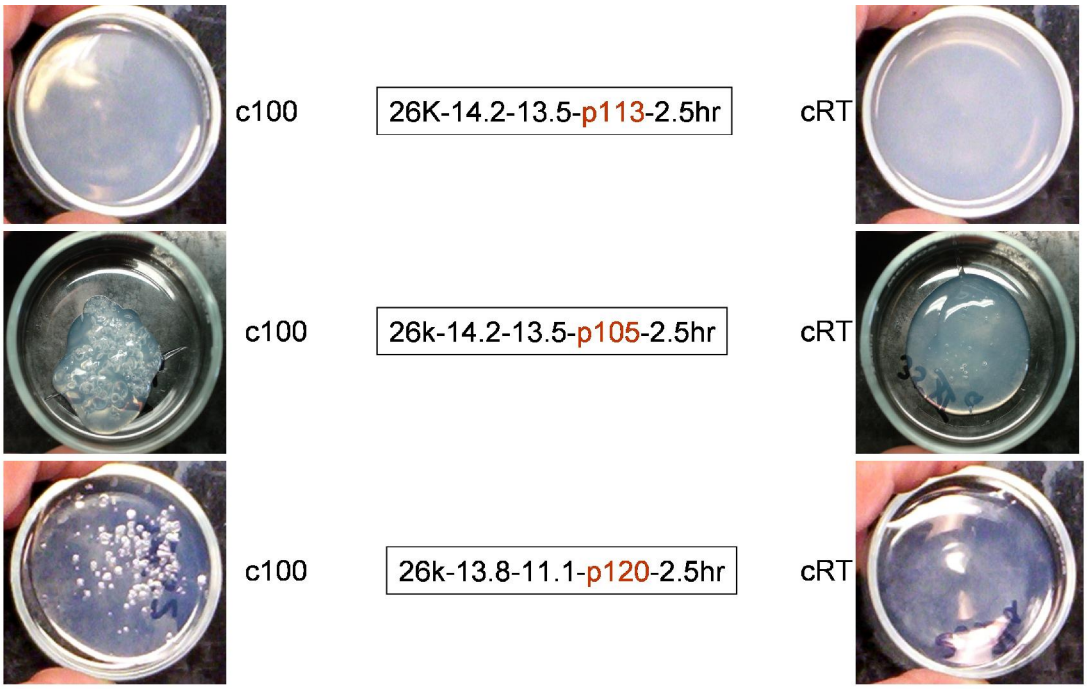

Figure 19. Effect of variable process heating and curing temperatures.

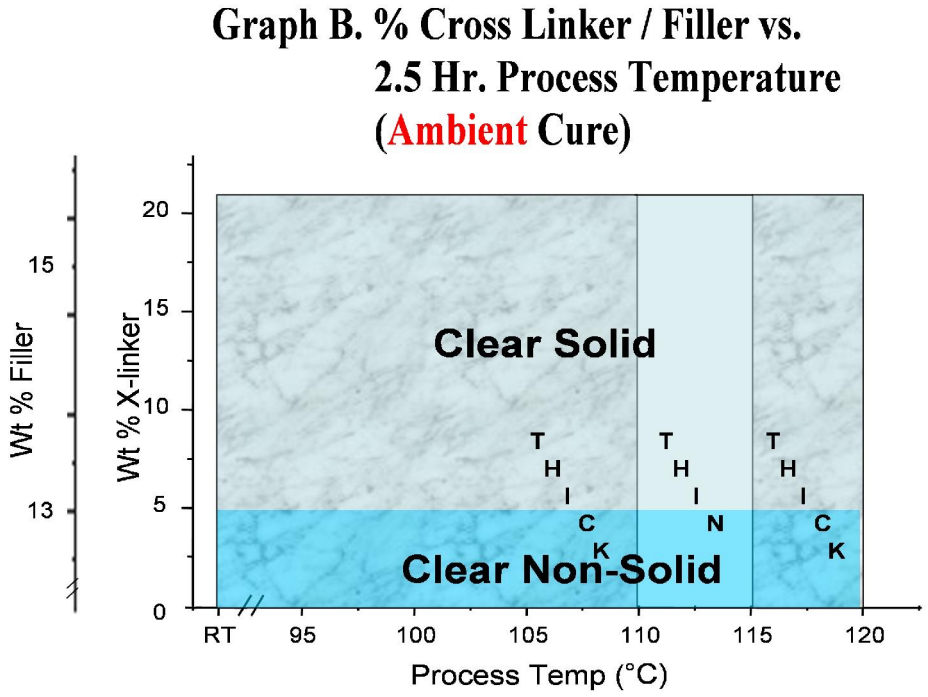

Curing at RT or 100ºC was found to result in the desired solid bubble free elastomer films only for materials containing over 5 wt% crosslinker combined with pre-

mixtures process heated for 2.5 hrs at 110°C to 115°C. Though RT cure was employed in the production of some elastomer samples in order to ensure that finished elastomers were unaffected by curing temperature and for comparison with the results of earlier experimenters, most samples were cured at 100ºC. With curing conditions defined, the following standard heated speed mixing [SHSM] protocol (Table 3) was adopted for the production of untreated fumed silica filled condensation cured silicone elastomer in further experimental work and was proposed as a standard protocol for undergraduate laboratory work.

Table 3. Standard Heated Speed Mixing Protocol

Pre-Processing

Admixture - Combine uFSN and PDMS in SpeedMixing cup.
Primary Mixing – SpeedMix for 3 one minute cycles @ 3,500 rpm.
Process Heating – Heat to 110-115ºC for 2.5 hours.
Secondary Mixing – SpeedMix for two 1 minute cycles @ 3,500 rpm.
Viscous pre-mixture

Reaction-Processing

Reactant Addition - Add crosslinker and catalyst to viscous pre-mixture.
Final Mixing – SpeedMix for two 1 minute cycles @ 3,500 rpm.
Sample Preparation – pour, dip, spin reaction mixture.
Curing – Maintain samples at ambient or 100ºC for 24 to 72 hours.
Finished Elastomer

SHSM Elastomer

Cover Slip Films: Imaging

While experiments to determine the conditions for Standard Heated Speed Mixing were being conducted, the experimental mixtures were also combined with appropriate crosslinker and used to dip and spin coat cover slips. Figure 20 shows typical examples of 100ºC cured, dip coated cover slips containing the range of crosslinker concentrations that produced solid, bubble-free films under SHSM conditions. All coatings, though solid, were soft, uneven, and contained gelled/granular inclusions. Dip coated SHSM samples cured at room temperature were visually indistinguishable from those cured at

100ºC. Spin coated samples were essentially identical to dip coated differing only in that spin coating resulted in somewhat thinner films. Figure 21 compares 20 times magnification micrographs of a dip coated film containing 5.9 wt% (14x) crosslinker and a similar micrograph of a spin coated film containing 16.6 wt% (45x) crosslinker. Though AFM examination was attempted, these surfaces also would not image.

Figure 20. Cured solid dip coatings of 14 wt% uFSN in PDMS with 5.4 to 20.9 wt% (12.5x – 60x) crosslinker (L → R) from Standard Heated Speed Mixing.

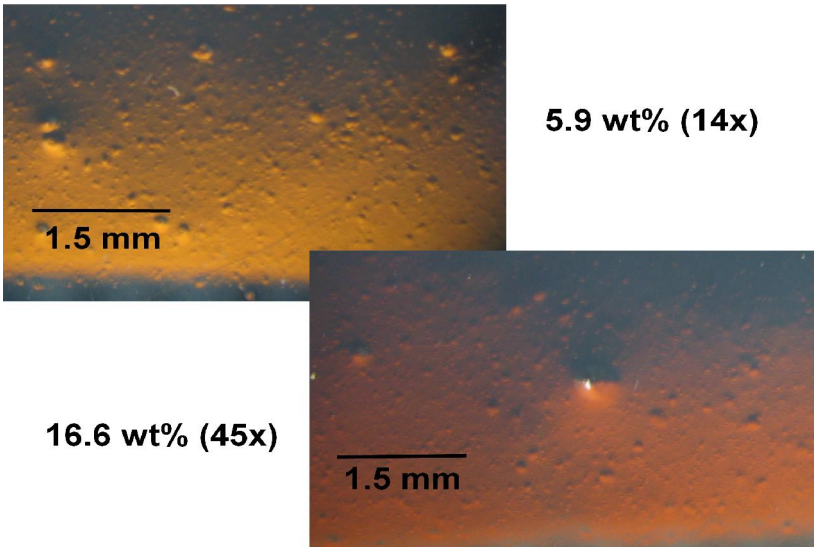

Figure 21. SHSM dip (upper) and spin (lower) coated surfaces (20X).

Poured Films: AFM

SHSM processing was employed to synthesize a series of elastomers containing from 5.9 to 20.9 wt% (14x to 60x) of ES40 crosslinker and sufficient Aerosil® 300 to result in cured elastomers containing 14 wt% uFSN. Unlike earlier samples these were poured to, and cured in, PTFE pans to facilitate the removal of elastomer plaques for later mechanical testing. Having been less than successful in producing elastomer films that could be examined by AFM through dip or spin coating, it was decided that thin poured films might prove more suitable. Accordingly, during the preparation of these plaques, small quantities of each reaction solution were also poured into the chambers of 2 well biological microscope slides. The side walls of the wells were carefully removed after curing, and the edges of the cured elastomer were trimmed to produce flat films approximately a millimeter thick. The surfaces of these films were examined by AFM on both a Veeco and Asylum instrument. After imaging some films were frozen in liquid nitrogen, fractured and examined by Asylum AFM for bulk morphology. Resulting images are presented in Appendix A.

Variations in phase angle indicative of harder Filler and softer PDMS regions were clearly visible on all images regardless of crosslinker content. On initial examination using the Veeco instrument it seemed that little silica was detected during a 20 µm by 20 µm scan of the 45x sample. This sample was reimaged at 20 µm by 20 µm using an Asylum AFM. The images from the two instruments are compared in Figure 22. Light and dark regions were clearly visible on the Asylum image. On closer examination the Veeco image was found to contain a multitude of faint discreet lighter regions dispersed in a darker matrix that might correspond to similar more distinct regions observed in the Asylum image. At a scale of 2 µm (Appendix A) images from both instruments displayed phase angle variations indicative of hard and soft regions. Regardless, the presence of regional phase variation in the Asylum images indicates the detectable presence of silica at all crosslinker concentrations even if the Veeco instrument did not always clearly reveal it.

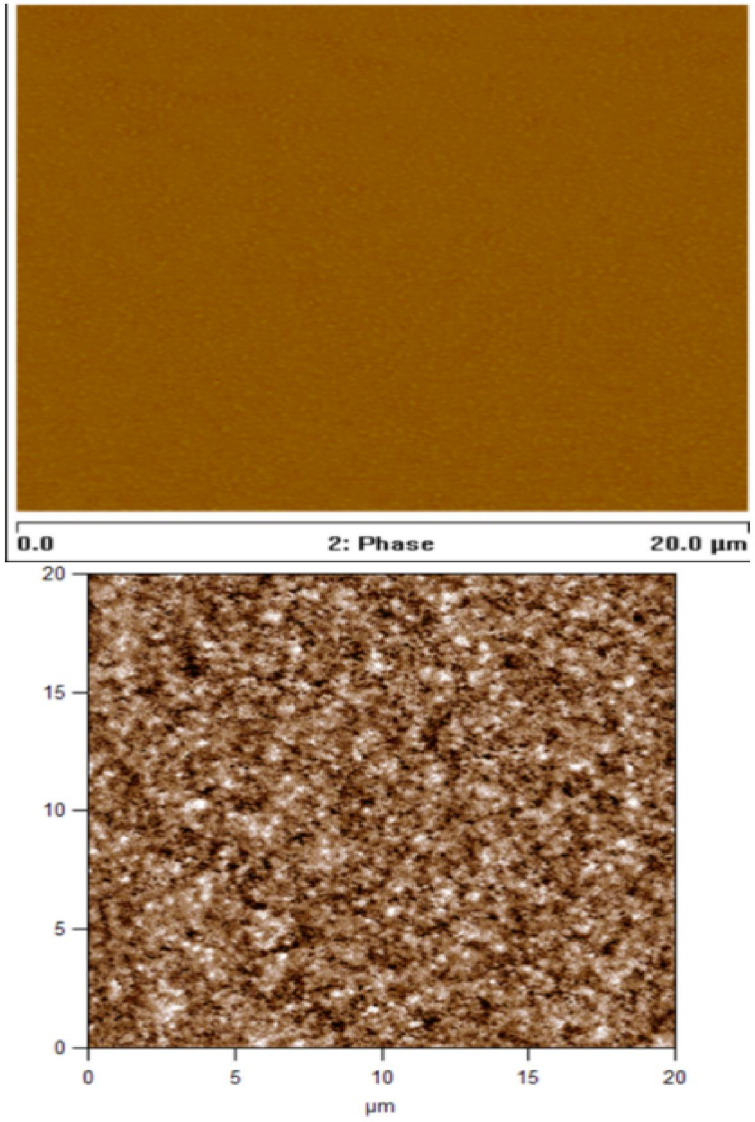

Figure 22. Comparison Veeco (top) and Asylum (bottom)
AFM images of the same 28x sample.

As in Chakrabarty's work silica was easily visible at a soft tapping set point ratio of 0.8. Unlike some earlier work, hard tapping was not required to reveal the silica. At this point, efforts to replicate the earlier inconsistent AFM results that had initially motivated this work were regretfully halted. It was felt that the newly developed Standard Heated Speed Mixing protocol differed too much from the techniques described in earlier work to give comparable results. It seems likely that earlier mixing techniques would have yielded inhomogeneous admixtures containing poorly dispersed and poorly

distributed uFSN. Such admixtures would be expected to cure to similarly inhomogeneous elastomers. The 14x composition at which Ogoshi and Inagi observed the disappearance of silica consisted of a cured elastomers containing > 91 vol% polymer. These researchers AFM imaged square regions of elastomer 5 μm - 0.5 μm on a side respectively. At the scale of silica agglomerates an inhomogeneous mixture containing < 9 vol% poorly dispersed silica might present some surface regions where little or no silica is present. If for some crosslinker concentration only silica-free regions were by chance imaged, while for other concentrations only silica bearing regions were imaged, then it might appear that fumed silica filler became undetectable by AFM on the surface of elastomer at certain crosslinker concentrations. This result would not be expected for elastomer synthesized with viscous liquid admixtures since the uFSN in these mixtures is dispersed to evenly distributed aggregates.

Poured Films: Mechanical Properties

Multiple dog bone samples of crosslinked elastomer unfilled, or filled with either 14 wt% tFSN, or 14wt% uFSN from SHSM were subjected to stress-strain testing to determine characteristic rupture stress and percent elongation (strain) at break. Results for samples containing 14x crosslinker are summarized in Table 4. Both treated and untreated fumed silica made significant improvements to the ultimate rupture stress and elongation at break of the silicone elastomer. The variation in the treated and untreated values lay within the standard deviation of either, thus the best that can be said is that the degree of improvement afforded by either filler to the ultimate tensile strength (~600%) or elongation at break (~200%) of the elastomer was about the same.

Table 4. Filler Reinforcement of Silicone Elastomer

	Rupture Stress (MPa)	Improvement %	Strain at Break (% elongation)	Improvement %
14x-No Filler	0.33	-	39.89	-
14x-14% uFSN	2.06	627	81.12	203
14x-14% tFSN	2.15	654	73.07	183

Over a range of crosslinker concentrations (14x to 60x) the ultimate tensile strength of the uFSN filled silicone elastomer appeared to increase by ~50% while the tensile strength of the tFSN filled elastomer remained roughly unchanged (Graph C). However, almost all crosslinker comparable stress results for the two materials were within a respective standard deviation of each other and linear fits were of poor quality, therefore this result is uncertain. Increasing crosslinker would be expected to increase mechanical strength of both uFSN and tFSN filled elastomers, due to increasing quantities of formed-in-place silica. More testing will be required to resolve this discrepancy. Nevertheless, it does appear that crosslinked elastomer containing the viscous admixture displays ultimate tensile strength similar to that of elastomer containing equivalent quantities of crosslinker and tFSN.

Graph C. Rupture Stress uFSN and tFSN (14 wt%) Filled Elastomer with Increasing Cross Linker

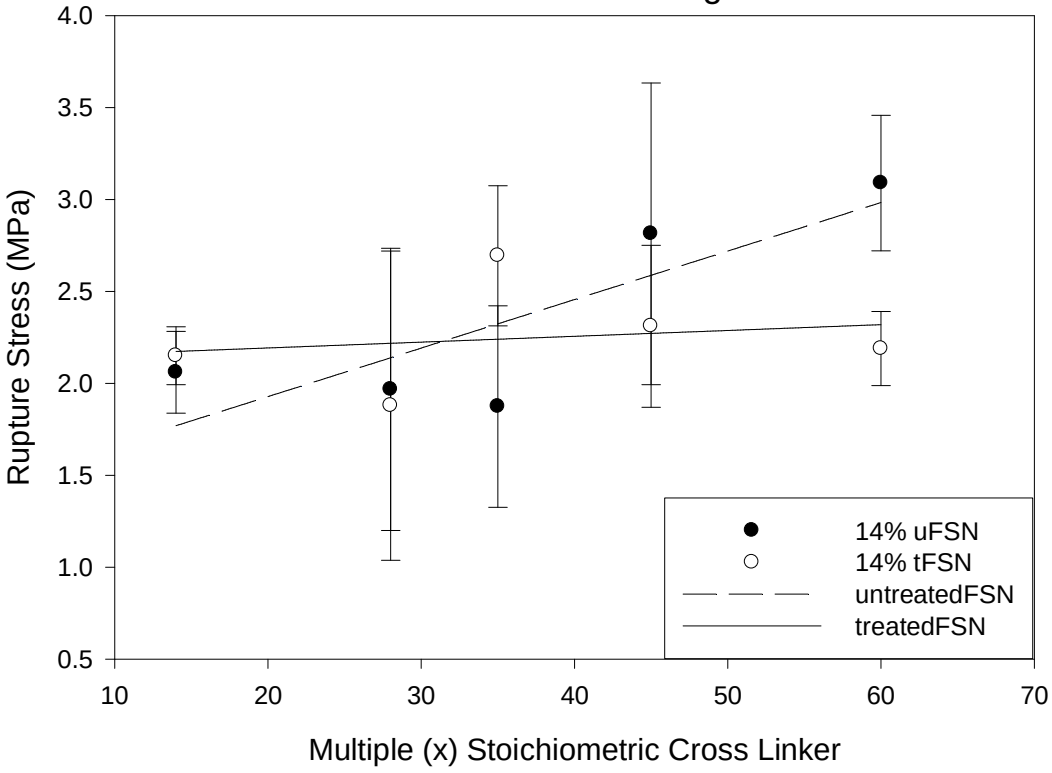

The percent elongation at break (rupture strain) of samples filled with either treated or viscous liquid untreated silica was also found approximately the same (within

SD) at any given crosslinker concentration with the extensibility of both materials decreasing exponentially as a function of increasing crosslinker (Graph D). A decrease in rupture strain as larger quantities of formed-in-place silica increased polymer crosslinking would be expected for both filled materials.

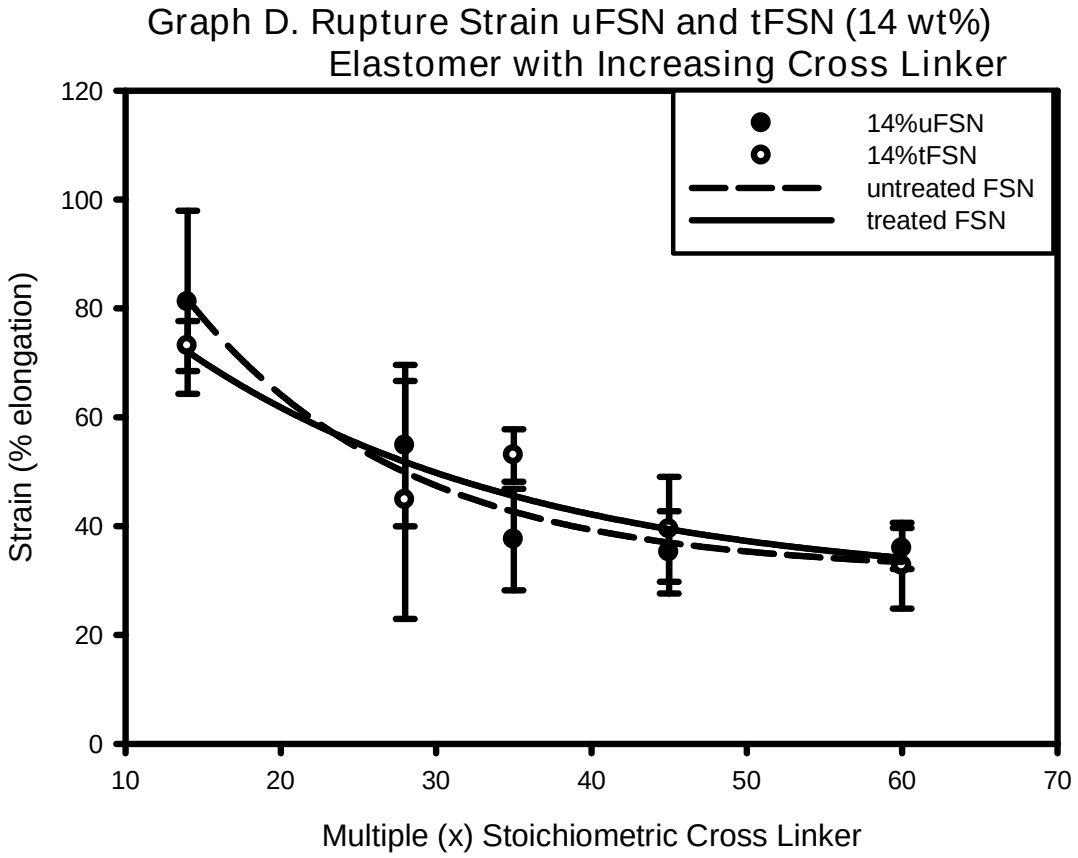

Pre-Mixture Liquefaction

The most striking phenomena observed in this work was the solid to liquid transition exhibited by heated uFSN/PDMS pre-mixtures during secondary high shear mixing (Figure 23). The two sources found in the literature that reported softening/liquefaction of PDMS/silica admixtures (DeGroot and Macosko, and Selimovik et al.,) both concluded from rheological data that the initial solidity of these mixtures was likely due to the presence of a solid silica-silica network within a polymer matrix[163, 164]

Both sources also believed that the observed softening/ liquefaction of these admixtures was due to the dispersive breakdown of the contained silica networks (summarized pp 58 – 60).

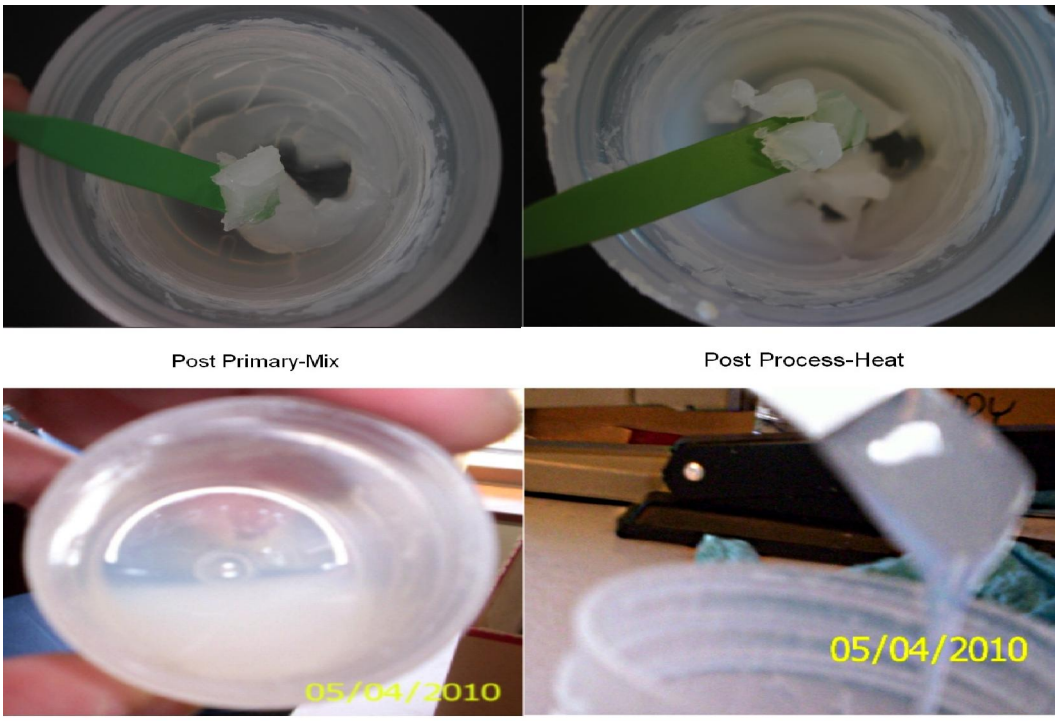

Figure 23. Example of PDMS/uFSN gel Liquefaction.

Dynamic Light Scattering

It had been assumed that a reduction in fumed silica particle size occurred during high shear speed mixing, but at no time had the extent of such dispersion been tested. Therefore, Dynamic Light Scattering was employed in an effort to determine the size of the fumed silica particles present in pre-mixtures during the several stages of pre-processing. While preparing PDMS diluted samples (1% or less solids) of pre-mixtures for examination by light scattering, it was noted that those containing fully pre-processed viscous liquid admixtures would easily pass through a 200 nm filter. It was also found that such a filter would rapidly clog when used to filter samples that contained solid admixtures that had only been pre-mixed, or had only been pre-mixed and process-heated. It was therefore concluded that secondary mixing of heated mixtures had

successfully reduced the size of most, if not all, of the silica particulates (agglomerates) in the initially solid admixtures to particles <200 nm in size (aggregates).

Though the preparation of samples for DLS yielded valuable data, examination of those samples by DLS was far less informative. For the dilute samples containing solid admixtures at suggested concentrations and whether filtered or not the instrument repeatedly returned the message: "data collected is unsuitable for analysis." A large excess of PDMS was used to solvate samples. It had been hoped that by using PDMS as a solvent the fumed silica within the pre-mixtures could be examined in an undamaged, native state similar to that found in the admixture. Perhaps this effort was too successful, since the incompletely pre-processed materials were never found fully dispersed in excess PDMS. These samples were always found to contain some ghostly translucent masses regardless of how much they had been mixed or how long they were allowed to stand. In unfiltered solutions accurate DLS sizing would be unlikely, since the instrument manufacturer indicated in their literature that DLS is unsuited to the analysis of such gels.[165,] Filtration would likely remove these gels leaving little particulate in the filtered solutions, thus also confounding sizing by DLS.

In contrast, samples containing fully pre-processed materials, whether filtered or not, would solvate in excess PDMS without problem. Upon dilution the viscous pre-mixtures easily formed the slightly turbid liquids that the instrument manufacturer indicated were most suitable for DLS. The instrument gave Z average mean hydrodynamic particle diameters of 50 - 70 nm. However, the Z average polydispersities (PDI) reported for these diameters were always one and the manufacture advised that a Z average mean with a PDI over 0.5 was unlikely to represent the actual size of particles. Even for Z average means with PDIs of 0.1 to 0.4, manufacturer literature indicated that mean values could only be used to say that, for similar samples, the particles in one sample were larger or smaller than the particles in another.[150] In that regard the unfiltered samples containing liquid admixtures did give the higher mean diameter values, perhaps indicating that some quantity of particles larger than 200 nm had been removed from the samples by filtration. However, the spread of values for the filtered (50 ± 25 nm)

overlapped the spread of values for the unfiltered (70 ± 35 nm), thus even this conclusion is uncertain. The analysis software also always reported that the instrument sample data was of low quality rendering the given values even more questionable. Neither higher nor lower concentration samples, nor longer count duration (up to 7,500 seconds) were found to improve the instrumental results. Also, silica granules like those found earlier on dipped cover slips were found to form on the walls of solution vials. If such granules were the result of agglomeration during sizing by light scattering, the DLS manufacture's literature indicated that accurate sizing was unlikely. A further complication was the implicit assumption of a spherical particle in the instrumental calculation of a hydrodynamic diameter. Fumed silica is well known to be a highly fractal material, and in discussion with manufacturer representatives it was learned that diameter values returned for such materials can be misleading.

Since DLS filtration showed that a reduction in the size of fumed silica particulates was accompanied by liquefaction, it was concluded (in agreement with the sparse literature) that agglomerated silica network structures larger than 200 nm were responsible for the solidity of the partially pre-processed admixtures. Such mixtures would contain agglomerated fumed silica with an effective volume exceeding that of spherical random close packing and by the Krieger-Dougherty solid-filled liquid viscosity relation (eq 25) would be expected to be solid. It was further concluded from DLS filtration that the liquidity of these mixtures after heating and secondary mixing was due to the reduction of those networks to particles the size of Aerosil® 300 fumed silica aggregates (average characteristic dimension ~100 nm). In agreement with percolation theory (eq 41) mixtures containing such particles in the concentration range of the experimental mixtures would be expected to be viscous liquids, because the small particles would effectively occupy less than the critical percolation volume.

Liquefying Filler Concentration Limit

In order to determine the maximum concentration of filler at which liquefaction of pre-mixtures would occur, a series of admixtures containing 16.2, 17.6, 20.3, and 25.8 wt% uFSN were subjected to standard heated speed mixing [SHSM] pre-processing.

Only the admixture with the lowest concentration of filler was found to form a viscous liquid pre-mixture. The mixtures with higher filler concentration remained solid. Increasing secondary-mixing from twice at 3,500 rpm to five times at 3,500 rpm failed to render liquid any of the higher filler mixtures. The maximum filler concentration at which pre-mixture liquefaction by SHSM was observed to occur was ~7.9 vol%. This is in reasonable agreement with the critical value of 7.8 vol% calculated (eq 41, p 50) for percolation based solidification of α, ω-hydroxyPDMS$_{26k}$ by fully dispersed (~100 nm aggregate) Aerosil®300. This result was seen as further proof that the dispersion of fumed silica agglomerates to aggregate size was responsible for admixture liquefaction.

These four pre-mixtures were intended for use in elastomer forming reaction-mixtures containing from 15 to 17 wt% crosslinker, and when these large quantities of low viscosity ES40 were added all the mixtures became viscous liquids. However the two samples containing the highest concentrations of filler were significantly thicker than the other two samples. When poured to plates the two lower filler reaction mixture samples spread into even films, while samples containing more filler did not (Figure 24).

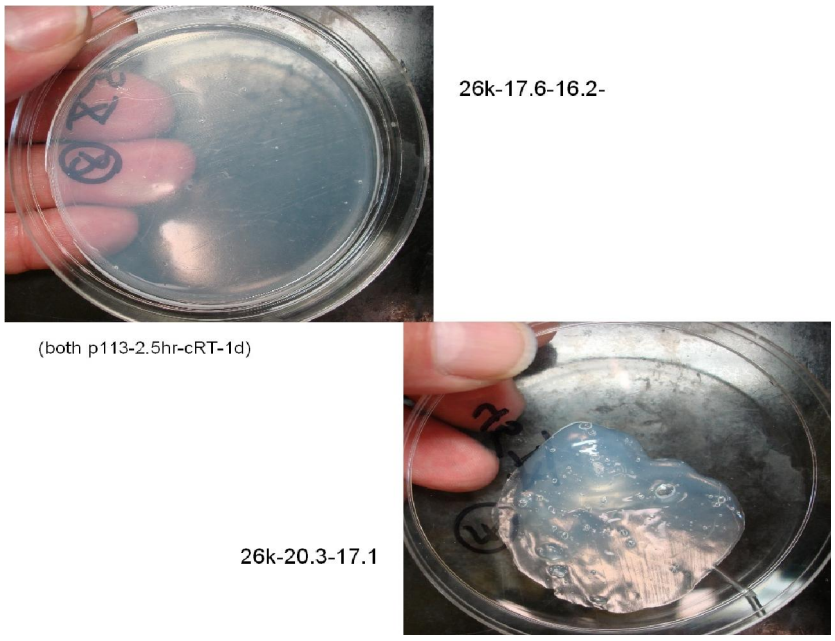

Figure 24. Finished Elastomer 17.6 wt% uFSN Vs. 20.3 wt% uFSN

Admixture Chemical Reactions

It appeared evident that heat processing had caused some structural change in the admixtures that rendered the included fumed silica agglomerate networks susceptible to shear thinning, but the nature of that change was unknown. Possible chemical reactions were examined to see if a chemical change had taken place. The heated admixtures contained only uFSN, hydroxy terminated PDMS, water as vapor and/or adsorbed on the silica surface, and air; thus few chemical reactions were believed possible. The oxidative stability of both uFSN and PDMS made chemical reactions with air at 110°C unlikely. However, to test the possibility weighed samples of uFSN were placed in sample containers that were then evacuated to <1 Torr and held under vacuum overnight while being heated to 120°C. After these vacuum packed samples of uFSN had cooled to ambient de-aerated PDMS sufficient to make the desired experimental mixtures was then added to each sample of silica by needle through a septa while maintaining vacuum. The resulting vacuum packed admixtures were then primary speed mixed and all became waxy solids like those of similar admixtures that had been primary mixed in air. Some vacuum packed samples were then heated to 110°C for 2.5 hours while others were held at ambient for a like period. At the end of that time all were subjected to secondary mixing. Also like earlier SHSM samples processed in air, only the process heated vacuum packed samples were found to liquefy. The absence of any difference in liquefaction behavior between air packed and vacuum packed admixtures under SHSM protocol tended to eliminated the possibility that a chemical reaction with air was responsible for admixture liquefaction.

Vacuum testing also rendered reactions of either PDMS or uFSN with water somewhat less likely to be causes of liquefaction. Hydrophobic PDMS typically contains little water. On the other hand, stored samples of hydrophilic Aerosil®300 were experimentally found by Thermal Gravimetric Analysis [TGA] to lose 3-5 wt% water on heating from ambient to 120°C. The elimination of at least this much water would be expected of Aerosil®300 samples heated to 120°C overnight under vacuum. However, when subjected to TGA, samples of vacuum heated uFSN still showed a small (~ 1 - 1.5 wt%) mass loss during TGA heating to 120°C. Samples of Aerosil®300 that were simply

dried in air at 120°C showed the same 1 – 1.5 wt% mass loss under TGA. This lost mass may represent water so tightly adsorbed on uFSN that neither boiling heat nor boiling heat and vacuum could displace it, but if so then why would this water only be displaced by similar heating in a nitrogen stream during TGA testing? It seems more likely that the small lost mass comes from the elimination of water adsorbed from atmosphere during the transfer of dried uFSN samples from oven to TGA. The low density of fumed silica and the small size of TGA sample pans limited Aerosil®300 TGA sample weight to ~10 mg. It is conceivable that 100 μg of water could be adsorbed in a short time on the 3 m^2 hydrophilic surface of such a sample. It was calculated earlier (p 33) that at 1.5 wt% water content all silanols present on an average Aerosil®300 agglomerate surface could be hydrogen bound to a water molecule. Therefore, the presence of water in admixtures can not be ignored, but it seems unlikely that the vacuum packed admixtures contained even 1 wt% water at the time of mixing. Thus, the possibility of liquefaction causing chemical silanol-water or PDMS-water reactions at 110°C appears small.

The high thermal stability of PDMS and uFSN made thermal decomposition at process temperature unlikely, but it was believed possible that mild heating might have resulted in condensation reactions of the PDMS hydroxy end groups and/or silica surface silanols. Condensation reactions between surface silanols on adjacent fumed silica aggregates was not considered a likely cause of liquefaction, since this would lead to larger aggregates and DLS filtering had already shown that only admixtures containing small aggregates would liquefy. Condensation reactions between adjacent (vicinal) surface silanols on the same aggregate were also considered unlikely since the literature indicated that such elimination reactions seldom occur below 200°C.[166]

Comparison by Gel Phase Chromatography of samples of unheated α,ω-hydroxy$PDMS_{26k}$ and samples heated to 110ºC for 2.5 hours showed that the heated samples displayed just a slight increase in molecular weight and little change in molecular weight distribution (Figure 25.). The small change in MW that was observed was within the variation that two consecutive samples of the same material had been found to display on the instrument. Inter-chain condensation of the low polydispersity 26

kDa PDMS would have been expected to lead to large increases in molecular weight. Since this was not observed, such a reaction is not believed to have occurred. The possibility of cyclic formation due to intra-chain condensation between chain-ends could not be ruled-out, but given the size of the PDMS molecules (~350 repeat units), such a reaction seemed even less likely than inter-chain condensation.

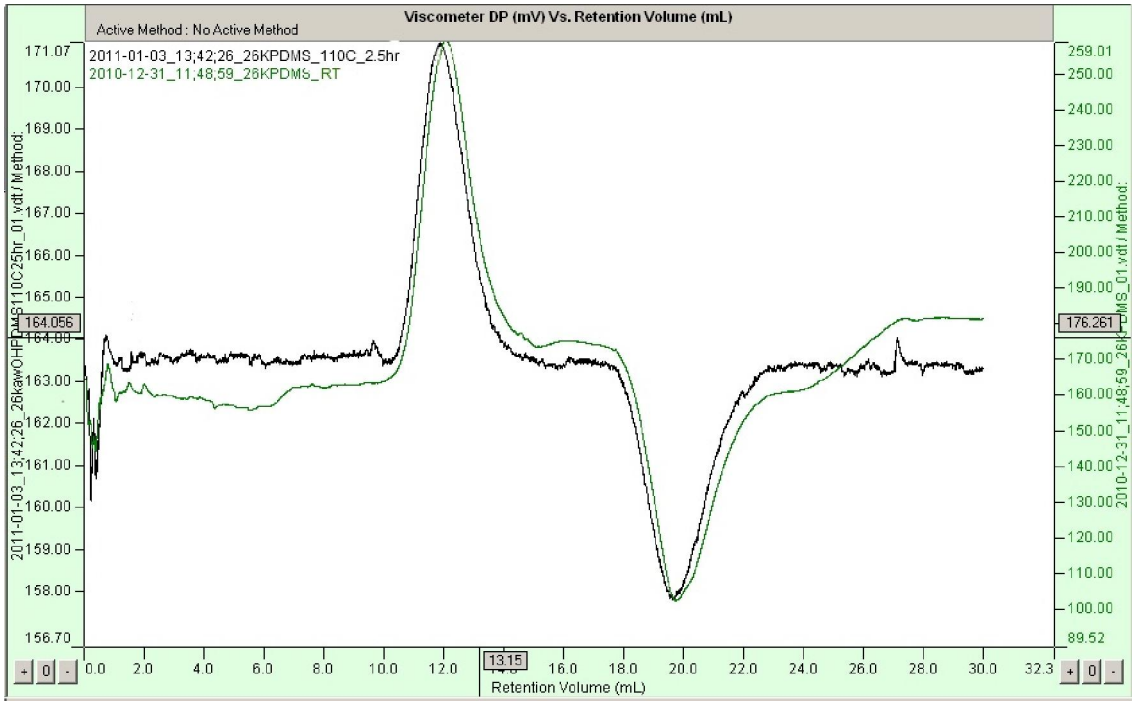

Figure 25. Example GPC Comparison, Room Temp and Process Heated PDMS

In a similar vein, it was thought possible that process-heating might have resulted in the condensation of PDMS end groups and fumed silica surface silanols. Such a reaction would be expected to result in a post-heating reduction of sample infra-red adsorption in the isolated silanol adsorption bands around 3750 $cm^{-1}$and 3,200 - 3,400 cm^{-1}.[167] Regions in which absorption signals might increase, due to the formation of covalent Si-O linkages, were not deemed relevant, because the literature indicated that such regions are obscured by much stronger absorption bands from other PDMS molecular structures.[147, 168]

Unfortunately, IR results, though not indicative of a reaction, were less than conclusive. Figure 26 shows a representative comparison of the FTIR adsorption spectra for an admixture as it underwent pre-processing. Traces have been separated for sake of clarity, and represent (lowest to highest) the adsorption spectra for: a sample admixture that had undergone primary mixing, the same sample of admixture after it had also undergone process heating, and the viscous liquid mixture that resulted from secondary mixing of the heated admixture.

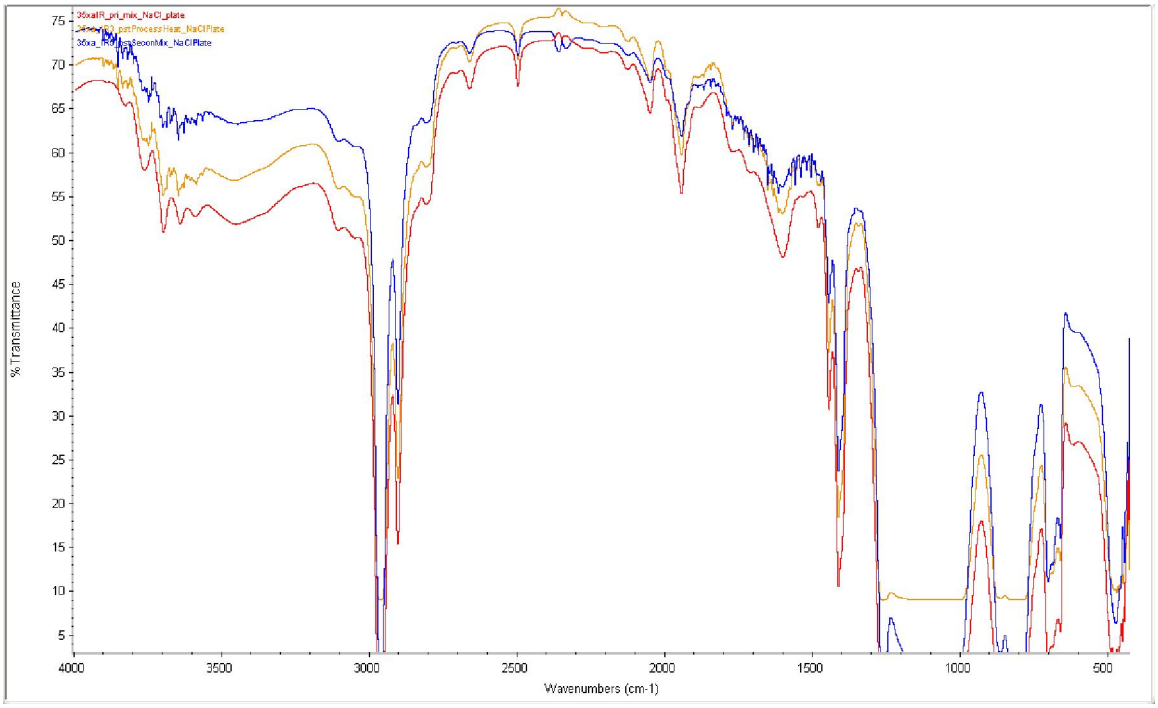

Figure 26. FTIR of an admixture during the stages of Pre-Processing (bottom: primary Mixed solid, middle: process heated solid, top: secondary mixed liquid)

In the 3750 cm^{-1} and the 3,200 - 3,400 cm^{-1} regions the primary-mixed and primary–mixed process-heated adsorption spectra were found to be nearly identical, differing only in that the heated sample had a more jagged trace. The sample tests were conducted ~3 hours apart, and comparison of background spectra conducted before each test revealed substantially more background noise in this region at the time of the second test. Unfortunately these regions also contain absorption bands for water, and therefore even small variations in humidity can affect IR signals here. In addition, though the initial

background measurement was conducted using the plate that was later used for the spectra of each primary-mixed sample and the spectra of that same sample after 2.5 hrs. of heat processing, the background for the heat processed sample had to be taken with a different plate in order that the same sample on the same plate might be examined both before and after heating. Thus, the software could only imperfectly subtract a background signal from the heat processed sample and this, along with interference due to water, is thought to have caused a jagged appearing post-heating absorption signal. However, the overall amount of absorption around 3,750 cm^{-1} and from 3,200 to 3,400 cm^{-1}, based on the depth and width of the absorption spectra in these regions, appeared nearly identical for both mixed and heated samples indicating that little, if any, reduction in free silanol occurred during heating. Though the IR spectra gave no direct indication that silanol condensation had occurred, the possibility that atmospheric water might have altered absorption in these regions leaves open the possibility that some silica/PDMS silanol condensation may nevertheless have taken place during process heating.

The IR spectrum for the viscous sample resulting from secondary mixing of the heated admixture, though of the same shape, appeared less intense than those of the two less pre-processed samples. However, because the viscous film applied to the plate could easily have been thinner than the film used in the earlier two tests, no quantitative conclusions could be drawn directly from the diminished absorption. The shape of the viscous fluid adsorption curve was however substantially the same as that of the solid heated mixture. These samples were tested at about the same time, so the jagged appearance of both curves is likely to be due to water present in the instrument. Due to this interference, condensation during secondary mixing can not be completely ruled out, but it appears unlikely.

It had been hoped that Attenuated Total Reflectance IR spectroscopy might yield more definitive results. For unknown reasons all spectra returned by the instrument showed no adsorption above ~3,000 cm^{-1}. Thus, no conclusions concerning silanol condensation could be drawn from ATRIR.

Admixture Physical Interactions

The energy supplied to the experimental solutions by speed mixing was greater during primary mixing before heating (3 one minute cycles) than during secondary mixing after heating (2 one minute cycles). Therefore, based on the particle size reduction that DLS filtering revealed only in secondary mixed samples, it was concluded that heating had either weakened the fumed silica network, or increased the dispersional effectiveness of mixing. Having found no evidence of chemical reactions that might cause such changes, physical interactions were investigated. It was initially thought that air within fumed silica agglomerates might slow the infiltration (wetting-in) of polymer and that heating might somehow speed air displacement. However, the lack of observed difference, described earlier, in the behavior of admixtures processed in air and those processed under vacuum tended to discount this possibility.

A heat induced lowering of polymer viscosity that might enhance mixing effectiveness was also considered. Though PDMS viscosity exhibits less temperature sensitivity than that of hydrocarbons, it was thought possible that the slightly lower viscosity of PDMS in a hot admixture might have occasioned the observed liquefaction.[169] An early investigation to examine this possibility involved the primary-mixing and process heating at SHSM conditions of several admixtures containing 13.1, 14.2, and 15.5 wt% uFSN (14x, 35x, and 60x). After process heating the samples were allowed to stand at ambient overnight before being subjected to secondary-mixing. All samples were observed to become pourable viscous liquids upon secondary mixing the following day. When these admixtures were further processed under SHSM conditions they were found to form even, translucent, bubble-free elastomer films indistinguishable from those formed from admixtures that had undergone secondary-mixing while hot. Thus, it was established that liquefaction occurred because the mixtures had been heated, but not because they were hot at the time of secondary mixing. Therefore admixture liquefaction due to a heat induced change in polymer viscosity with a consequent change in mixing effectiveness was considered unlikely.

The sole physical interaction known to occur between the components of these admixtures is the adsorption of polymer on filler, also known as the formation of bound rubber [BR]. The extent and rate of BR formation in fumed silica/PDMS admixtures has been well studied (pp 38– 46), and is remarkable for its slow pace (weeks to years) at room temperature. However the rate of formation of silica bound polymer is also known to be highly temperature sensitive. Cohen-Addad and others noted that adsorption was more rapid at elevated temperatures, but have not thus far published an exact relationship. Both Selemovik et al. and DeGroot and Macosko suggested a relationship between BR formation and softening/liquefaction of silica/PDMS admixtures. Therefore, it was decided that examining the BR content and ability to shear liquefy of admixtures processed at different temperatures and sampled at different points during pre-processing might reveal something about the nature of the thermal/shear induced structural change.

In order to eliminate any variation due to composition, all samples initially consisted of roughly 5g of a pre-mixture containing 14.2 wt% (eq 49) Aerosil®300 in α, ω-hydroxy$PDMS_{26k}$. Such a filler loading lies about midway between the lowest and highest employed in this work and was considered likely to give representative bound rubber values. Serial extractions of unbound polymer were carried out with identical quantities of cyclohexane solvent. Cyclohexane was chosen because a large quantity of high purity was readily available and published work considered it a good solvent for PDMS.[170] The quantity of PDMS extracted was found to decrease from several grams during the first extraction to several hundred milligrams during the second extraction to several tens of milligrams during the third extraction. A fourth extraction was found to yield milligrams of unbound polymer; but, since this mass was too small to allow for further examination of the extract, solvent extractions were generally limited to three per sample. Several sources reported that fumed silica adsorbed PDMS would undergo full thermal degradation at around 450ºC under an inert atmosphere to form a mixture of volatile low MW cyclic siloxane oligamers, and a number of investigators reported successfully using Thermal Gravimetric Analysis [TGA] to determine the Bound Rubber content of silica/PDMS mixtures.[171, 172, 173, 174, 175] Bound Rubber determinations were made by examining the mass loss of dried samples of the residues remaining after solvent

extraction during TGA heating. Extracts, dried of solvent, were also examined by TGA to allow for the determination polymer/filler concentration and thus the degree to which the constituents of the initial mixtures were recovered.

After an initial extraction all solvated samples were observed to become nearly transparent gels. These gels were found to be more difficult to disperse in solvent than the initial admixtures. During further extractions, gels from samples that had undergone full pre-processing were found to be more difficult to disperse than those that had undergone primary mixing and process heating; and gels that had undergone primary mixing and process heating were found to be more difficult to disperse than gels that had only undergone primary mixing. It was curious to note that while admixture cohesive energy (as indicated by resistance to shear) decreased during SHSM pre-processing steps, the extraction of unbound polymer and solvent swelling of the materials from those steps resulted in gels with increasing cohesive energy. Upon drying the gels were found to become white, randomly shaped particulates visually ranging from 5 mm diameter grains to fine powders in size. Some dried samples also displayed needle-like particulates as much as a centimeter in length. All dried particulates were brittle enough that finger pressure was sufficient to break them apart.

Extraction involved numerous transfers of materials accompanied by much taring of containers and weighing of samples, thus occasioning loss of material and measurement errors. However, an average overall recovery of 97.3 % of starting material with a standard deviation of 2 % was achieved for an average mass loss of ~ 2 wt% per 5 g sample. Recovery of PDMS, the largest component by mass in the mixtures, was 96.2% with a deviation of 2.2 %. Average uFSN recovery exceeded the initial filler content by 3.3% with a standard deviation of 3.3%. Given that the initial mass of uFSN was around 900 mg per sample this equates to an average positive error of 30 ± 30 mg, and is likely to have been caused by the multiplicative propagation of TGA uncertainty, an unconscious bias in rounding or cumulative mass determination errors. Though, when tested, a sample of pure α, ω-hydroxyPDMS$_{26k}$ was found to be completely eliminated during TGA examination, it is also possible that during TGA testing a high temperature

chemical interaction between PDMS and Fumed silica, or the oxidation of PDMS due to the incomplete exclusion of oxygen may have caused a small increase in silica mass. Full experimental sample mass and TGA based compositional data are presented in Appendix B.

Two identical admixtures were sampled at the end of each standard pre-processing step. Directly after mixing the solid admixtures were found to contain 0.24 - 0.25 g BR/g uFSN (B_0 for this system). After heat processing at 110ºC for 2.5 hours, the Bound Rubber in each solid mixture was found to have increased to 0.58 - 0.61 g PDMS/g uFSN. Following secondary-mixings that liquefied the heated admixtures, BR contents of 0.59 and 0.60 g/g were found. It was notable that the waxy solids present after heat processing were found to contain substantially the same level of BR as the viscous liquids that resulted from the secondary-mixing of those heated solids. Thus, a change in Bound Rubber content during the secondary-mixing that liquefies these admixtures could not be considered the cause of that liquefaction.

Thermal Variation BR Formation

To determine the thermal variability of BR formation a series of primary-mixed solutions were heat processed for 2.5 hours at a number of temperatures ranging from ambient (~25ºC) to 110 ºC, but were not then subjected to secondary mixing. Samples of the resulting waxy solids were extracted and the residues were examined by TGA. Within the experimental range Bound Rubber content was found to increase exponentially with increasing process-heating temperature (Graph E). It was recognized that Bound Rubber content could not be expected to increase indefinitely, and a limiting (saturation) value of 0.85 g bound polymer/g filler for the experimental mixtures was calculated from the Cohen-Addad relations (eqs 35 and 36). It was further assumed that this value could only be achieved at high temperature, and a theoretical data point was thereby generated and included in the data set. The data was then fitted to a more physically realistic sigmoidal function. However, it is unlikely that either function applies at much above 200ºC, since PDMS silanol homo-condensation reactions become probable above this temperature.[176]

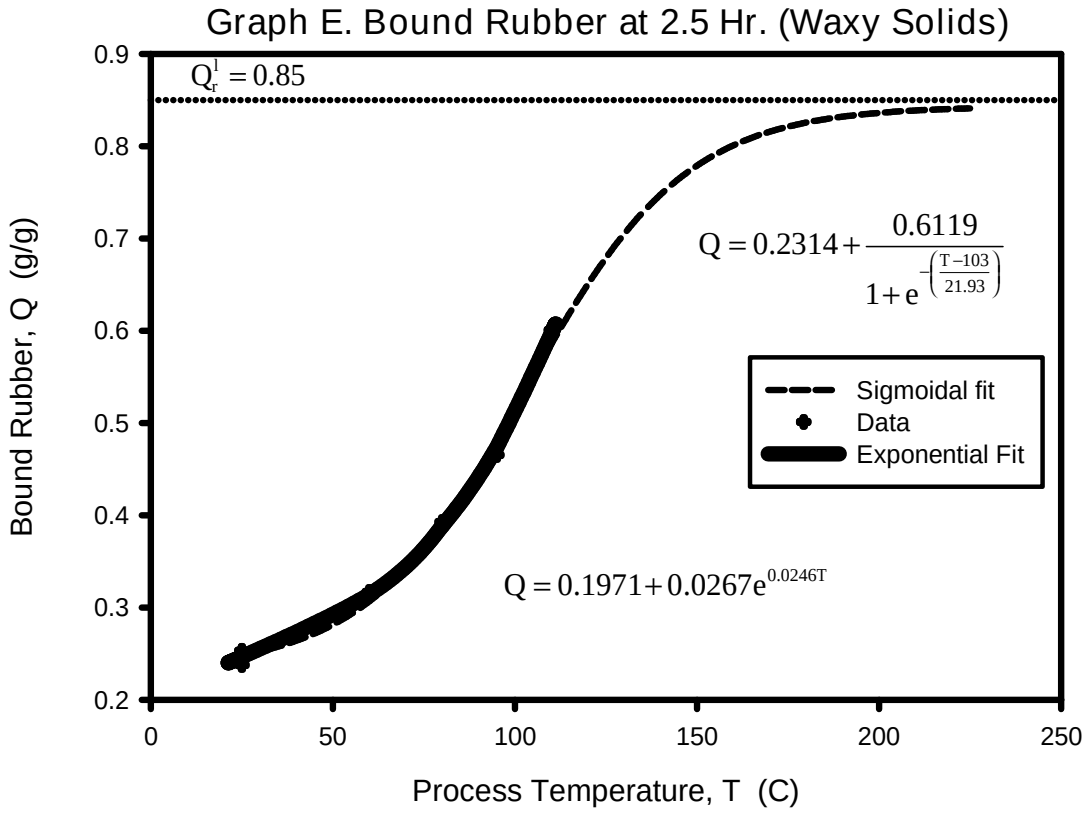

A number of admixtures were pre-processed at various temperatures for periods >2.5 hours, and then periodically sampled. These samples were then extracted, and their residues tested for Bound Rubber content (Graph F). As was expected, from the Cohen-Addad dynamic adsorption relation (eq 36) the Bound Rubber content of all samples was found to increase over time. By varying the characteristic time (τ) in the dynamic adsorption relation curves were fitted to the adsorption data at each temperature. The BR increase over process time at any given temperature was found to correlate well with the asymptotic type of growth curve that might be expected from the Cohen-Addad relation (Graph F). The samples treated at 110ºC showed the fastest increase and were found to have nearly reached saturation after 24 hours of heating, while samples process aged at ambient showed a much slower increase and would be expected to require six or more months to reach bound polymer saturation.

Graph F. Bound Rubber Formation

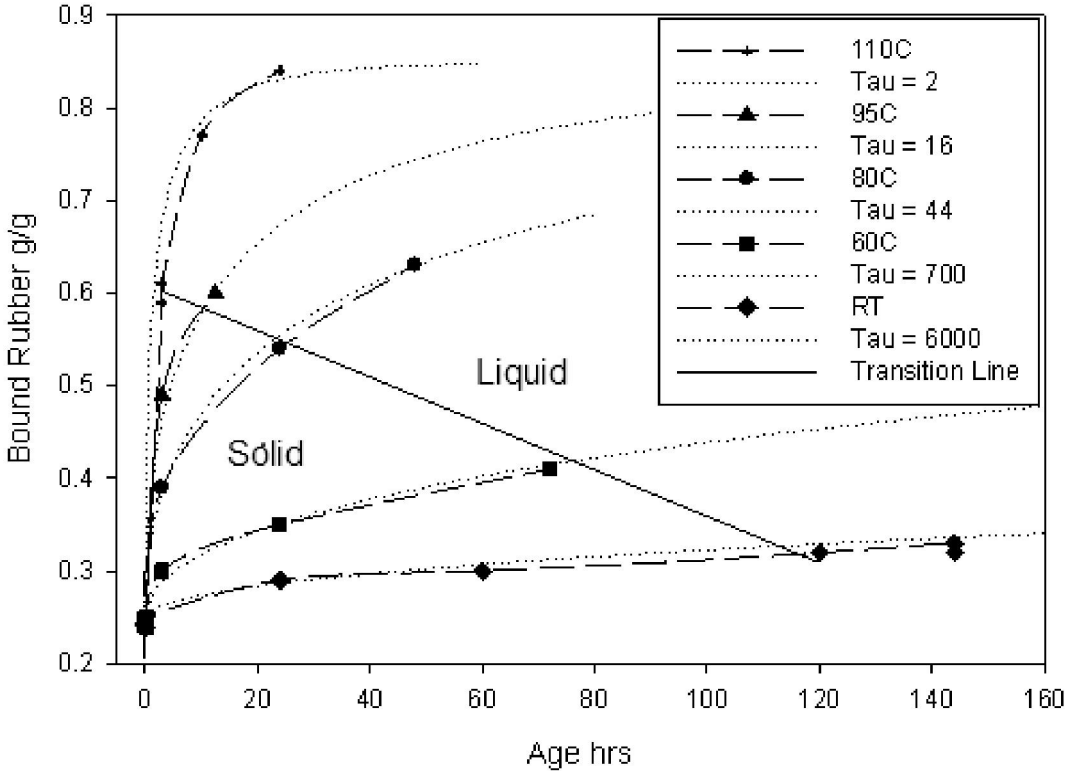

Thermal Variation of BR at Liquefaction

When samples were heat processed for 2.5 hours at different process temperatures, only the samples processed at 110 ºC were found to form viscous liquids upon immediate secondary-mixing. Unexpectedly, however, it was also discovered that samples processed at lower temperatures would undergo a solid/liquid change upon secondary mixing if they were held at the lower temperatures for longer periods of time. The required aging time was found to increase roughly linearly as BR content at liquefaction dropped. (Graph F). Admixtures processed at room temperature were found to contain 0.32 g/g bound rubber when first shear thin-able, while identical mixtures processed at 110ºC were found to contain ~ 0.60 g/g at the time of first liquefaction. Materials processed at intermediate temperatures contained intermediate quantities of bound polymer at the age of first liquefaction. Since 0.32 grams of adsorbed polymer per g of filler sufficed to render an admixture shear thin-able, then by the models proposed by DeGroot and Macosko, and Selimovik et al. such a quantity of BR should also have been

sufficient to liquefy any similar mixture by either pulling apart, or isolating the filler aggregates. However, at higher processing temperatures far more adsorbed polymer was found at the age that solid admixtures of identical composition would first liquefy. Hence, the absolute quantity of adsorbed polymer (at least above 0.32 g/g for this system) does not appear to be the cause of the age dependent solid to liquid transition under shear.

It does appear that the underlying process responsible for this shear induced change can (like adsorption) be accelerated by heating, but the thermal variation of "age to shear liquefy" and "age to 66% adsorption (τ)" seem to differ. The best fit curve to data for "Liquefying Age" vs. Temperature was a decreasing sigmoid over the 25-110°C range (Graph G).

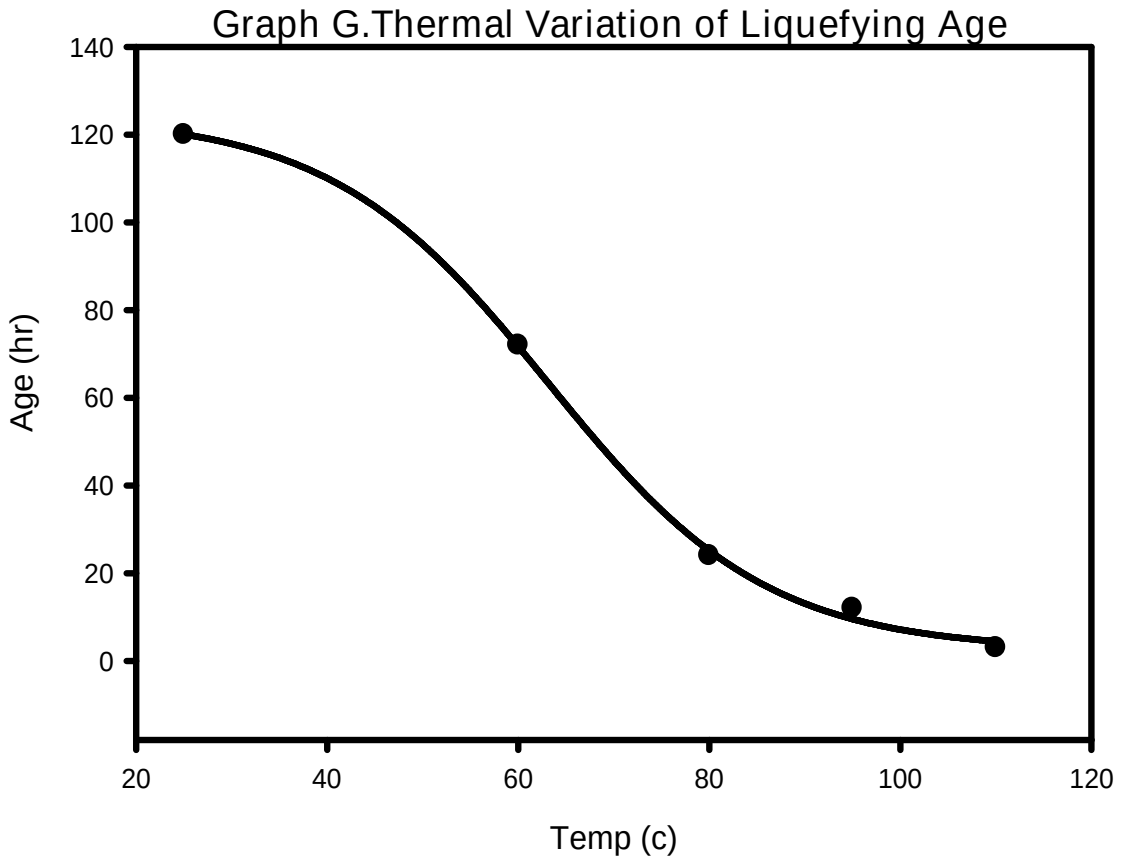

In contrast the best fit to the data for Age (τ) at 66% Adsorption vs. Temperature decayed exponentially over the same temperature range (Graph H).

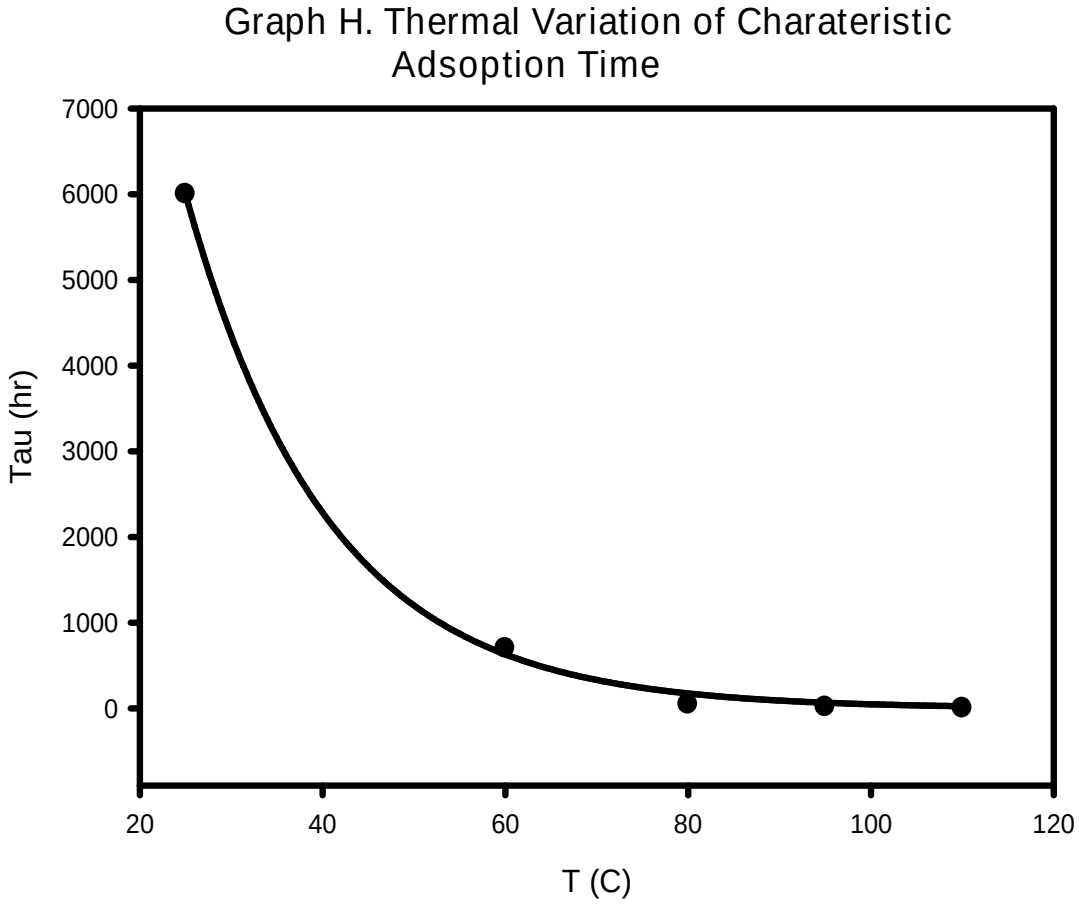

If polymer adsorption leads to liquefaction, then that shear enhancing adsorption must differ from the adsorption to saturation described by Cohen-Addad. If it is assumed that none of the instantaneously adsorbed polymer (B_0 = 29 wt% saturation) causes shear enhancement and further assumed that no Cohen-Addad surface adsorption occurs during shear enhancing adsorption, then from the results for RT adsorption (Graph F) PDMS must achieve this weakening by the adsorption of no more than 8 wt% of the quantity of polymer adsorbed at saturation. (Since it is likely that some Cohen-Addad type adsorption does concurrently occur, the required percentage is probably <8 wt%.) At ambient adsorbing this 8 wt% would require at least 5 days, while at 110°C 8 wt% adsorption could be achieved in no less than 2.5 hrs. In contrast, by the Cohen-Addad relation at ambient, the adsorption of another 24% of the saturation quantity of BR (B_0 + 8% +Cohen-Addad = 66% saturation, at tau) would require several months, while at

110°C the same degree of adsorption could be achieved during the same 2.5 hours required for shear enhancing adsorption. Thus, shear enhancing adsorption is far less susceptible to thermal acceleration than adsorption to saturation.

The network of agglomerated silica aggregates that is believed to render these admixtures solid is likely held together by numerous interaggregate silanol-silanol hydrogen bonds. It is believed that adsorption of polymer in interaggregate bonding regions would disrupt interaggregate bonds, thus weakening the agglomerate network and making it more susceptible to shear liquefaction. If many interaggregate silanols were already occupied by polymer at the time shearing dispersed the agglomerate network, then no sharp increase in the quantity of BR or the rate of BR formation due to adsorption on newly unoccupied silanols would be observed at the time of liquefaction. This is consistent with the observation that process heated solids and the viscous liquids to which they were sheared contained about the same quantities of BR. From earlier theoretical discussions (pp 31 - 32, 47) for an average Aerosil®300 aggregate the regions where interaggregate hydrogen bonds exist are likely ~40 nm^2 in area, about a nanometer in thickness, and numerous enough (~80) to occupy roughly 27% of the filler surface. To weaken the agglomerate network PDMS molecules would need to infiltrate interaggregate spatial volumes about the size of a few polymer molecules, and while doing so would need to disrupt some fraction of the roughly 80 hydrogen bonds in each volume. Polymer adsorption in these regions would likely be quite different from the diffusive adsorption described by Cohen-Addad, and would also be likely to proceed with kinetics distinct from that described for the open aggregate surface.

Admixture Re-solidification

A commonly reported Bound Rubber dependent effect that was also observed in this work with viscous admixtures was solution hardening upon further aging (crepe hardening). The viscous samples which were processed at room temperature for 5 to 6 days (containing 0.32-0.33 g/g of Bound Rubber) were observed to return to a waxy solid state within a day of secondary-mixing induced liquefaction. In contrast, a sample

processed at 110ºC for 24 hours and containing roughly saturation quantities of Bound Rubber (~0.85 g/g) has remained a viscous liquid for nearly a year. Lacking a suitable instrument to measure the viscosity of aging mixtures, a simple flow test was devised to gauge the relative rate at which solutions containing differing quantities of Bound Rubber would re-solidify.

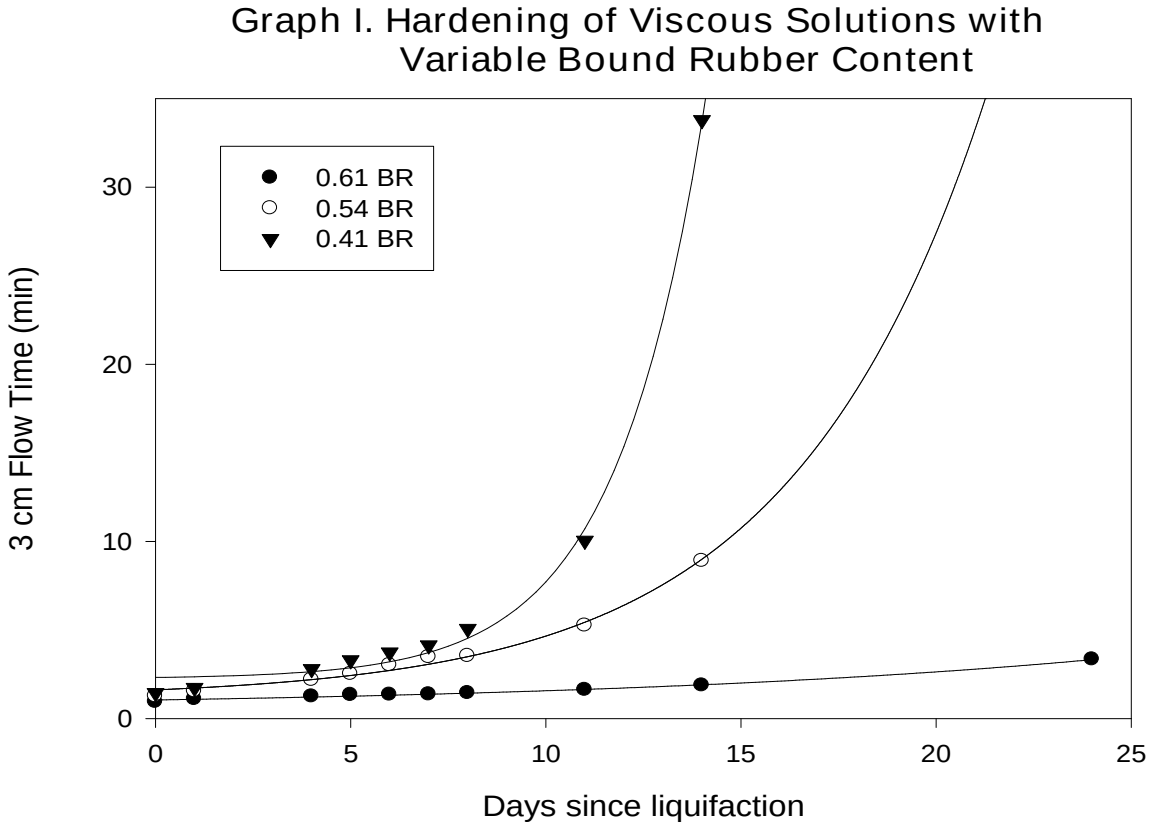

The time required for equivalent masses of viscous admixtures containing differing quantities of Bound Rubber to flow 3 cm was found to increase with decreasing Bound Rubber content (Graph I). Initially the difference was small. The sample containing 0.54 g/g required 30% longer, and the sample containing 0.41 g/g required 50% longer, to flow the distance than did the sample containing 0.61 g/g. As time passed, this difference increased. By the end of 2 weeks for the 0.41 g/g sample, and by the end of slightly over 3 weeks for the 0.54 g/g sample, each took over 10 times longer to cover the distance than did the sample containing 0.61 g/g of Bound Rubber. Though at 30 minutes to flow 3 cm the samples containing lower quantities of bound rubber could not

be considered fully solid, this was arbitrarily selected as a cut- off to simplify graphing, since at the end of 24 days the 0.54 g/g sample required over 3.5 hours to cover the distance and the 0.41 g/g sample was not observed to flow at all. Fitting an exponential to the 0.61 g/g sample data points gives a 30 minute to flow 3 cm re-solidification age of about a month and a half. Consistent with this result, a number of samples processed like this sample (under SHSM conditions) were observed to remain slowly pourable for as much as 2 months after liquefaction.

Earlier, it was found likely that liquefaction occurs because a polymer strengthening network of hydrogen bonded agglomerated aggregates is destroyed by secondary mixing. The re-hardening of these solutions then most likely results from the re-establishment of those hydrogen bonded silica networks, in which case the availability of silica surface silanols for hydrogen bonding would determine how quickly such a network reformed. The greater the silica bound rubber content the fewer the available silanols, and the slower would be re-solidification. In a viscous liquid the rotational/translational (Brownian) movement of separated aggregates with unbound silanols could establish an agglomeration network so long as the effective aggregate volume exceeded the critical volume for spherical random close packing. For the "just mixed" (lowest BR content) samples where BR = B_0 = 0.32 g/g on 14.2 wt% Aerosil®300 in α, ω-hydroxyPDMS$_{26k}$ the Eggers/Schummer relation (eq 43) gives a coated filler based β modifier of 2 to the actual uFSN vol % of 6.85 for an effective vol % of 13.7. The percolation based critical volume (eq 41) for these solutions was computed to be 8.8 vol %, thus as was observed this low BR solution would be expected to become solid due to the formation of a filler based network with an effective volume greater than the critical gelation value.

A similar analysis can be made for the saturated filler (0.85 g/g) sample. With a β value of ~3, an age hardening solution might also be expected based on the polymer coated filler having an effective volume (20.85 vol%) greater than the admixture's critical volume for gelation. However, an underlying assumption of the Flory-Stockmayer percolation theory is that the network forming species will form a network. As originally

developed, this theory was applied to monomers with chemically active groups that would react with each other to form a covalently bound polymer network. As applied to uFSN filled PDMS, this assumes that aggregates will hydrogen bond with each other to form an agglomerate network. However, at Bound Rubber saturation few silanols remain available to re-bind the agglomerate network. Therefore, rather than forming a space encompassing network, the aggregates tend to remain separate coated particles surrounded by free polymer. The critical volume relation no longer applies, just as it would not apply to a solution of monomers containing no reactive groups. At Bound Rubber saturation liquefied uFSN/PDMS solution viscosity should follow Kreiger-Dougherty behavior (eq 25) and display ~ 70% higher viscosity than that of the PDMS alone, regardless of viscous solution age. Visibly, though solutions containing saturated filler were found to become slightly thicker over time, they have not yet been observed to re-solidify and have retained a honey like viscosity (2 - 10 Pa·s) after over a year.

This interpretation also gives some theoretical insight into the solid/liquid nature of these admixtures. At the time of primary mixing fumed silica agglomerates present so large an effective volume and particle size that the Kreiger-Dougherty solid filled fluid viscosity relation and the Flory-Stockmayer gelation theory both predict the observed solid admixtures. The rapid adsorption of polymer to B_0 predicted by Cohen-Addad further reinforces the prediction of solidity, because the polymer coating of filler would, by the Eggers/Schummer theory, be expected to further increase the effective particle size and volume of filler. However, to remain solid both Kreiger-Dougherty and Flory-Stockmayer require that the fumed silica maintains large sized agglomerates in a network of high effective volume. As originally devised by Flory and Stockmayer the network was conceived of as a molecular network held together by covalent bonds. Once formed the dissolution of such a network would not be expected. In contrast, once weakened by infiltrating polymer the numerous but weak hydrogen bonds of the nano-scale fumed silica network can be ruptured by strong shear forces. Once agglomerates have been shear reduced to aggregate size, both Kreiger-Dougherty and Flory-Stockmayer would predict liquid admixtures, but the Cohen-Addad described formation of BR would still predict

that, due to Eggers/Schummer filler coating, a solid admixture should be obtained. However, viscous liquid admixtures are observed.

Silicone coated filler aggregates, though effectively large enough to form gel networks, appears to only form those networks slowly. Silicone polymer molecules show little interaction with each other in the bulk as is exemplified by silicone's relatively low viscosity. Thus silicone coated filler particles should also show little interaction with surrounding bulk polymer. Though adsorbed polymer increases the size of filler it simultaneously reduces the silanol sites available for silica network formation. The unstated Flory-Stockmayer assumption is that larger molecules become more likely to bind with each other, while for PDMS coated filler quite the opposite is the case. Therefore, though the Eggers/Schummer theory predicts solid materials for polymer coated fully dispersed admixtures, it does not account for the lowering of intra-particle reactivity caused by adsorbed polymer coating, nor does it consider the length of time required for such mixtures to solidify due to coating. Thus, these theories allow for a period of time when admixtures of sufficiently dispersed fumed silica may be viscous liquids while hydrogen bonded strengthening networks form. At Bound Rubber saturation the liquid period becomes so extended that hardening may never be observed.

Conclusions

The original thesis of this work that, "variations in the processing conditions employed in earlier studies caused the observed crosslinker dependent variation in AFM phase angle detection of fumed silica on the surface of filled silicone elastomers," was never conclusively tested. No combination of the processing conditions reported in the earlier papers was found that allowed for the replication of films suitable for examination by AFM. In the current work no "disappearance" of fumed silica from the surface of any elastomer film that could be examined by AFM was ever observed regardless of crosslinker concentration. However, the films examined by AFM in this study were

processed under Standard Heated Speed Mixing [SHSM] conditions quite different from the process conditions described in the earlier works. It is suspected that the earlier elastomers contained poorly dispersed and distributed uFSN agglomerates, and that at the scale of AFM imaging the examination of surface regions lacking in fumed silica on one sample and the examination of silica rich regions on another sample may have given the appearance of crosslinker dependent detect ability of silica.

The SHSM protocol developed in this work has been found to reliably produce clear, even, bubble-free, uFSN-filled silicone elastomer films suitable for use in undergraduate experiments. That SHSM represents the “best” processing conditions has been demonstrated by an examination of the deleterious effects on elastomer quality of processing under conditions (time, temperature, concentration, etc.) outside of those prescribed for SHSM. Mechanical testing has shown that silicone elastomers produced under SHSH conditions display ultimate tensile strength and are as extensible as similarly crosslinked elastomer reinforced with a like concentration of treated fumed silica.

In agreement with DeGroot and Macosko, and Selemovik et al. it has been concluded that the initial solidity of the experimental PDMS/uFSN admixtures arose from the presence of fumed silica agglomerate networks. As introduced, uFSN consists of silanol bearing agglomerates of such large size and effective volume that experimental admixture solidification is consistent with accepted theories describing both percolation based solidifying network formation due to large particle size, and solid-filled liquid viscosity based solidification due to the occupation by uFSN agglomerates of a volume effectively in excess of spherical random close packing. It was also concluded from filtration results that the subsequent liquefaction of these admixtures was due to the destructive dispersal of these networks to the size of constituent aggregates. Consistent with theory, for sufficiently small aggregates at most experimental concentrations, the volume effectively occupied by fully dispersed filler was found to be below both the percolation critical and random close packing for spheres, thereby allowing for the existence of the observed liquid admixtures for some period of time. Further it was also

found that the adsorption of polymer on filler increases the period over which an admixture may remain liquid.

The lack of evidence of chemical or physical interactions, other than the formation of bound rubber, in these admixtures lead to the conclusion that the shear enhancing process is adsorption related. However, identical admixtures processed at different temperatures were found to contain different quantities of adsorbed polymer at the age of first liquefaction, and the manner in which that liquefying age varied over processing temperature was found to differ from the manner in which overall BR formation thermally varies. Therefore, neither the reduction of agglomerates by aggregate bridging adsorbed polymer (DeGroot and Macosko), nor a similar reduction solely due to particle isolating adsorbed polymer (Selimovik et al.) seems a likely cause of shear liquefaction. It appears instead, since the liquefying adsorption does not appear to occur via the adsorption to saturation mechanism described by Cohen-Addad, that liquefaction occurs due to some other type of polymer adsorption phenomena. It is proposed that polymer adsorption in the interaggregate hydrogen bonding region, which would both enhance admixture shear thinning by weakening the solidifying silica network and proceed in a manner kinetically distinct from that of overall BR formation on the bare silica surface, is the most likely cause of the observed admixture shear induced liquefaction.

Future Directions

It remains to be determined whether the suspected shear-inducing adsorption differs in other way(s) from the adsorption to saturation described by Cohen-Addad. It has been found that liquefaction occurs up to the critical solidifying filler concentration and can be accelerated by heat, but how the time to first liquefaction varies with filler concentration remains unknown. DeGroot and Macosko found accelerated softening at higher filler levels, while Selimovik et al. (and Cohen-Addad) found softening to be faster at higher polymer levels. Similarly, Cohen-Addad adsorption has been found to occur more rapidly for higher MW polymer, but the effect of polymer MW on time to

first solidification has yet to be tested. Any relationship between uFSN surface area (available silanols) and rate of liquefaction should also be investigated. Lower surface area uFSN would be expected to agglomerate more weakly than fumed silica of higher surface area and therefore lower surface area uFSN might also be expected to liquefy more quickly at lower BR concentrations. It remains to be seen if this is the case. Ultimately it is hoped the discovery of some relation between these variables will allow for the construction of an expression describing shear-inducing adsorption as a component of (but distinct from) adsorption to saturation.

Further rheological studies of the liquefied admixtures may also prove enlightening. Some variations in the viscosities of admixtures processed at different temperatures were observed during the course of the present work. However, lack of suitable instrumentation prevented quantification of such variation. Liquid admixtures containing less bound rubber appeared somewhat thicker than those containing more BR, but the degree of difference needs to be assessed. The change in viscosity as viscous liquid admixtures crepe harden should also be revisited with better instrumentation. It was noted that re-hardened admixtures could be easily returned to a liquid state by one minute of speed mixing perhaps indicating that re-hardening bonding differs from the agglomeration bonding present in the initial admixture.

Knowledge of the mechanical properties of elastomers containing the new viscous admixtures is far from satisfactory. The sparse testing performed in the course of this study was only intended to indicate that viscous admixtures containing uFSN provide roughly the same degree of reinforcement to silicone elastomer as do admixtures containing like quantities of tFSN and crosslinker. Much more testing will be required to quantify that reinforcement of PDMS. The mechanical testing of elastomers containing viscous uFSN admixtures processed at different temperatures (and therefore containing differing quantities of BR) is of particular interest. Incompletely treated fumed silica has been shown to form somewhat stronger elastomer than fully tFSN. It is thought that the same may be true for less than fully BR saturated uFSN. If so, then it may prove possible

to somewhat tailor filled silicone elastomer mechanical properties via process temperature.

The question of crosslinker dependent variation in the AFM phase angle based detect-ability of uFSN on filled silicone elastomer surfaces remains unresolved. It is suspected that this phenomenon arises from insufficient sampling of inhomogeneous surfaces. However, until elastomers similar to those of earlier experimenters can be replicated this theory will remain unproven.

It is known that PDMS with hydroxy end groups is absorbed ~10 times faster than PDMS with methyl end groups. However, a preliminary test of an admixture of 26 kDa vinyl terminated PDMS and 14 wt% uFSN processed at 110°C was found to require roughly 50 times longer to first liquefy than a similarly treated mixture containing hydroxy terminated PDMS. It would appear that viscous liquid admixtures containing PDMS with different functional groups can be produced. This would allow for the synthesis of liquid admixture derived silicone elastomers by different crosslinking reactions. Therefore, it is believed that an examination of the liquefaction behavior of admixtures of uFSN and non-hydroxy terminated PDMS might also prove instructive.

Appendix I

Tapping Mode

Phase and 3D

AFM Images

of

Cured PDMS Elastomers

Containing

5.9 to 20.9 wt% ES40

And

12.3 wt% uFSN

(14x to 60x crosslinker compositions)

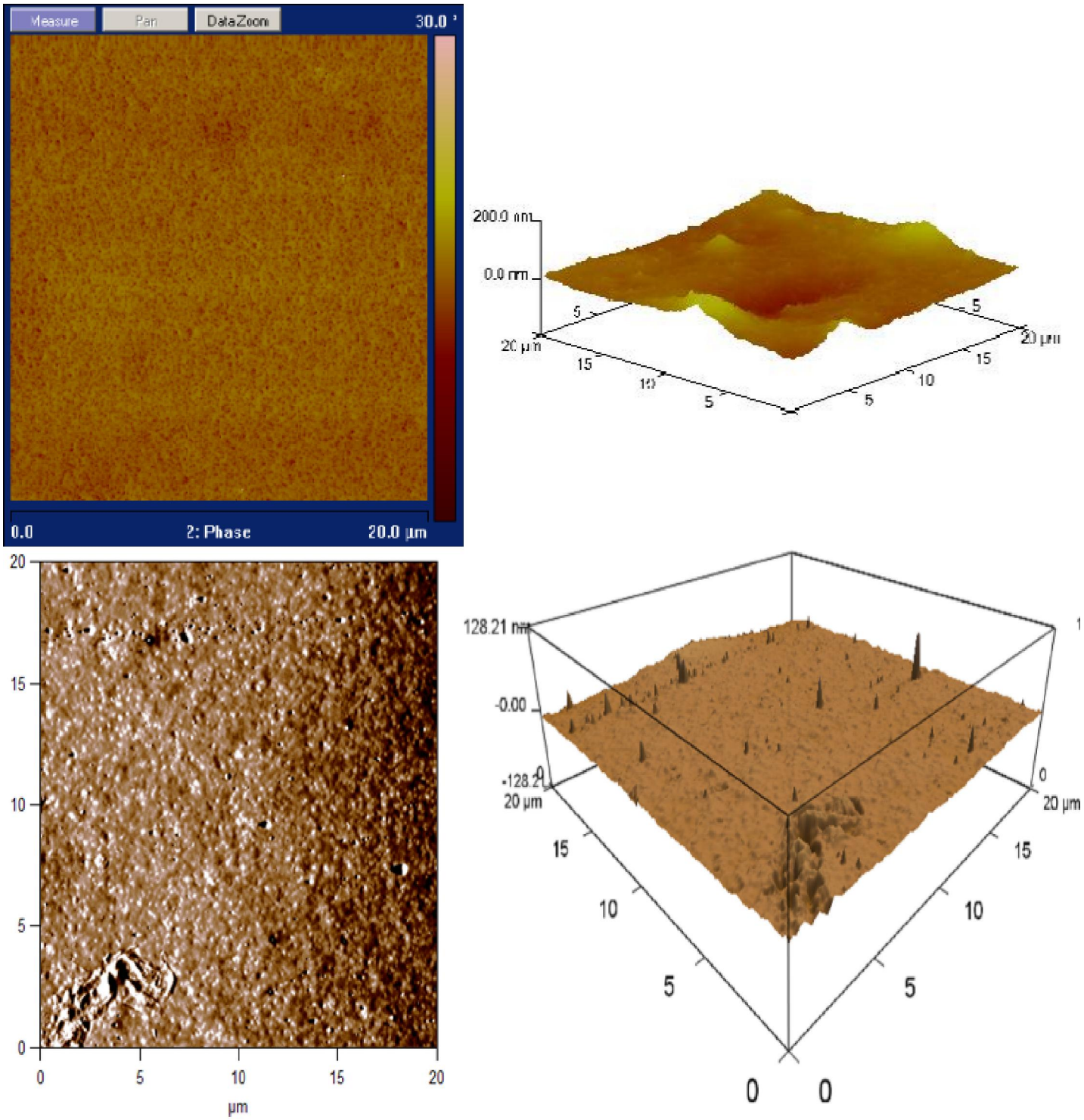

14x -20 µm Surfaces

Phase Contrast (left) and 3D Height (right) surface images from Veeco instrument (upper pair) and Asylum instrument (lower pair)

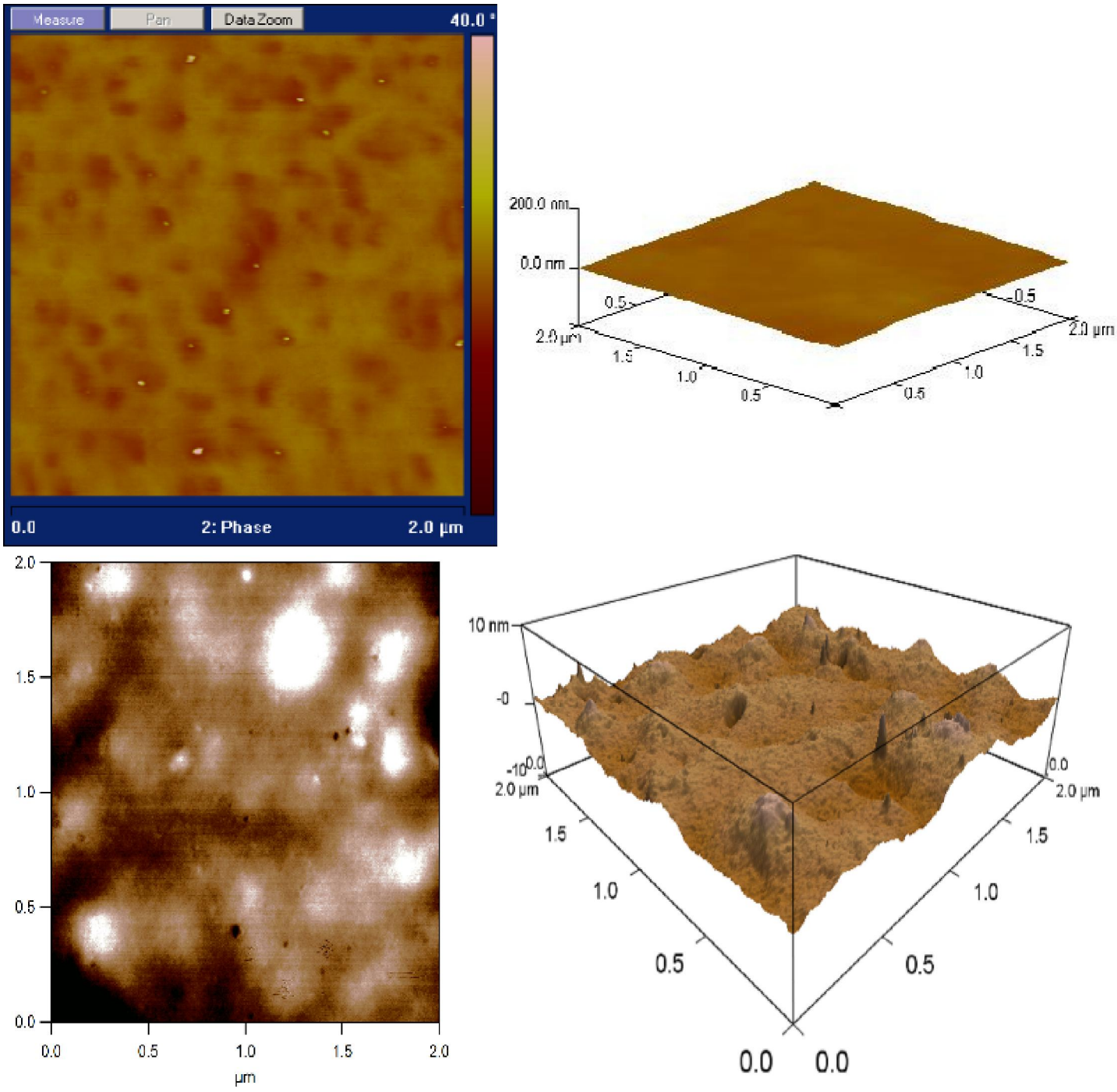

14x -2 µm Surfaces

Phase Contrast (left) and 3D Height (right) surface images from Veeco instrument (upper pair) and Asylum instrument (lower pair)

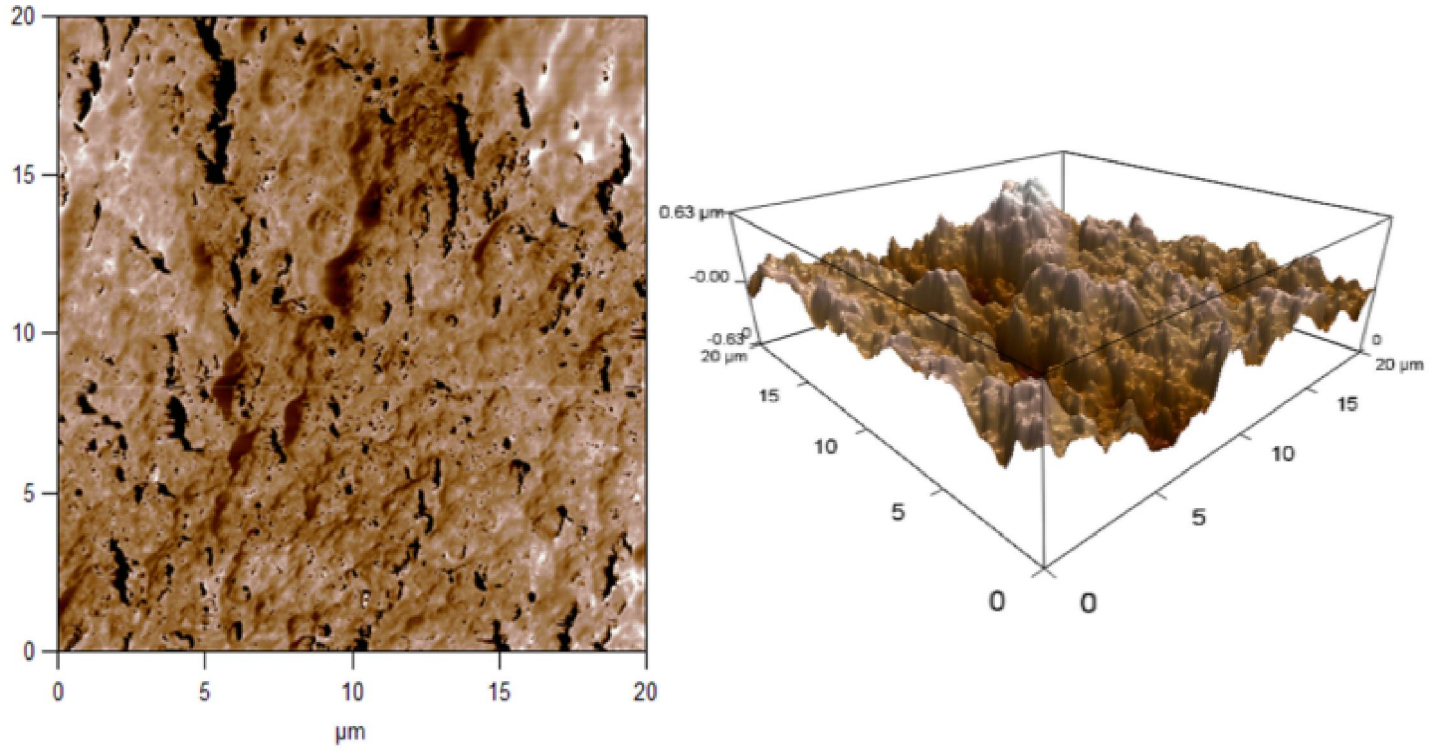

14x -20 µm Fracture Surface

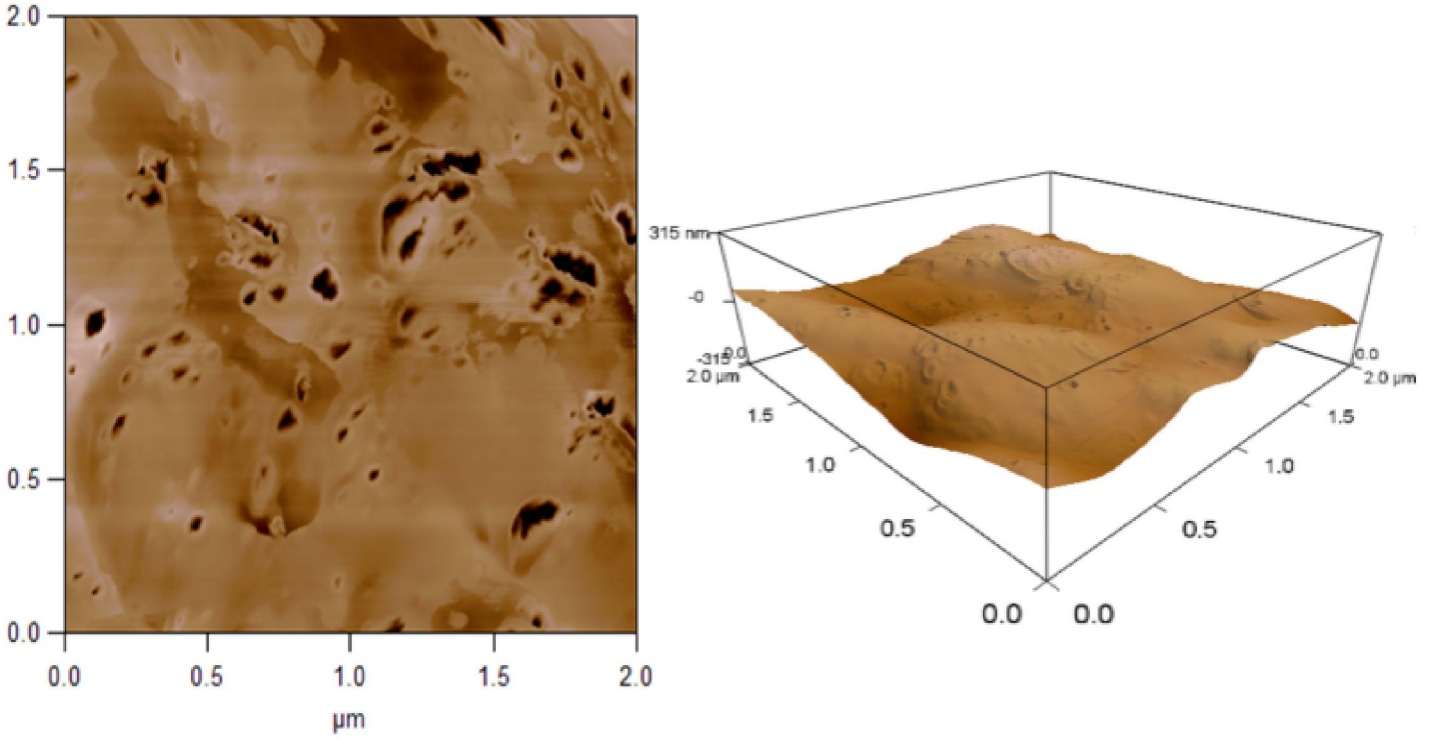

14x -2 µm Fracture Surface

Phase Contrast (left) and 3D Height (right) surface images from Asylum instrument

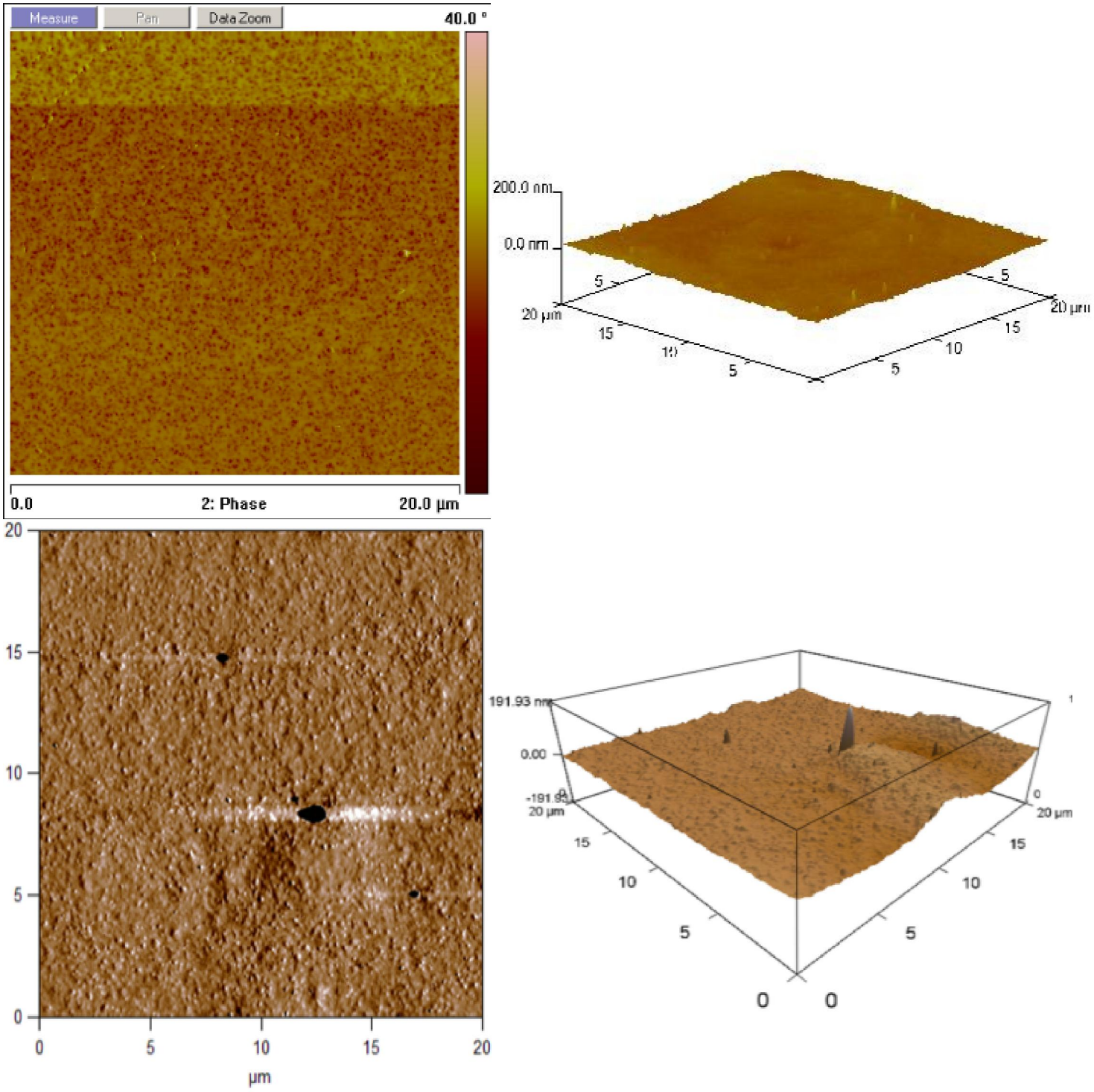

28x -20 µm Surfaces

Phase Contrast (left) and 3D Height (right) surface images from Veeco instrument (upper pair) and Asylum instrument (lower pair)

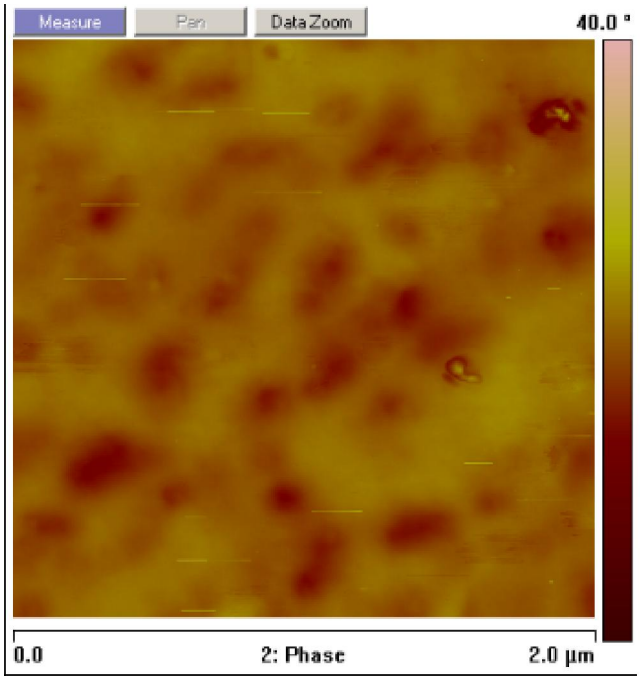

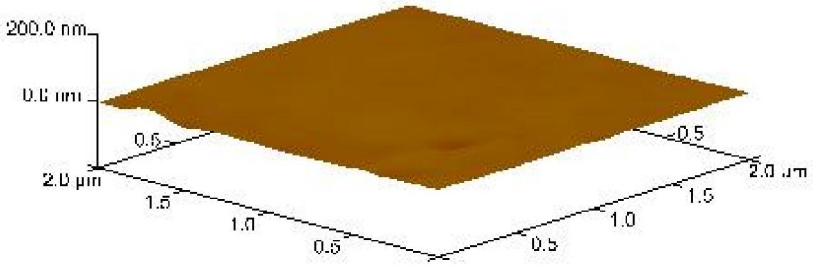

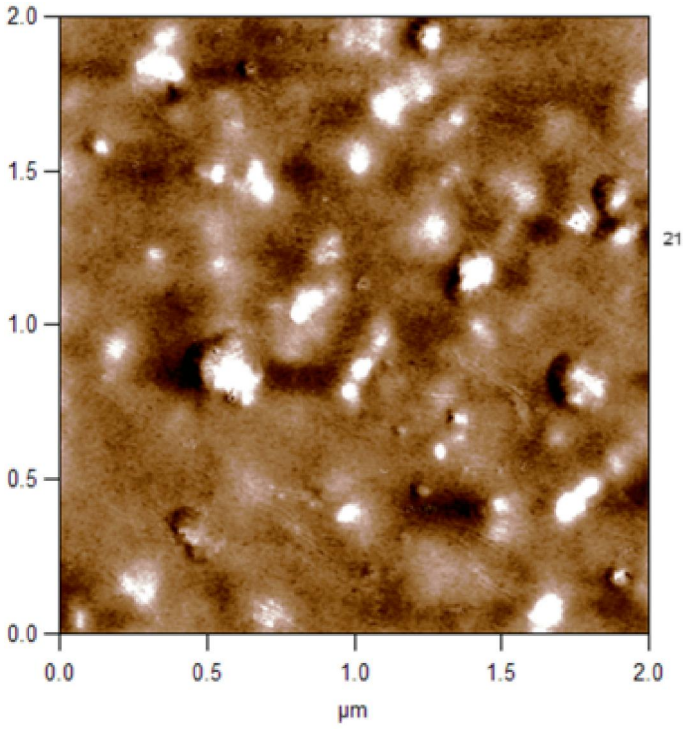

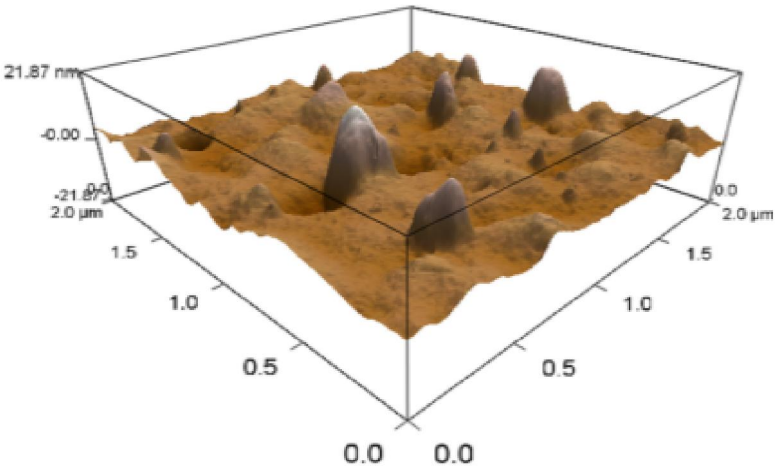

28x -2 µm Surfaces

Phase Contrast (left) and 3D Height (right) surface images from
Veeco instrument (upper pair) and Asylum instrument (lower pair)

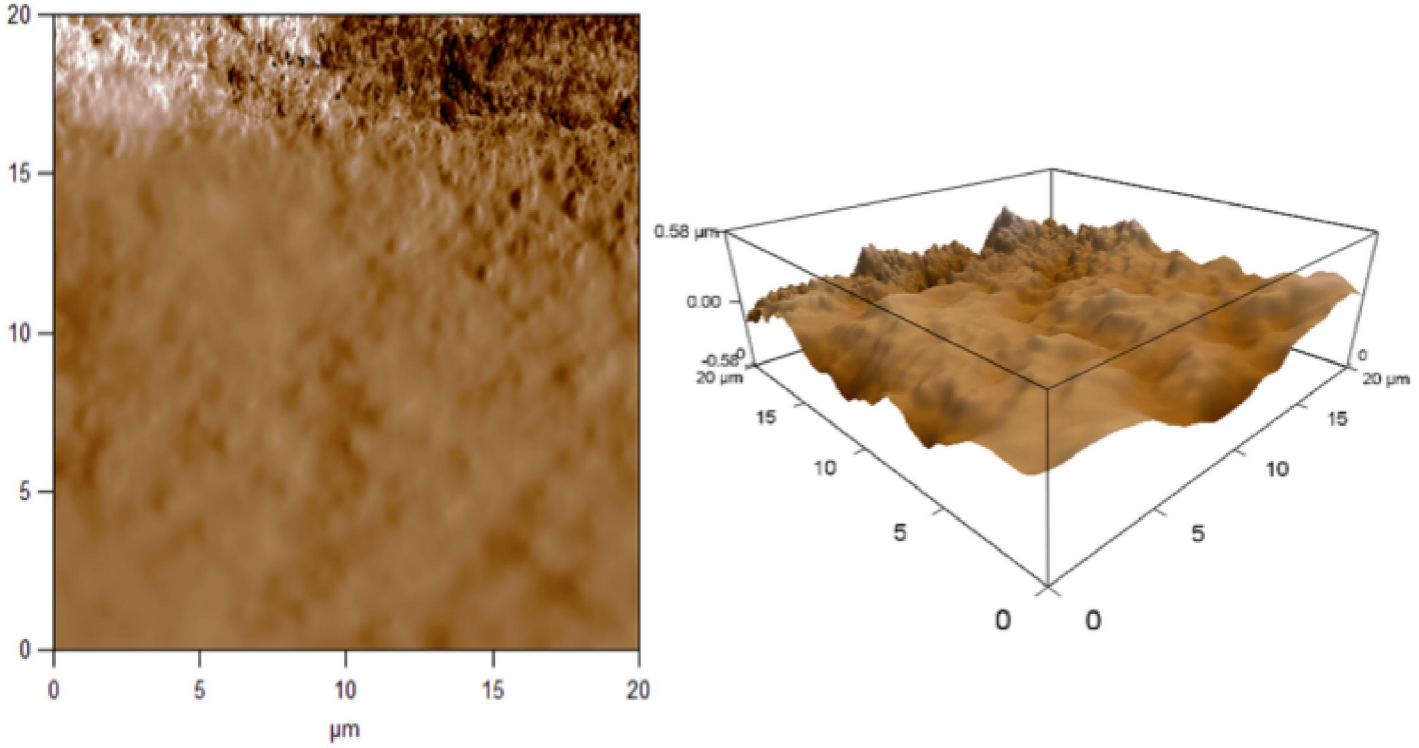

28x -20 µm Fracture Surface

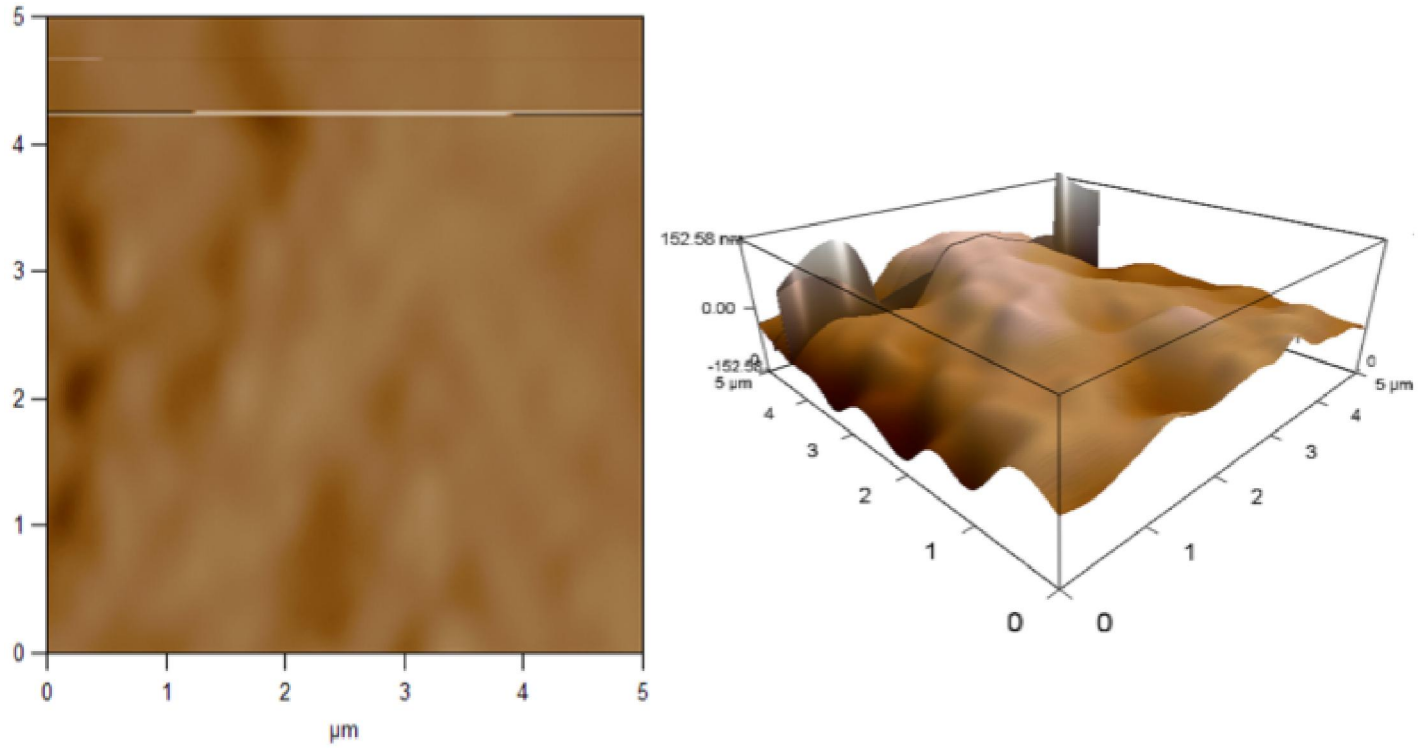

28x -5 µm Fracture Surface

Phase Contrast (left) and 3D Height (right) surface images from Asylum instrument

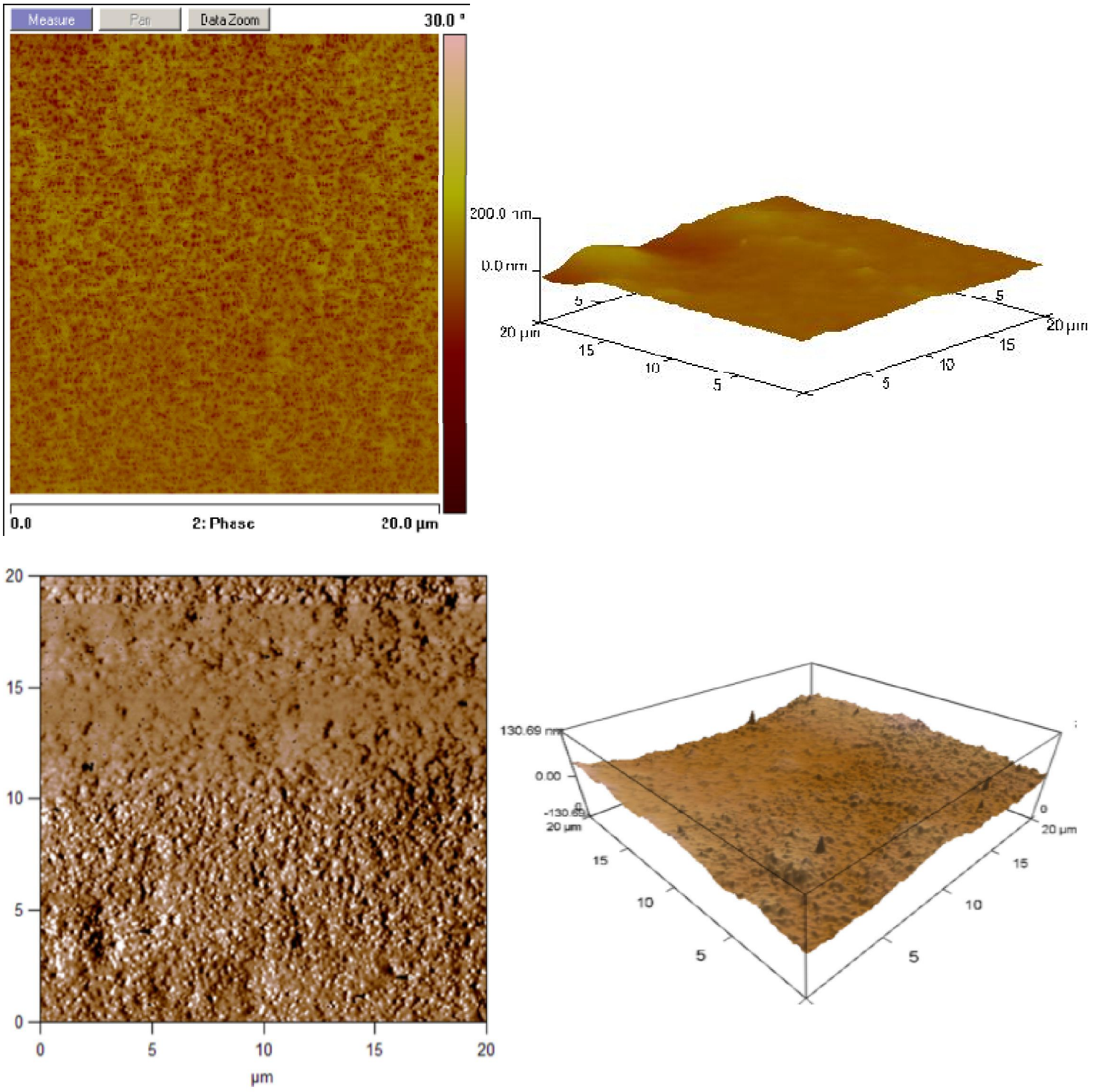

35x -20 Surfaces

Phase Contrast (left) and 3D Height (right) surface images from
Veeco instrument (upper pair) and Asylum instrument (lower pair)

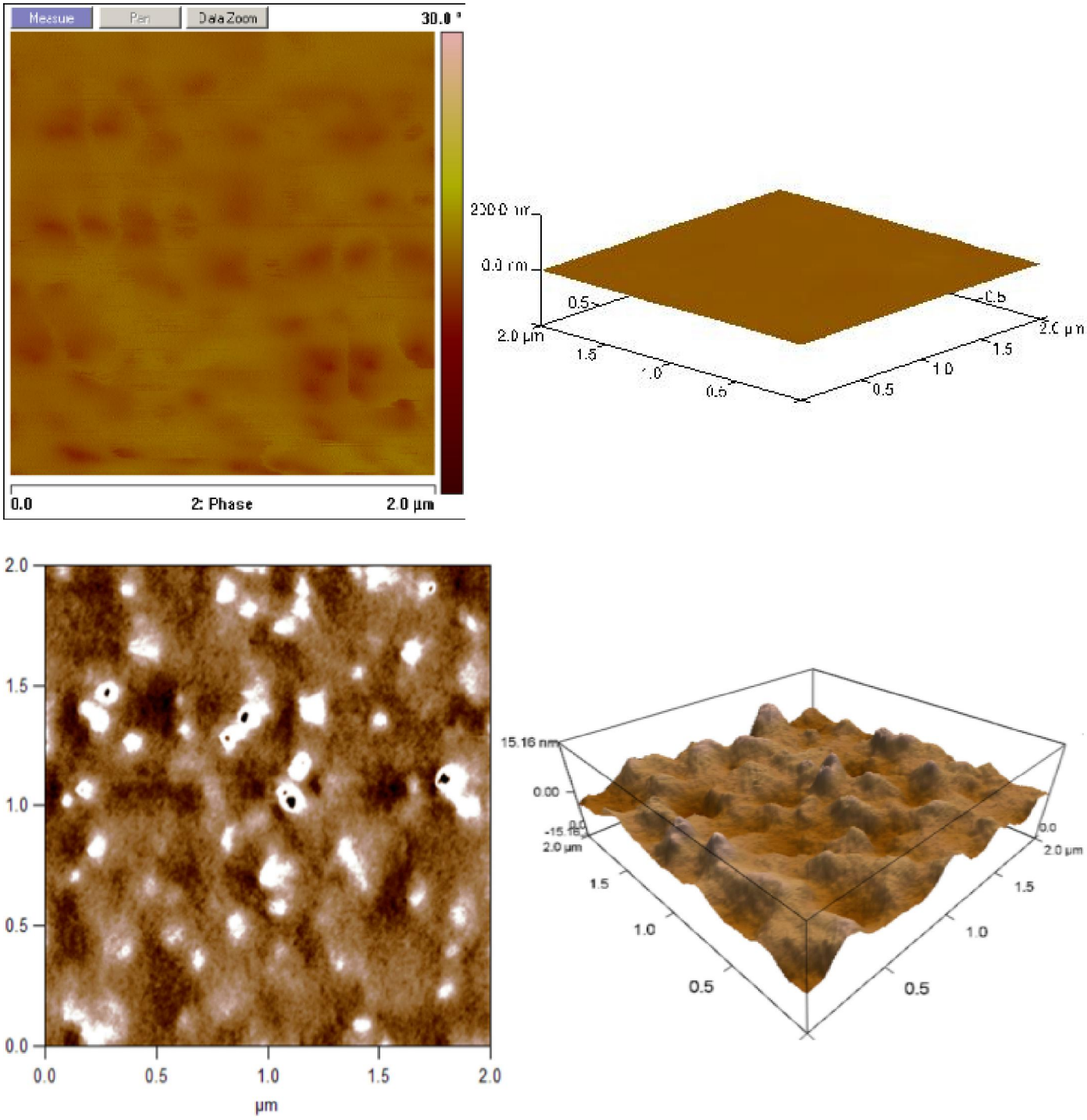

35x -2 Surfaces

Phase Contrast (left) and 3D Height (right) surface images from Veeco instrument (upper pair) and Asylum instrument (lower pair)

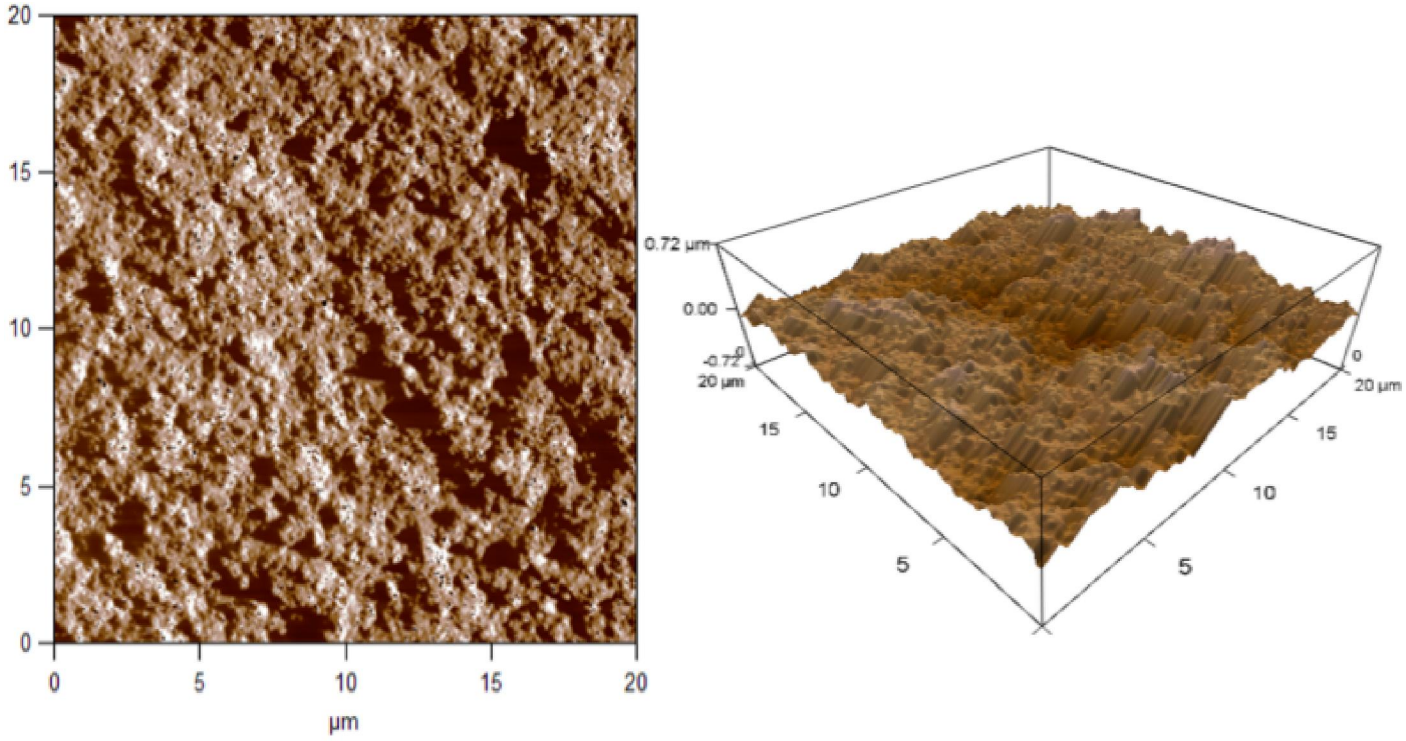

35x -20 Fracture Surface

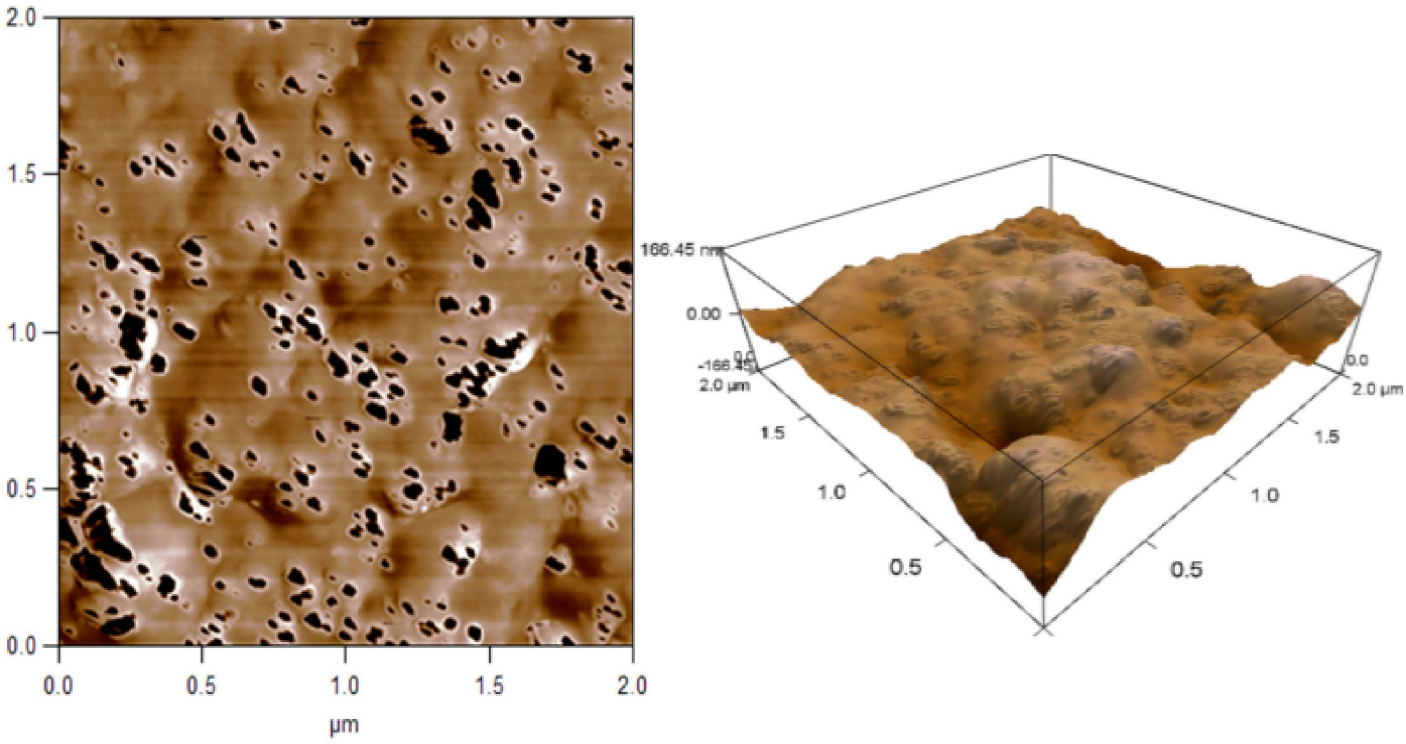

35x -2 Fracture Surface

Phase Contrast (left) and 3D Height (right) surface images from Asylum instrument

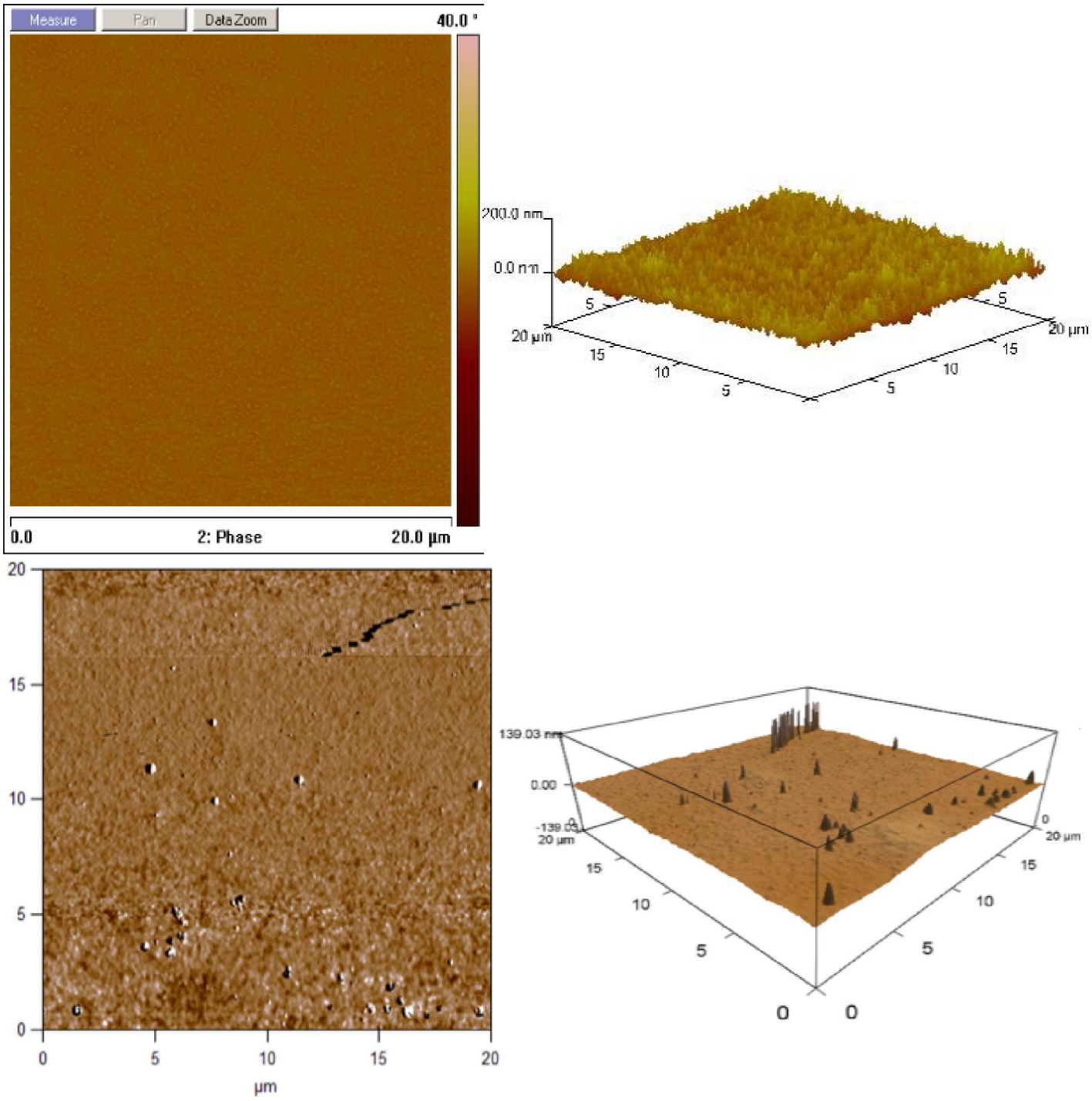

45x -20 µm Surfaces

Phase Contrast (left) and 3D Height (right) surface images from Veeco instrument (upper pair) and Asylum instrument (lower pair)

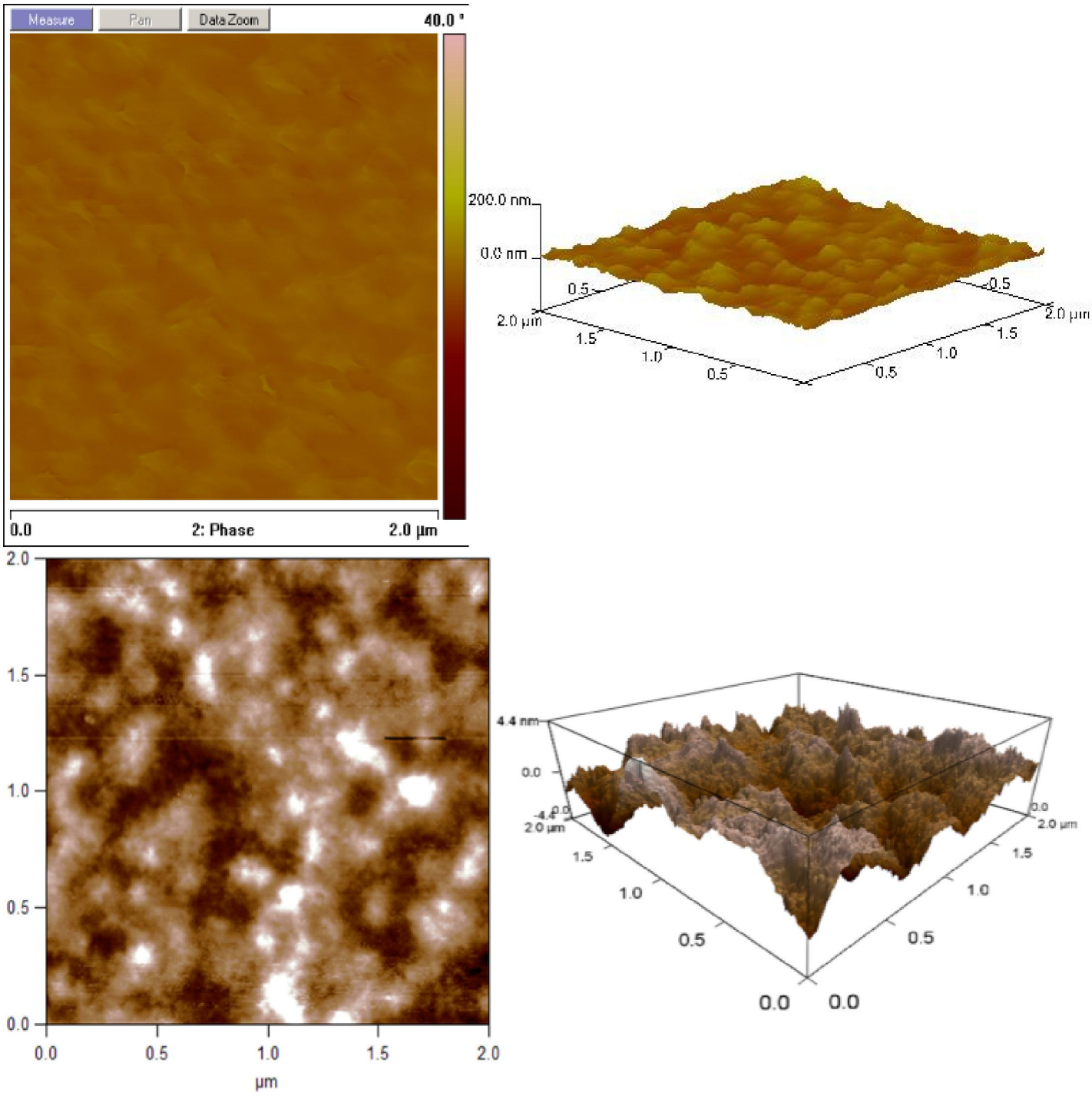

45x -2 µm Surfaces

Phase Contrast (left) and 3D Height (right) surface images from
Veeco instrument (upper pair) and Asylum instrument (lower pair)

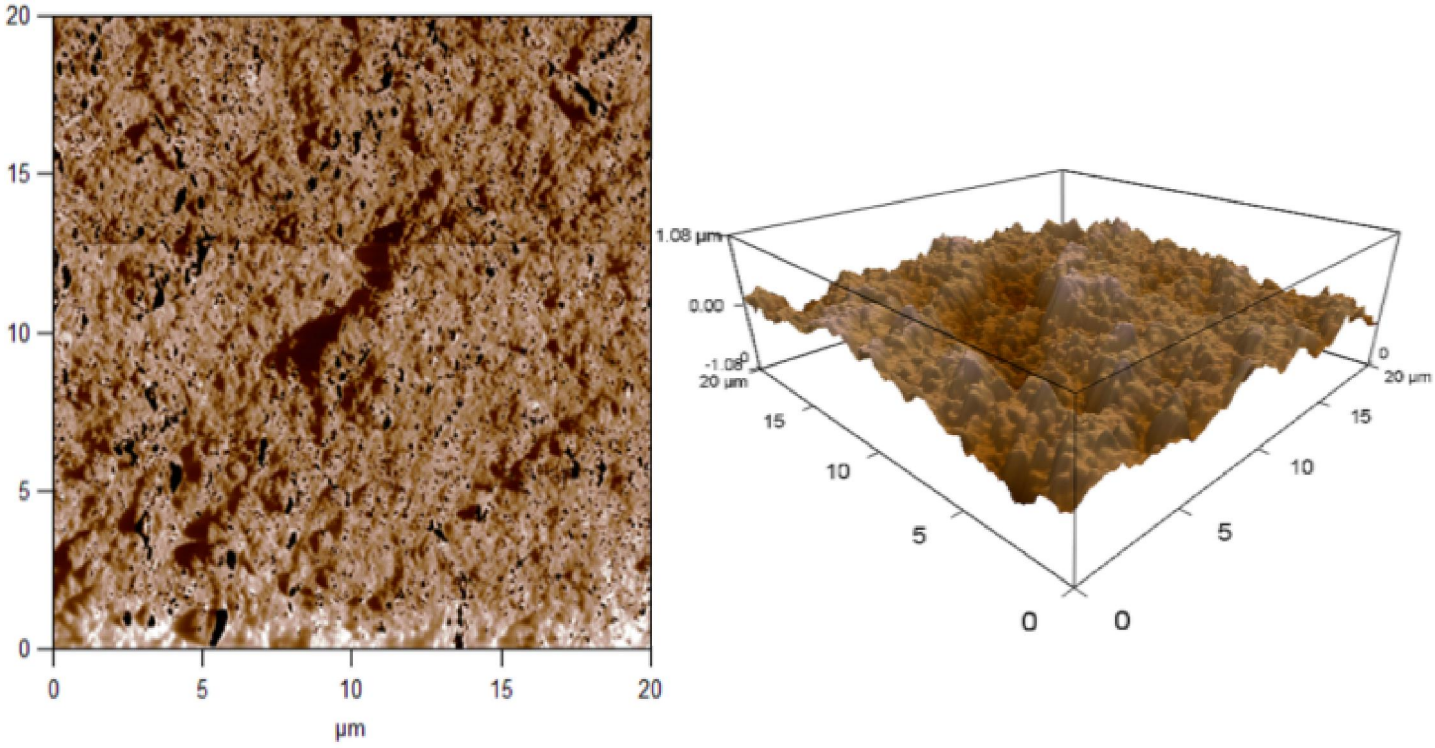

45x -20 µm Fracture Surface

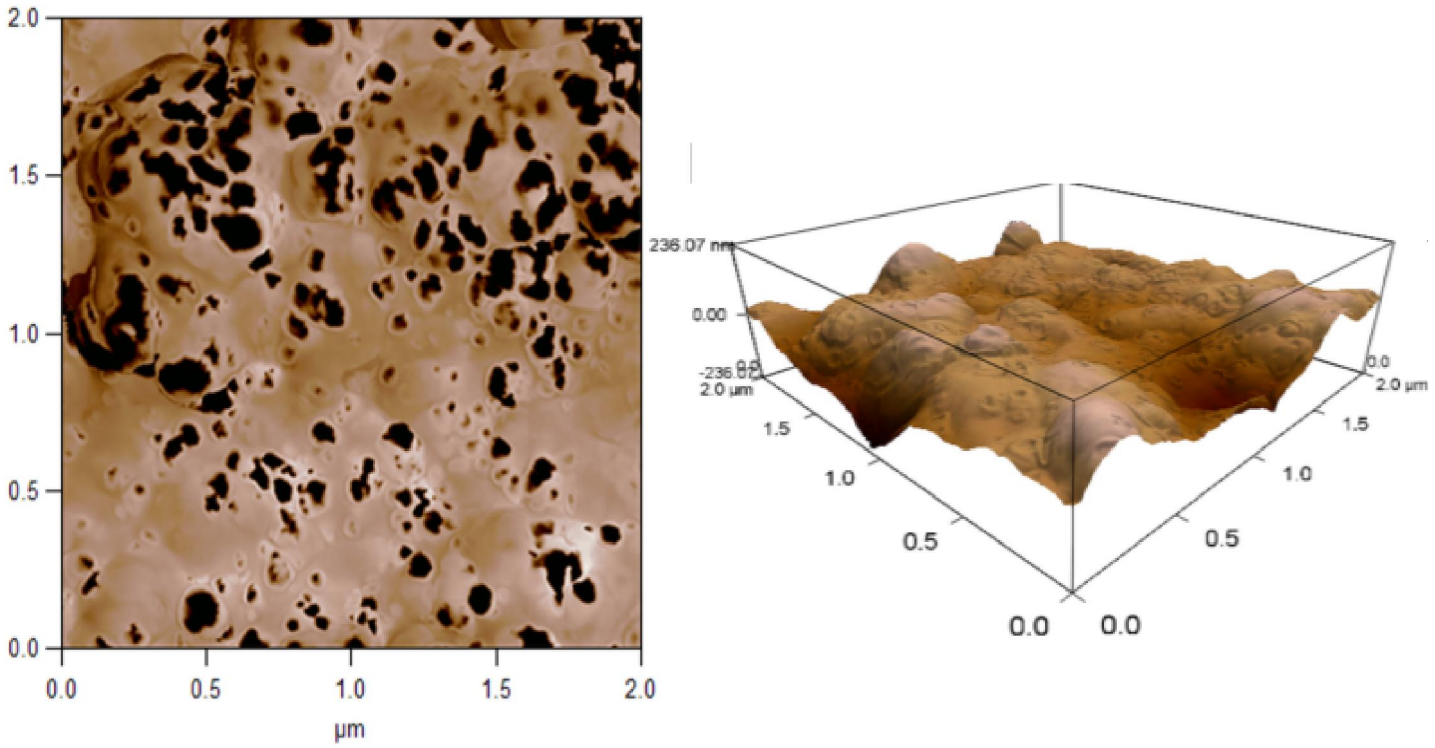

45x -2 µm Fracture Surface

Phase Contrast (left) and 3D Height (right) surface images from Asylum instrument

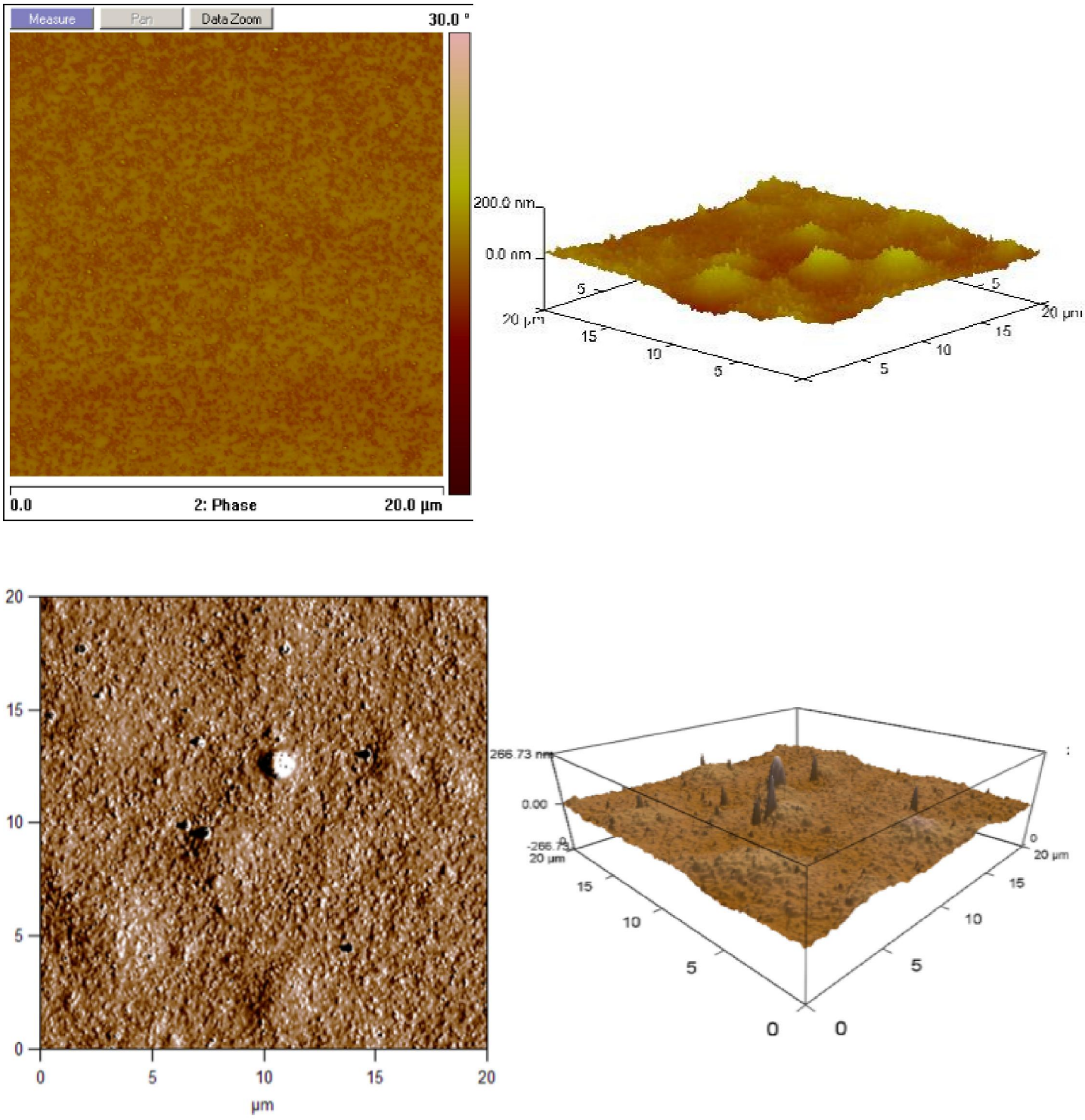

60x -20 Surfaces

Phase Contrast (left) and 3D Height (right) surface images from Veeco instrument (upper pair) and Asylum instrument (lower pair)

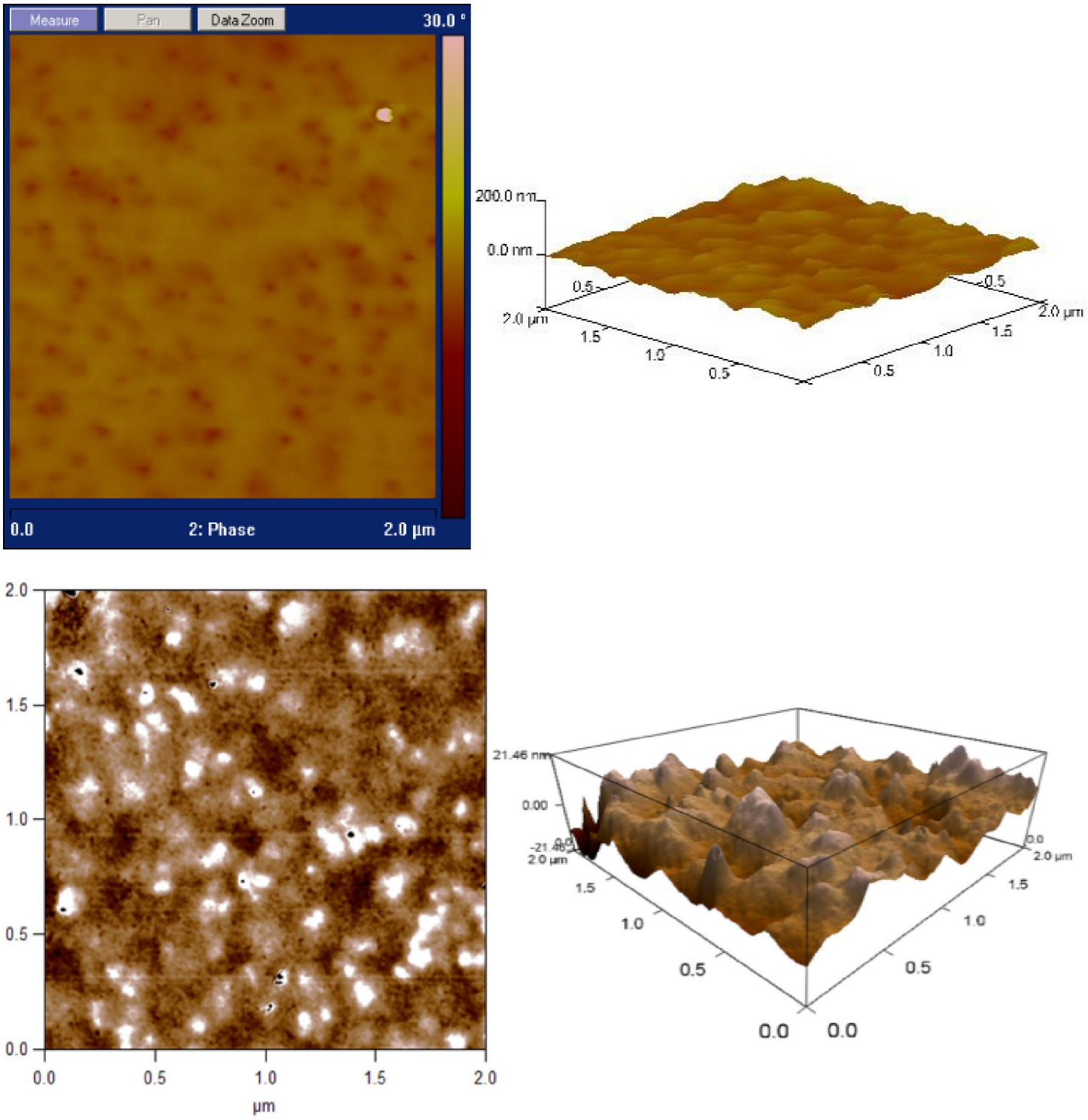

60x -2 Surfaces

Phase Contrast (left) and 3D Height (right) surface images from Veeco instrument (upper pair) and Asylum instrument (lower pair)

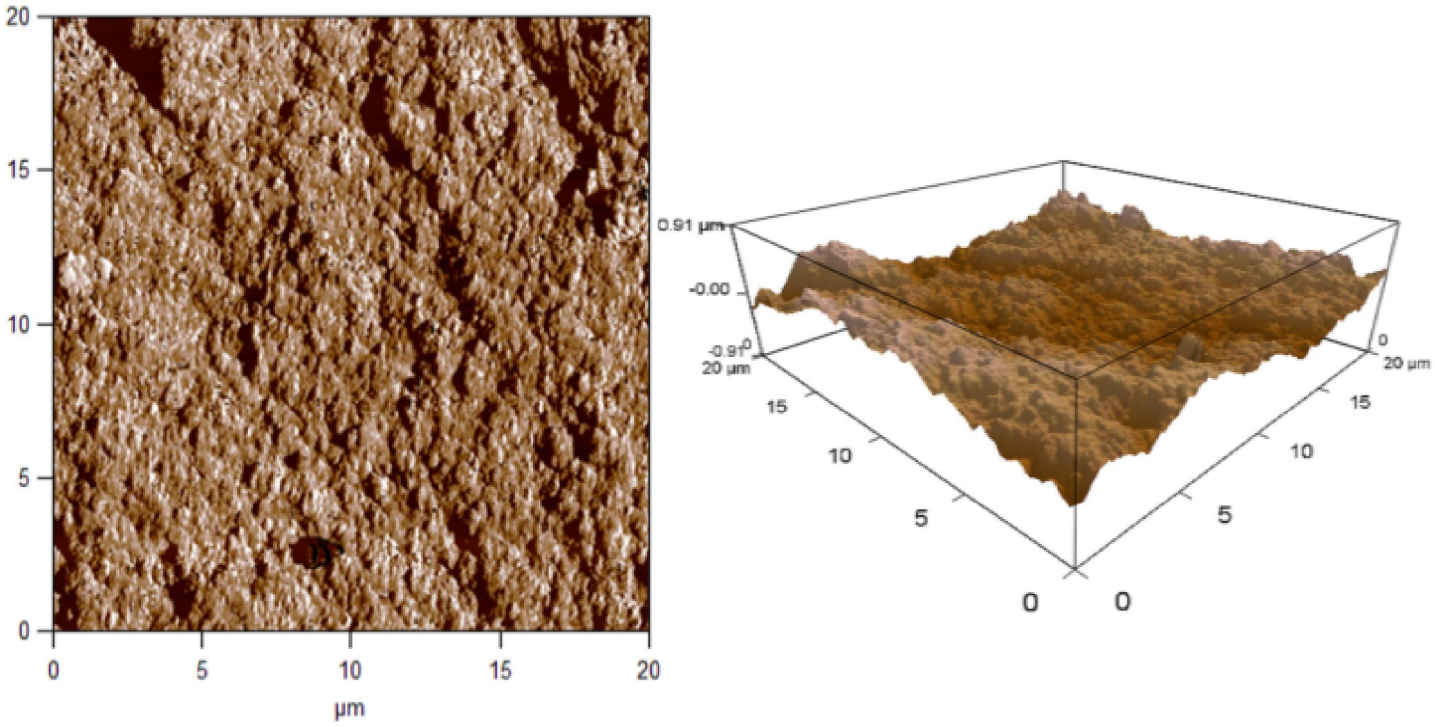

60x -20 Fracture Surface

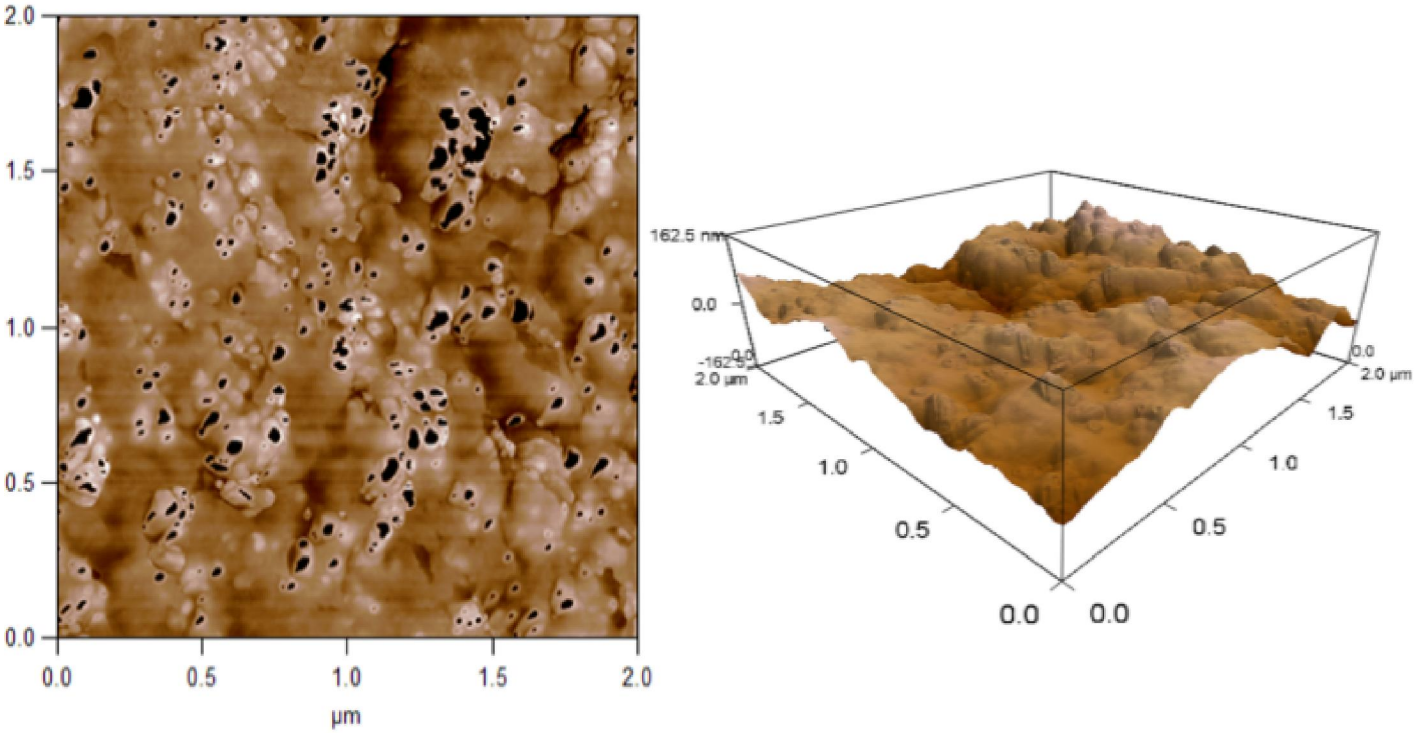

60x -2 Fracture Surface

Phase Contrast (left) and 3D Height (right) surface images from Asylum instrument

Appendix II

Mass and TGA Data
for the
Determination
of
Bound Rubber Content
in
PDMS/ uFSN Admixtures

Temp	Proc	Sample Mass			1st Extr Mass			2nd Extr Mass			3rd Extr Mass			Resid Mass			Recov Mass			Bound Rubber
C	Time hr	(g)	PDMS	uFSN	(g)	PDMS	uFSN	(g)	PDMS	uFSN	(g)	PDMS	uFSN	(g)	PDMS	uFSN	(g)	PDMS	uFSN	g/g
25	0.1	5.003	4.293	0.710	3.320	3.320	0.000	0.550	0.547	0.003	0.089	0.089	0.000	0.926	0.178	0.748	4.885	4.134	0.751	0.24
		%	85.8	14.2		100.0	0.0		99.5	0.5		100.0	0.0		19.2	80.8	97.6	96.3	105.7	
25	0.1	4.997	4.287	0.710	3.419	3.405	0.014	0.491	0.487	0.004	0.111	0.111	0.000	0.912	0.184	0.728	4.933	4.188	0.745	0.25
		%	85.8	14.2		99.6	0.4		99.2	0.8		100.0	0.0		20.2	79.8	98.7	97.7	105.0	
60	3.0	4.999	4.289	0.710	3.581	3.438	0.143	0.335	0.328	0.007	0.029	0.029	0.000	0.795	0.184	0.580	4.740	3.979	0.729	0.32
		%	85.8	14.2		96.0	4.0		98.0	2.0		100.0	0.0		23.1	72.9	94.8	92.8	102.8	
60	72.0	5.000	4.290	0.710	3.699	3.618	0.081	0.279	0.276	0.003	0.030	0.030	0.000	0.938	0.271	0.667	4.946	4.194	0.752	0.41
		%	85.8	14.2		97.8	2.2		98.8	1.2		100.0	0.0		28.9	71.1	98.9	97.8	105.9	
80	3.0	5.000	4.290	0.710	2.810	2.810	0.000	0.880	0.880	0.000	0.060	0.025	0.035	1.040	0.293	0.747	4.790	4.009	0.781	0.39
		%	85.8	14.2		100.0	0.0		100.0	0.0		42.2	57.8		28.2	71.8	95.8	93.4	110.1	
80	24.0	4.982	4.275	0.707	3.757	3.757	0.000							1.115	0.392	0.723	4.872	4.149	0.723	0.54
		%	85.8	14.2		100.0	0.0								35.2	64.8	97.8	97.1	102.1	
80	48.0	5.000	4.290	0.710	3.040	3.040	0.000	0.540	0.540	0.000	0.060	0.026	0.034	1.140	0.439	0.701	4.780	4.044	0.735	0.63
		%	85.8	14.2		100.0	0.0		100.0	0.0		43.5	56.5		38.5	61.5	95.6	94.3	103.6	
95	3.0	4.999	4.289	0.710	3.959	3.856	0.103							0.944	0.309	0.635	4.903	4.165	0.738	0.49
		%	85.8	14.2		97.4	2.6								32.8	67.2	98.1	97.1	103.9	
95	12.0	5.000	4.290	0.710	2.860	2.849	0.011	0.740	0.740	0.000	0.110	0.048	0.062	1.010	0.378	0.632	4.720	4.015	0.706	0.60
		%	85.8	14.2		99.6	0.4		100.0	0.0		43.4	56.6		37.4	62.6	94.4	93.6	99.4	

(cont.)

Temp	Proc	Sample Mass			1st Extr Mass			2nd Extr Mass			3rd Extr Mass			Resid Mass			Recov Mass			Bound Rubber
C	Time hr	(g)	PDMS	uFSN	(g)	PDMS	uFSN	(g)	PDMS	uFSN	(g)	PDMS	uFSN	(g)	PDMS	uFSN	(g)	PDMS	uFSN	g/g
110	3.0	4.998	4.288	0.710	3.279	3.259	0.020	0.431	0.430	0.001	0.046	0.046	0.000	1.134	0.426	0.708	4.890	4.161	0.729	0.60
		%	85.8	14.2		99.4	0.6		99.7	0.3		100.0	0.0		37.6	62.4	97.8	97.0	102.7	
110	3.0	4.995	4.286	0.709	3.644	3.580	0.064	0.202	0.199	0.003	0.030	0.030	0.000	1.083	0.402	0.681	4.959	4.211	0.748	0.59
		%	85.8	14.2		98.2	1.8		98.6	1.4		100.0	0.0		37.1	62.9	99.3	98.3	105.5	
110	3.0	5.005	4.294	0.711	3.323	3.323	0.000	0.390	0.389	0.001	0.049	0.049	0.000	1.208	0.443	0.765	4.970	4.204	0.766	0.58
		%	85.8	14.2		100.0	0.0		99.7	0.3		100.0	0.0		36.7	63.3	99.3	97.9	107.8	
110	3.0	4.971	4.265	0.706	3.662	3.622	0.040	0.169	0.166	0.003	0.035	0.035	0.000	1.091	0.413	0.678	4.957	4.237	0.720	0.61
		%	85.8	14.2		98.9	1.1		98.5	1.5		100.0	0.0		37.9	62.1	99.7	99.3	102.0	
110	12.5	5.000	4.290	0.710	2.870	2.870	0.000	0.670	0.669	0.001	0.060	0.027	0.033	1.180	0.512	0.668	4.780	4.078	0.702	0.77
		%	85.8	14.2		100.0	0.0		99.9	0.1		44.3	55.7		43.4	56.6	95.6	95.1	98.8	
110	24.0	5.000	4.290	0.710	3.130	3.036	0.094	0.410	0.410	0.000	0.110	0.053	0.057	0.970	0.442	0.528	4.620	3.941	0.679	0.84
		%	85.8	14.2		97.0	3.0		100.0	0.0		47.8	52.2		45.6	54.4	92.4	91.9	95.6	
25	120.0	5.007	4.296	0.711	4.115	3.982	0.133							0.806	0.193	0.613	4.921	4.176	0.745	0.32
		%	85.8	14.2		96.8	3.2								24.0	76.0	98.3	97.2	104.8	
25	144.0	4.997	4.287	0.710	4.025	3.957	0.068							0.875	0.215	0.660	4.900	4.172	0.728	0.33
		%	85.8	14.2		98.3	1.7								24.6	75.4	98.1	97.3	102.6	
25	144.0	4.991	4.282	0.709	4.481	4.091	0.390							0.433	0.106	0.327	4.914	4.197	0.717	0.32
		%	85.8	14.2		91.3	8.7								24.4	75.6	98.5	98.0	101.2	
																Avg	97.3	96.2	103.3	
																SD	2.0	2.2	3.3	

References

[1] Dow-Corning, "Highlights from the history of Dow Corning Corporation, the silicone pioneer," (2008).
[2] Dow-Corning, "Material Safety Data Sheet, Dow Corning 4 Electrical Insulating Compound Ver. 1.4," (2009).
[3] Eugene Rochow, Silicon and silicones : about Stone-age tools, antique pottery, modern ceramics, computers, space materials and how they all got that way (Berlin u.a.: Springer, 1987). p. 87.
[4] Eugene Rochow. Methyl Silicones and Related Products. U.S. Patent 2258218, Issued 1941/10/07.
[5] James Franklin Hyde. Insulated Conductor and Insulation Therefor. U.S. Patent 2386466, Issued 1945/10/09.
[6] Geoffrey Martin and Frederic Stanley Kipping, "XXXVIII.-Benzyl and ethyl derivatives of silicon tetrachloride," Journal of the Chemical Society, Transactions 95(1909). pp 302-314.
[7] Neil R. Thomas, "Frederic Stanley Kipping—Pioneer in Silicon Chemistry: His Life & Legacy," Silicon 2(2010). pp 187-193.
[8] Nm9J, "Essential 2 Flexible," PCARA Update 2010. pp 4-7.
[9] A. J. O'Lenick Jr, "Basic Silicone Chemistry," Silicone Spectator(2009), http://www.siliconespectator.com/articles/Silicone_Spectator_January_2009.pdf.
[10] "Silicone 8. High temperature and Chemical resistant Silicone Rubber," http://www.chemcases.com/silicon/sil8cone.htm.
[11] J. Burkhardt and G. ed Koerner, "Chemistry and Technology of Polysiloxanes," in Silicones, chemistry and technology (CRC Press, 1992).
[12] Richard G. Jones, Ando Wataru, and Julian Chojnowski, Silicon-Containing Polymers: The Science and Technology of Their Synthesis and Applications (Springer, 2001). p. 8.
[13] J. Chojnowski, S. Rubinsztajn, and L. Wilczek, "Acid-catalyzed condensation of model hydroxyl-terminated dimethylsiloxane oligomers - cyclization vs. linear condensation: intra-inter catalysis," Macromolecules 20, no. 10 (1987). pp 2345-2355.
[14] Jones, Wataru, and Chojnowski, Silicon-Containing Polymers: The Science and Technology of Their Synthesis and Applications. p. 6.
[15] Roger DeJaeger and Mario Gleria, Silicon-based inorganic polymers (Nova Science, 2008). p. 11.
[16] J. Rich et al., "Silicon Compounds, Silicones," in Kirk-Othmer Encyclopedia of Chemical Technology (1997). p. 5.
[17] Claire Jalbert et al., "Molecular weight dependence and end-group effects on the surface tension of poly(dimethylsiloxane)," Macromolecules 26, no. 12 (1993). pp 3069-3074.
[18] Rich et al., "Silicon Compounds, Silicones." p. 2.
[19] Rob Roy McGregor, Silicones and their uses (McGraw-Hill, 1954). p. 27.
[20] DeJaeger and Gleria, Silicon-based inorganic polymers. p. 63.
[21] Linus Pauling, "The nature of silicon-oxygen bonds," American Mineralogist 65(1980).pp 321-323.
[22] DeJaeger and Gleria, Silicon-based inorganic polymers. p. 3.
[23] Geoff Rayner-Canham and Tina Overton, Descriptive Inorganic Chemistry (W. H. Freeman, 2006). p. 311.
[24] Dow-Corning, "Silicone™ Chemistry – Silicone vs. Organic Polymers," http://www.dowcorning.com/content/discover/discoverchem/si-vs-organic.aspx?e=Physical+%26+Chemical+Properties.
[25] DeJaeger and Gleria, Silicon-based inorganic polymers. p. 3.
[26] J. E. Mark, "Some interesting things about polysiloxanes," Accounts of chemical research 37, no. 12 (2004). pp 946-953.
[27] Centre Europeen des Silicones, "Diagram of Typical Silicone Molecule - Modified," http://www.silicones-science.com/chemistry/basic-structure.
[28] Vadapalli Chandrasekhar, Inorganic and Organometallic Polymers (Berlin: Springer, 2005). p. 242.
[29] Ibid. p. 241.
[30] Ibid. p. 243.

[31] S. Wu, "VI," in Polymer Handbook, ed. J. Brandrup and E. H. Immergut (New York, NY: Wiley-Interscience, 1989).
[32] DeJaeger and Gleria, Silicon-based inorganic polymers. p. 64.
[33] Stuart M. Lee, Reference book for composites technology (CRC Press, 1989). p. 67.
[34] Alex C. Kuo and James E. ed Mark, Poly(dimethylsiloxane) in "Polymer data handbook" (Oxford University Press, 2009). p. 546.
[35] R. N. Lichtenthaler, D. D. Liu, and J. M. Prausnitz, "Specific Volumes of Dimethylsiloxane Polymers to 900 Bars," Macromolecules 11, no. 1 (1978). pp 192-195.
[36] Rich et al., "Silicon Compounds, Silicones." p. 21.
[37] Anil K. Bhowmick and Howard L. Stephens, Handbook of elastomers (CRC Press, 2001). p. 625.
[38] Eugène Papirer, Adsorption on silica surfaces (CRC Press, 2000). p. 46.
[39] Ibid. p. 47.
[40] Bhowmick and Stephens, Handbook of elastomers. p. 606
[41] Rochow, Silicon and silicones : about Stone-age tools, antique pottery, modern ceramics, computers, space materials and how they all got that way. p. 61.
[42] James Falender, "Presentation - The History of Chemistry in Dow Corning," (2006). Slide 23.
[43] "United States Synthetic Rubber Program, 1939-1945," http://portal.acs.org/portal/acs/corg/content?_nfpb=true&_pageLabel=PP_ARTICLEMAIN&node_id=929&content_id=CTP_004465&use_sec=true&sec_url_var=region1&__uuid=79ab49b0-b47d-4eaa-af0d-54af31408c4b.
[44] Frank Zephyr and Aldo Musacchio, "The International Natural Rubber Market, 1870-1930 | Economic History Services," http://eh.net/encyclopedia/article/frank.international.rubber.market.
[45] Ibid.
[46] "United States Synthetic Rubber Program, 1939-1945".
[47] "Silicones 4. Corning and the First Silicones for High Temperature Insulation," http://www.chemcases.com/silicon/sil4cone.htm.
[48] Dallas T. Hurd and Alden P. Armagnac, "How You'll Use the New Silicones," Popular Science 1948. p. 132.
[49] Earl L. Warrick. Method for Making Rubbery Polymeric Organo-Siloxane Compositions. U.S. Patent 2,460,795, Issued 1949/02/01.
[50] Hurd and Armagnac, "How You'll Use the New Silicones." p. 32.
[51] A. K. Jershow, Silicone Elastomers, RAPRA Review Reports,Report 137, vol. 12 (Rapara Technology Ltd., 2001). p. 7.
[52] Keith E. Polmanteer. Siloxane Elastomers. U.S. Patent 2927907, Issued 1960/03/08.
[53] Jershow, Silicone Elastomers, RAPRA Review Reports,Report 137, 12. p. 25.
[54] Matthew Butts, James Cella, and Christina Darkangelo Wood, "Silicones Kirk-Othmer Encyclopedia of Chemical Technology," Kirk-Othmer Encyclopedia of Chemical Technology (2002). p. 8.
[55] Frederik Willem van Der Weij, "The action of tin compounds in condensation - type RTV silicone rubbers," Die Makromolekulare Chemie 181, no. 12 (1980). pp 2541-2548.
[56] Bhowmick and Stephens, Handbook of elastomers. p. 616.
[57] K. A. Smith, "A study of the hydrolysis of methoxysilanes in a two-phase system," The Journal of Organic Chemistry 51, no. 20 (1986). pp 3827-3830.
[58] M. Guibergia-Pierron and G. Sauvet, "Heterofunctional condensation of alkoxysilanes and silanols–I. Synthesis of definite polysiloxane networks," European polymer journal 28, no. 1 (1992). pp 29-36.
[59] G. L. Witucki, "A silane primer: chemistry and applications of alkoxy silanes," Journal of coatings technology 65(1993). pp 57-60.
[60] D. W. McCarthy, J. E. Mark, and D. W. Schaefer, "Synthesis, structure, and properties of hybrid organic-inorganic composites based on polysiloxanes. I. Poly (dimethylsiloxane) elastomers containing silica," Journal of Polymer Science-B-Polymer Physics Edition 36, no. 7 (1998). pp 1167-1189.
[61] R. N. Meals, "Silicones," Annals of the New York Academy of Sciences 125, no. 1 (1965). pp 137-146.
[62] G. E. Silicones, "RTV162 MSDS," (2003).
[63] S. J. Clarson, K. Dodgson, and J. A. Semlyen, "Studies of cyclic and linear poly(dimethylsiloxanes): 19. Glass transition temperatures and crystallization behaviour," Polymer 26, no. 6 (1985). pp 930-934.
[64] Materials Momentive Performance, "RTV162 Data Sheet," (Momentive Performance Materials, Inc, 2010).

[65] McGregor, Silicones and their uses. p. 149.
[66] Momentive Performance, "RTV162 Data Sheet."
[67] Etsu Shin, "Characteristic Properties of Silicone Rubber Compounds," (Shin-Etsu, 2005).
[68] Rochow, Silicon and silicones : about Stone-age tools, antique pottery, modern ceramics, computers, space materials and how they all got that way. pp. 108, 114.
[69] Walter Waddell, "Production, classification and properties of natural rubber--part 2 - - Free Online Library,"
http://www.thefreelibrary.com/_/print/cite.aspx?url=http%3A%2F%2Fwww.thefreelibrary.com%2FProduction%2C%2Bclassification%2Band%2Bproperties%2Bof%2Bnatural%2Brubber--part%2B2.-a0137862033&author=Waddell,+Walter+H.&title=Production,+classification+and+properties+of+natural+rubber--part+2&artId=137862033&pubDate=2005-09-01.
[70] W. Hechtl, "Chemistry and Technology of Room-Temperature-Vulcanizable Silicone Rubber," in Silicones Chemistry and Technology (CRC Press, 1992). p. 50.
[71] Charles Goodyear, "Processes for the Fabrication of a Less Rigid, Flexible or Elastic Rubber," Dingler's Polytechnisches Journal 139(1856). pp 376-386.
[72] B. B. Boonstra, "Role of particulate fillers in elastomer reinforcement: A review," Polymer 20, no. 6 (1979). pp 691-704.
[73] Evonik-Degussa, "Technical Bulletin Number 11, Fine Particles, Basic Characteristics of Aerosil Fumed Silica," (Degussa AG, Applied Technology Aerosil, 2006). p. 8.
[74] Gamal M. S. El Shafie, "Silica Surface Chemical Properties," in Adsorption on silica surfaces, ed. Eugène Papirer (CRC Press, 2000). p. 37.
[75] David Boldridge, "Morphological Characterization of Fumed Silica Aggregates," Aerosol Science and Technology 44(2010). pp 182-186.
[76] Werner Michel, "Fumed Silicas Reinforce Elastomers," (Degussa GmbH, Applied Technology Aerosil, 2007).
[77] Nikhil Ravindra Agashe, "in-situ Small Angle X-Ray Scattering Studies of Continuous Nano-Particle Synthesis in Premixed Diffusion Flames" (University of Cincinnati, 2004).
[78] Stephen J. Clarson and J. A. Semlyen, Siloxane polymers (Prentice Hall, 1993). p. 514.
[79] A. Camenzind, W. R. Caseri, and S. E. Pratsinis, "Flame-made nanoparticles for nanocomposites," Nano Today 5, no. 1 (2010). pp 48-65.
[80] Evonik-Degussa, "Technical Bulletin Number 11, Fine Particles, Basic Characteristics of Aerosil Fumed Silica."
[81] C. M. Sorensen, "Light scattering by fractal aggregates: a review," Aerosol Science and Technology 35, no. 2 (2001). pp 648-687.
[82] Boldridge, "Morphological Characterization of Fumed Silica Aggregates."
[83] E. Schaer et al., "Experimental tracking of silica dispersion into silicone polymer," Powder technology 168, no. 3 (2006). pp 156-166.
[84] C. Oh and C. M. Sorensen, "The Effect of Overlap between Monomers on the Determination of Fractal Cluster Morphology," Journal of Colloid and Interface Science 193, no. 1 (1997). pp 17-25.
[85] D. W. Schaefer, K. D. Keefer, and Luciano Pietronero, "Analysis of Fractal Properties of Materials," in Fractals in physics: proceedings of the Sixth International Symposium on Fractals in Physics, ICTP, Trieste, Italy, July 9-12, 1985 (North-Holland, 1986). p. 39.
[86] David Avnir, Dina Farin, and Peter Pfeifer, "Chemistry in noninteger dimensions between two and three. II. Fractal surfaces of adsorbents," The Journal of Chemical Physics 79, no. 7 (1983). p 3566.
[87] Adrian Camenzind et al., "Nanostructure Evolution: From Aggregated to Spherical SiO2 Particles Made in Diffusion Flames," European Journal of Inorganic Chemistry 2008, no. 6 (2008). Pp 911-918.
[88] Jean L. Leblanc, Filled Polymers: Science and Industrial Applications (CRC Press, 2009). pp 68-69.
[89] Evonik-Degussa, "Technical Bulletin Number 11, Fine Particles, Basic Characteristics of Aerosil Fumed Silica." p. 37.
[90] J. Mathias and G. Wannemacher, "Basic characteristics and applications of aerosil:: 30. The chemistry and physics of the aerosil Surface," Journal of colloid and interface science 125, no. 1 (1988). pp 61-68.
[91] Evonik-Degussa, "Technical Bulletin Number 11, Fine Particles, Basic Characteristics of Aerosil Fumed Silica." p. 41.
[92] Papirer, Adsorption on silica surfaces. p. 87.
[93] Ibid. p. 37.

[94] Bhowmick and Stephens, Handbook of elastomers. p. 631.
[95] Earl L. Warrick. Siloxane Elastomers. U.S. Patent 2541137, Issued 1951/02/13.
[96] Wilfred Lynch, Handbook of silicone rubber fabrication (Van Nostrand Reinhold, 1978). p. 27.
[97] Evonik-Degussa, "Successful Use of AEROSIL Fumed Silica in Liquid Systems TI 1279," (Evonik Degussa GmbH, 2009). p. 5- 6.
[98] A. Einstein, "A New Determination of Molecular Dimensions," Annalen der Physik 19, 34(1906). p 289.
[99] E. Guth, "Theory of filler reinforcement," Journal of Applied Physics 16, no. 1 (1945). pp 20-25.
[100] D J Beaucage Kohls, G, "Rational Design of reinforced rubber," Current Opinion in Solid State and Materials Science 6(2002). Pp 183-194.
[101] Irvin M. Krieger, "A Mechanism for Non-Newtonian Flow in Suspensions of Rigid Spheres," Journal of Rheology 3(1959). p. 137.
[102] Dietrich Stauffer and Amnon Aharony, Introduction to percolation theory (CRC Press, 1994).
[103] Patricio Jeraldo, "Critical Phenomena in Percolation Theory," (2005). On line Essay University of Illinois. http://guava.physics.uiuc.edu/~nigel/courses/563/Essays_2005/PDF/jeraldo.pdf
[104] F. Bohin, D. L. Feke, and I. Manas-Zloczower, "Determination of the infiltration kinetics of polymer into filler agglomerates using transient buoyancy measurements," Powder technology 83, no. 2 (1995). pp 159-162.
[105] Jv DeGroot and Cw Macosko, "Aging Phenomena in Silica-Filled Polydimethylsiloxane," Journal of Colloid and Interface Science 217, no. 1 (1999). pp 86-93.
[106] L. L. Popovich, D. L. Feke, and I. Manas-Zloczower, "Influence of physical and interfacial characteristics on the wetting and spreading of fluids on powders," Powder technology 104, no. 1 (1999). pp 68-74.
[107] A. M. Bueche, "Filler reinforcement of silicone rubber," Journal of Polymer Science 25, no. 109 (1957). pp 139-149.
[108] E. L. Warrick and P. C. Lauterbur, "Filler phenomena in silicone rubber," Industrial & Engineering Chemistry 47, no. 3 (1955). pp 486-491.
[109] G. Berrod et al., "Reinforcement of siloxane elastomers by silica. Chemical interactions between an oligomer of poly(dimethylsiloxane) and a fumed silica," Journal of Applied Polymer Science 26, no. 3 (1981). pp 833-845.
[110] L. Leger, H. Hervert, and M. Deruelle, "Adsorption of polydimethylsiloxane chains on plane silica surfaces," in Adsorption on silica surfaces (Dekker, New York, 2000). pp 597-619.
[111] Petr Vondráček and Miroslav Schätz, "NH3 modified swelling of silica filled silicone rubber," Journal of Applied Polymer Science 23, no. 9 (1979). pp 2681-2694.
[112] Seila Selimovic, Sarah M. Maynard, and Yue Hu, "Aging effects of precipitated silica in poly(dimethylsiloxane)," Journal of Rheology 51(2007). p 325.
[113] B. B. Boonstra, "Reinforcement by Fillers," in Rubber Technology and Manufacture, ed. C. M. Blow and C. Hepburn (London: Butterworth, 1982). p. 269.
[114] Petr Vondráček and Miroslav Schätz, "Bound rubber and “crepe hardening” in silicone rubber," Journal of Applied Polymer Science 21, no. 12 (1977). pp 3211-3222.
[115] Clarson and Semlyen, Siloxane polymers. p 517.
[116] K. E. Polmanteer and C. W. Lentz, "Reinforcement Studies—Effect of Silica Structure on Properties and Crosslink Density," Rubber Chemistry and Technology 48(1975). p 795.
[117] G. Berrod et al., "Reinforcement of siloxane elastomers by silica. Interactions between an oligomer of poly(dimethylsiloxane) and a fumed silica," Journal of Applied Polymer Science 23, no. 9 (1979). pp 2579-2590.
[118] Erik Geissler, Anne- Marie Hecht, and Ferenc Horkay, "Structure of polymer solutions and gels containing fillers," Macromolecular Symposia 171, no. 1 (2001). pp 171-190.
[119] H. Barthel and E. Nikitina, "INS and IR study of intermolecular interactions at the fumed silica-polydimethylsiloxane interphase, Part 3. Sicica-siloxane adsorption complexes," Silicon Chemistry 1, no. 4 (2002). pp 261-279.
[120] Mesfin Tsige et al., "Interactions and structure of poly(dimethylsiloxane) at silicon dioxide surfaces: Electronic structure and molecular dynamics studies," Journal of Chemical Physics 118, no. 11 (2003). pp 5132-5143.

[121] James S. Smith et al., "A molecular dynamics simulation and quantum chemistry study of poly(dimethylsiloxane)–silica nanoparticle interactions," Journal of Polymer Science Part B: Polymer Physics 45, no. 13 (2007). pp 1599-1615.
[122] V. M. Litvinov and H. W. Spiess, "2H NMR study of molecular motions in polydimethylsiloxane and its mixtures with aerosils," Die Makromolekulare Chemie 192, no. 12 (1991). pp 3005-3019.
[123] S. Chandrasekhar, "Stochastic Problems in Physics and Astronomy," Reviews of Modern Physics 15, no. 1 (1943). pp 1-89.
[124] J. P. Cohen-Addad, "Silica-siloxane mixtures. Structure of the adsorbed layer: Chain length dependence," Polymer 30, no. 10 (1989). pp 1820-1823.
[125] J. P. Cohen-Addad and R. Ebengou, "Silica–siloxane mixtures. Investigations into adsorption properties of end-methylated and end-hydroxylated chains," Polymer 33, no. 2 (1992). pp 379-383.
[126] J. P. Cohen Addad and S. Touzet, "Poly (dimethylsiloxane)-silica mixtures: intermediate states of adsorption and swelling properties," Polymer 34, no. 16 (1993). pp 3490-3498.
[127] P. Levresse, D. L. Feke, and I. Manas-Zloczower, "Analysis of the formation of bound poly(dimethylsiloxane) on silica," Polymer 39, no. 17 (1998). pp 3919-3924.
[128] Leblanc, Filled Polymers: Science and Industrial Applications. pp. 250-252.
[129] J. P. Cohen-Addad et al., "Hydroxyl or methyl terminated poly (dimethylsiloxane) chains: kinetics of adsorption on silica in mechanical mixtures," Polymer 30, no. 1 (1989). pp 143-146.
[130] Clarson and Semlyen, Siloxane polymers. pp. 522-524.
[131] Leblanc, Filled Polymers: Science and Industrial Applications. p. 250.
[132] Clarson and Semlyen, Siloxane polymers. p. 523.
[133] J. P. Cohen-Addad and L. Dujourdy, "Silica concentration dependence of the kinetics of polydimethylsiloxane adsorption on aggregates," Polymer Bulletin 41, no. 2 (1998). pp 253-260.
[134] Levresse, Feke, and Manas-Zloczower, "Analysis of the formation of bound poly(dimethylsiloxane) on silica."
[135] Aranguren, Mora, and Macosko, "Compounding Fumed Silicas into Polydimethylsiloxane: Bound Rubber and Final Aggregate Size," Journal of Colloid and Interface Science 195, no. 2 (1997). pp 329-337.
[136] M. Seipenbusch et al., "Interparticle forces in silica nanoparticle agglomerates," Journal of Nanoparticle Research 12(2009). pp 2037-2044.
[137] Evonik-Degussa, "Technical Bulletin Number 11, Fine Particles, Basic Characteristics of Aerosil Fumed Silica." p. 8.
[138]Schaer et al., "Experimental tracking of silica dispersion into silicone polymer."
[139] F. Bohin, I. Manas-Zloczower, and D. L. Feke, "Kinetics of dispersion for sparse agglomerates in simple shear flows: Application to silica agglomerates in silicone polymers," Chemical engineering science 51, no. 23 (1996). pp 5193-5204.
[140] J. F. Boyle, I. Manas-Zloczower, and D. L. Feke, "Hydrodynamic analysis of the mechanisms of agglomerate dispersion," Powder technology 153, no. 2 (2005). pp 127-133.
[141] P. J. Flory, "Constitution of Three-dimensional Polymers and the Theory of Gelation," The Journal of Physical Chemistry 46, no. 1 (1942). pp 132-140.
[142] Walter H. Stockmayer, "Theory of Molecular Size Distribution and Gel Formation in Branched-Chain Polymers," The Journal of Chemical Physics 11(1943). p 45.
[143] Camenzind, Caseri, and Pratsinis, "Flame-made nanoparticles for nanocomposites."
[144] Clarson and Semlyen, Siloxane polymers. p. 525.
[145] H. Eggers and P. Schummer, "Reinforcement Mechanisms in Carbon Black and Silica Loaded Rubber Melts at Low Stresses," Rubber Chemistry and Technology 69(1996). p 253.
[146] McCarthy, Mark, and Schaefer, "Synthesis, structure, and properties of hybrid organic-inorganic composites based on polysiloxanes. I. Poly (dimethylsiloxane) elastomers containing silica."
[147] Camenzind, Caseri, and Pratsinis, "Flame-made nanoparticles for nanocomposites." p. 56.
[148] Evonik-Degussa, "Technical Bulletin Pigments No12 - Degussa Silicas for HTV Silicone Rubber," (Evonik Degussa GmbH, 2004). p. 20.
[149] M. Wang, M. D. Morris, and Y. Kutsovsky, "Effect of Fumed Silica Surface Area on Silicone Rubber Reinforcement," KAUTSCHUK UND GUMMI KUNSTSTOFFE 61, no. 3 (2008). p 107.
[150] B. B. Boonstra, H. Cochrane, and E. M. Dánnenberg, "Reinforcement of Silicone Rubber by Particulate Silica," Rubber Chemistry and Technology 48(1975). p 558.

[151] J. E. Mark, C. Y. Jiang, and M. Y. Tang, "Simultaneous curing and filling of elastomers," Macromolecules 17, no. 12 (1984). pp 2613-2616.
[152] Y. P Ning et al., "Particle sizes of reinforcing silica precipitated into elastomeric networks," Journal of Applied Polymer Science 29, no. 10 (1984). pp 3209-3212.
[153] Burak Erman and James E. Mark, Structures and properties of rubberlike networks (Oxford University Press, 1997).
[154] C. C. Sun and J. E. Mark, "Comparisons among the reinforcing effects provided by various silica-based fillers in a siloxane elastomer," Polymer 30, no. 1 (1989). pp 104-106.
[155] McCarthy, Mark, and Schaefer, "Synthesis, structure, and properties of hybrid organic-inorganic composites based on polysiloxanes. I. Poly (dimethylsiloxane) elastomers containing silica."
[156] Tomoki Ogoshi et al., "Tapping Mode AFM Evidence for an Amorphous Reticular Phase in a Condensation-Cured Hybrid Elastomer: α,ω-Dihydroxypoly(dimethylsiloxane)/Poly(diethoxysiloxane)/Fumed Silica Nanoparticles," Journal of the American Chemical Society 126(2004). pp 12284-12285.
[157] Shinsuke Inagi et al., "Appearing, Disappearing, and Reappearing Fumed Silica Nanoparticles: Tapping-Mode AFM Evidence in a Condensation Cured Polydimethylsiloxane Hybrid Elastomer," Chemistry of Materials 19(2007). pp 2141-2143.
[158] S. Chakrabarty et al., "Processing dependence of surface morphology in condensation cured PDMS nanocomposites," Polymer 51(2010). pp 5756-5763.
[159] Ogoshi, "Ogoshi_Supporting Information JACS.doc."
[160] Inagi, "Inagi_Supporting Information Chem Mater.doc."
[161] Chakrabarty, "Souvik_Polym2010SuppInfo and unpublished notes."
[162] "SpeedMixer™ - DAC 150 FV," http://www.speedmixer.com/dac150.1fv.php.
[163] Selimovic, Maynard, and Hu, "Aging effects of precipitated silica in poly(dimethylsiloxane)."
[164] DeGroot and Macosko, "Aging Phenomena in Silica-Filled Polydimethylsiloxane."
[165] Malvern, "Chapter 6 Sample Preparation," in Zetasizer Nano Series User Manual (Malvern Instruments Ltd., 2004).
[166] Papirer, Adsorption on silica surfaces., p 49.
[167] Kuo and Mark, Poly(dimethylsiloxane) in "Polymer data handbook".
[168] Aranguren, Mora, and Macosko, "Compounding Fumed Silicas into Polydimethylsiloxane: Bound Rubber and Final Aggregate Size."
[169] Lee, Reference book for composites technology.
[170] Jessamine Ng Lee, Cheolmin Park, and George M. Whitesides, "Solvent compatibility of poly(dimethylsiloxane)-based microfluidic devices," Analytical Chemistry 75, no. 23 (2003). pp 6544-6554.
[171] P. R. Dvornic, "High Temperature Stability of Polysiloxanes," Silicon Compounds: Silanes and Silicones, Gelest Catalog (2004).
[172] Rajesh Tiwari, "Special Report/Instrumentation:Thermal Techniques for Material Characterization," (2008). Published On Line by Ceramic Industry Magazine. http://www.ceramicindustry.com/articles/special-report-instrumentation-thermal-techniques-for-material-characterization
[173] Levresse, Feke, and Manas-Zloczower, "Analysis of the formation of bound poly(dimethylsiloxane) on silica."
[174] DeGroot and Macosko, "Aging Phenomena in Silica-Filled Polydimethylsiloxane."
[175] S. D. Burnside and E. P. Giannelis, "Nanostructure and properties of polysiloxane-layered silicate nanocomposites," Journal of Polymer Science Part B: Polymer Physics 38, no. 12 (2000). pp 1594-1604.
[176] Berrod et al., "Reinforcement of siloxane elastomers by silica. Chemical interactions between an oligomer of poly(dimethylsiloxane) and a fumed silica."